Organic-Inorganic Hybrid and Halide Perovskites

A New Breed of Exciting Advanced Functional Materials

PROFESSOR CNR RAO PRIZE LECTURE IN ADVANCED MATERIALS 2021

Satishchandra Ogale
Research Institute for Sustainable Energy (TCG-CREST), Kolkata
Department of Physics and Centre for Energy Science, IISER Pune
satishogale@iiserpune.ac.in, satishogale@gmail.com

Funding : CSIR, MNRE, DST (Nanomission), UK-India (APEX-I,II, SUNRISE, DIT, BRNS (DAE), Govt of India

Salute to the Highly Eminent Scientist & Torch-Bearer of Indian Science


CENTRE FOR
ENERGY
SCIENCE

https://www.conserve-energy-future.com/causes-effects-of-industrial-pollution.php

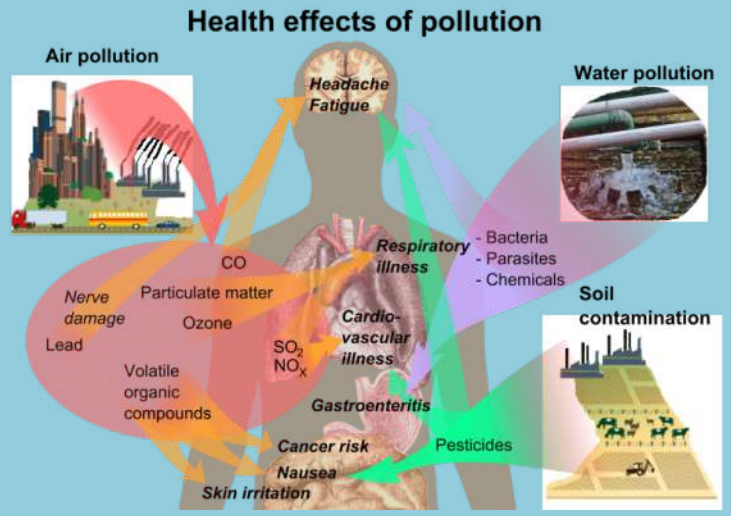

https://ec.europa.eu/jrc/en/news/air-quality-traffic-measures-could-effectively-reduce-no2-concentrations-40-europe-s-cities

Global CO2 emissions continue to rise

Emissions in gigatonnes of carbon dioxide

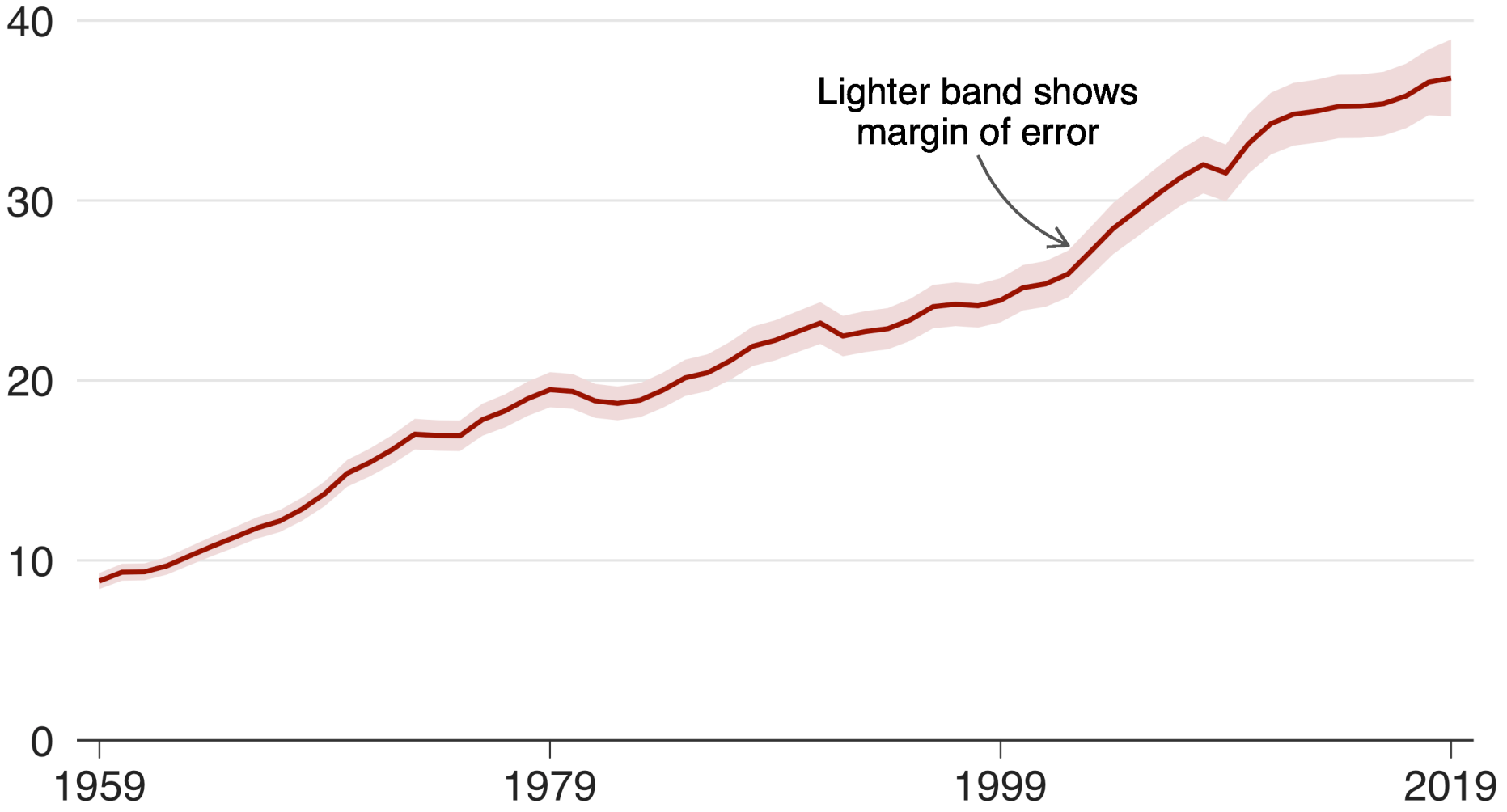

Source: Global Carbon Project/CICERO

BBC

David Roberts in Climate and Energy


ABB
ABB
Protoscar


ZERO EMISSION
BYD

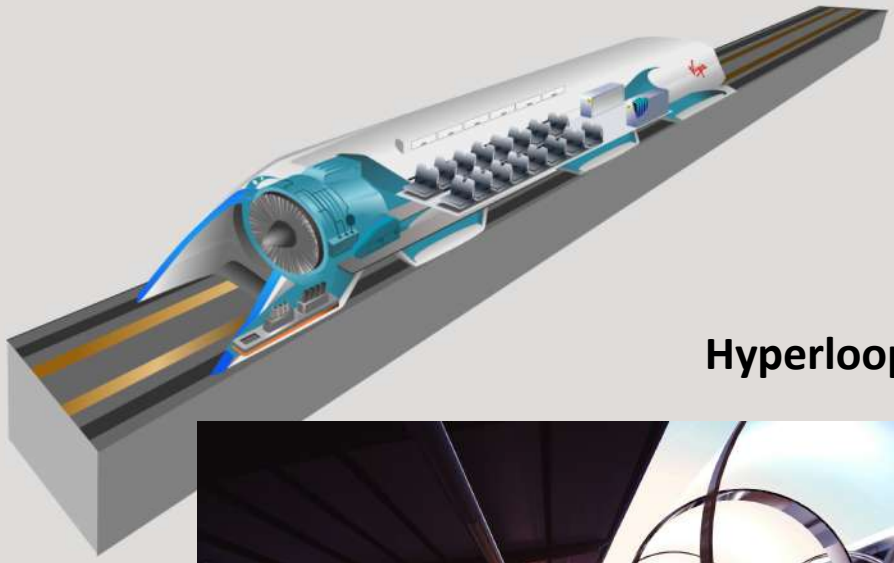

Hyperloop

Source : Internet

Space Race

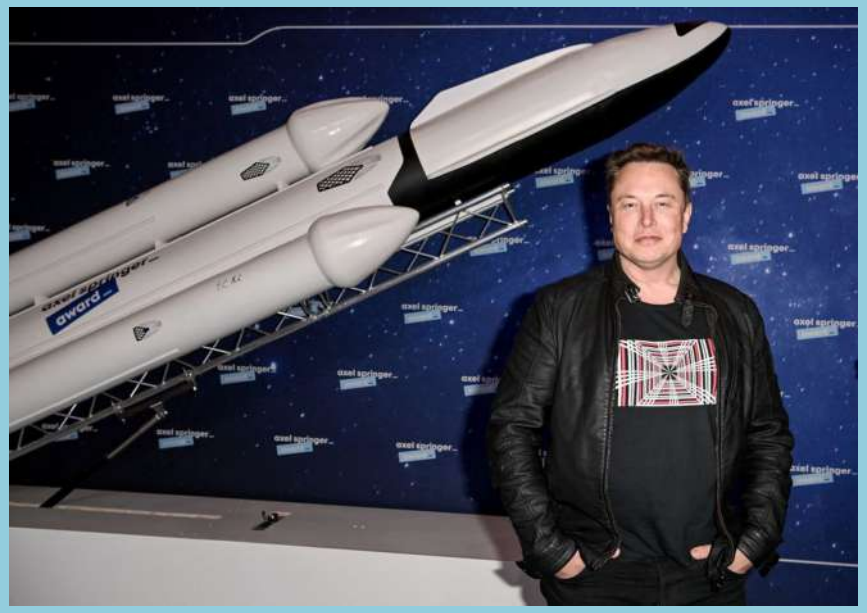

Next Generation Device Systems

- **Ultra High Performing**
- **Flexible**
- **Thin**
- **Light Weight**
- **Self Powered or Low powered**
- **Robust**

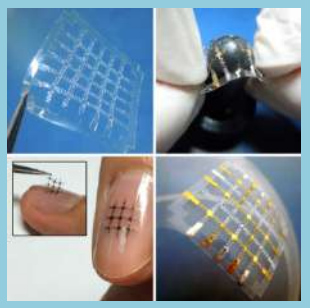

Robotics, AI, Machine Learning, Data Science

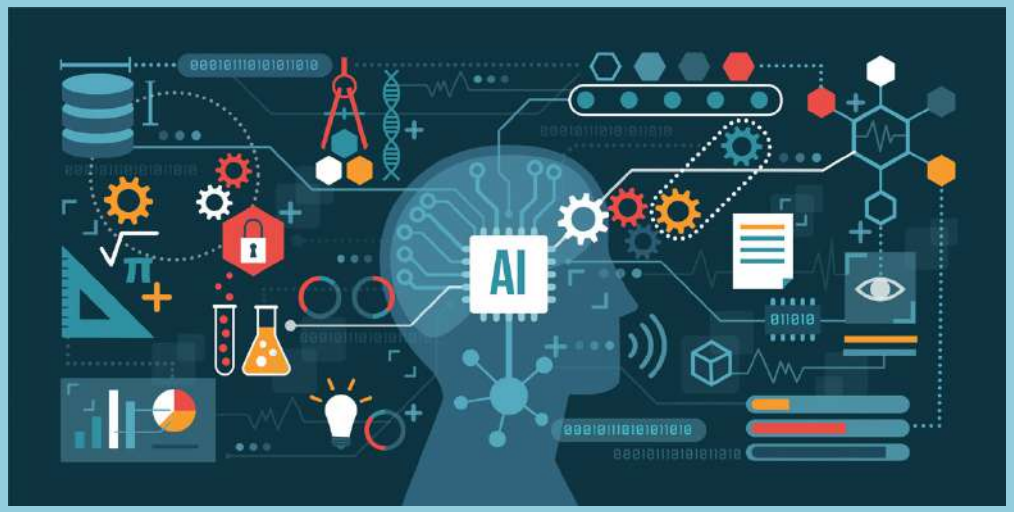

Haotian Mai And Caitlin Dawson | August 10, 2020

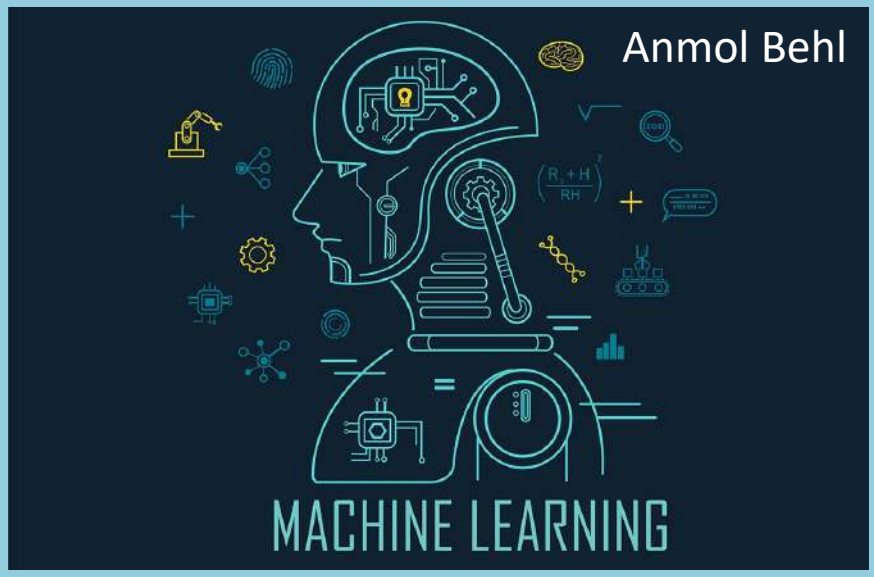

http://www.kiwidatascience.com/

https://en.wikipedia.org/wiki/Robotics

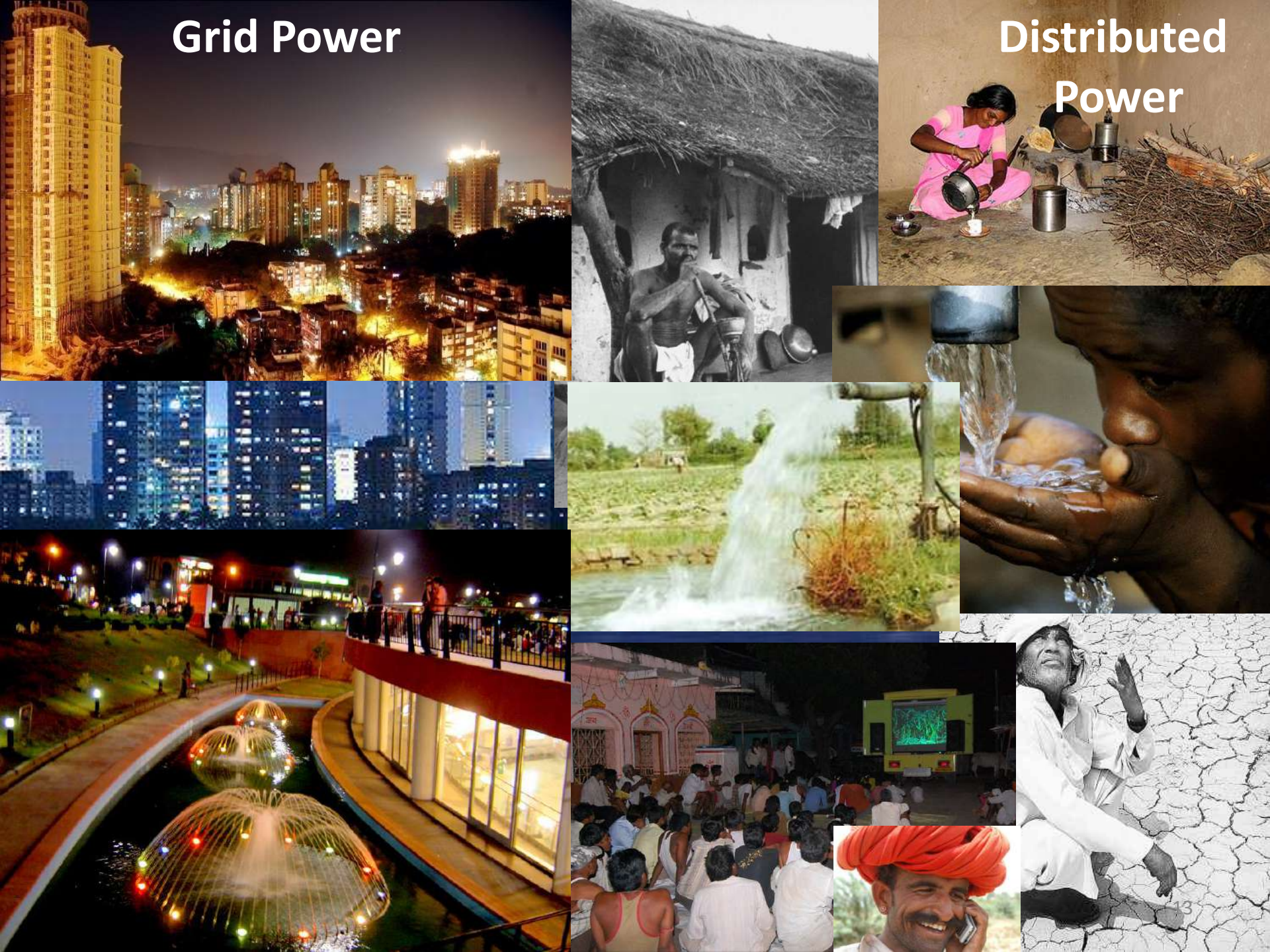
Grid Power
Distributed Power

Conversion

Solar Cells, Solar Water Splitting for Hydrogen
CO_2 Reduction to Clean Fuels

Metal Oxides, Sulfides, Semiconductor QDs
Hybrid & Halide Perovskites, 2D Materials

Dyes, Functional Polymers,
Ionic liquids, gels, organo-metallics

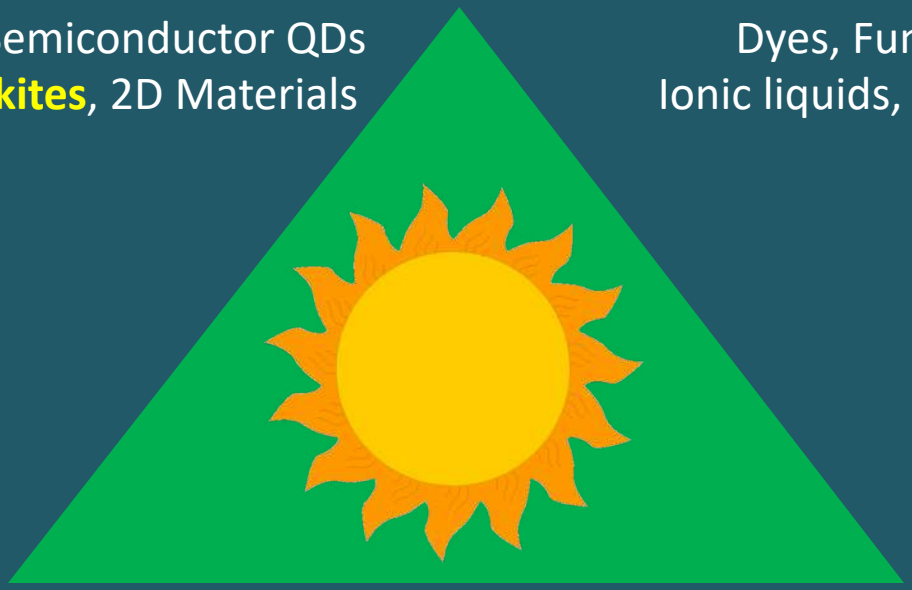

Storage

Super-capacitor, Li/Na Battery
Alternate Battery Chemistries
Phase Change Materials

Conservation

Solid State Lighting (LED)
Smart Systems

Functional High Surface Area Carbon, Metal Oxides/sulfides, Conducting Polymers,
Engineered Hetero-junction systems and Interfaces

High Tc superconductors, CMR Manganites, Ferroelectrics, Piezoelectrics, Multiferroics …

Very Interesting Structural, Chemical, Bonding, Valence, Orbital configurations

Intriguing phase diagrams and Broad Range of Exciting Property Portfolio

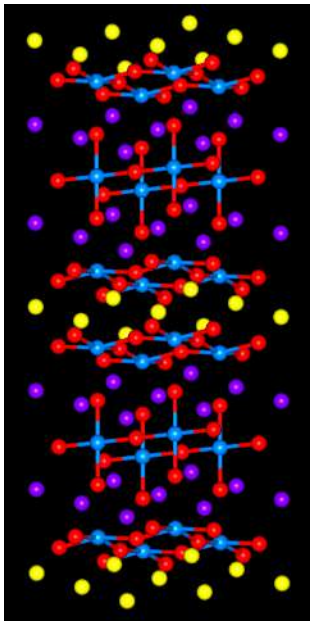

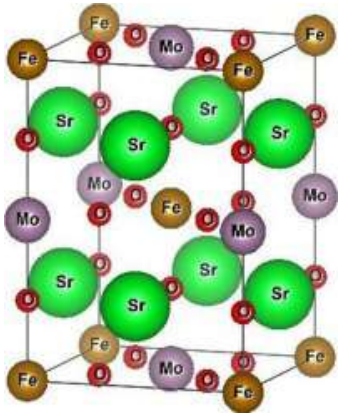

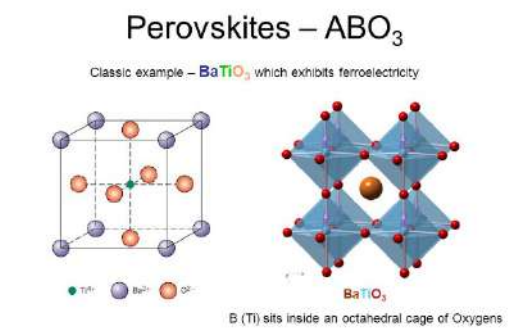

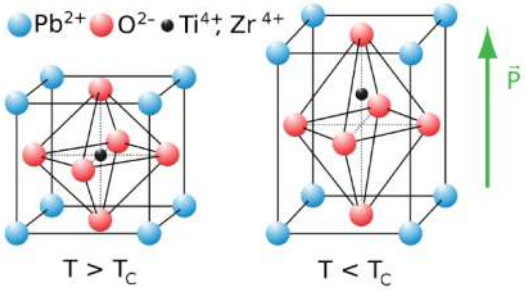

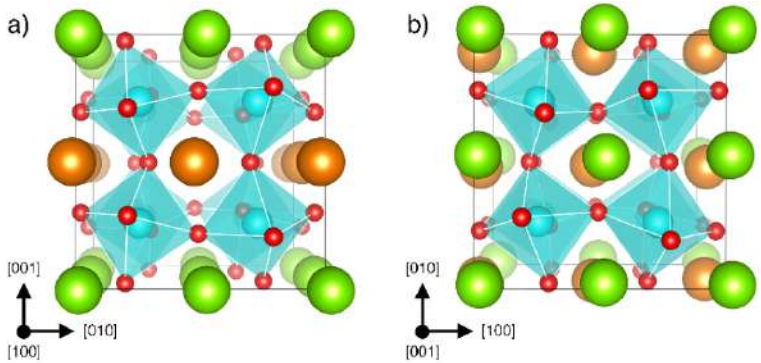

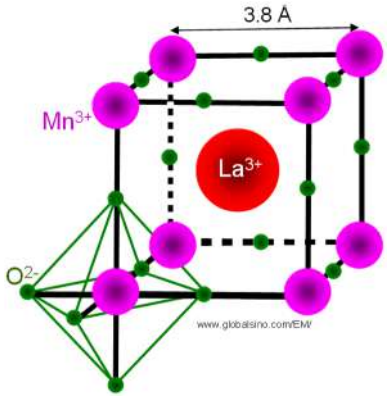

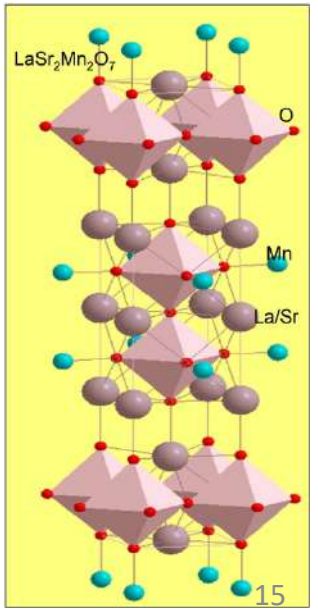

Hybrid Perovskites

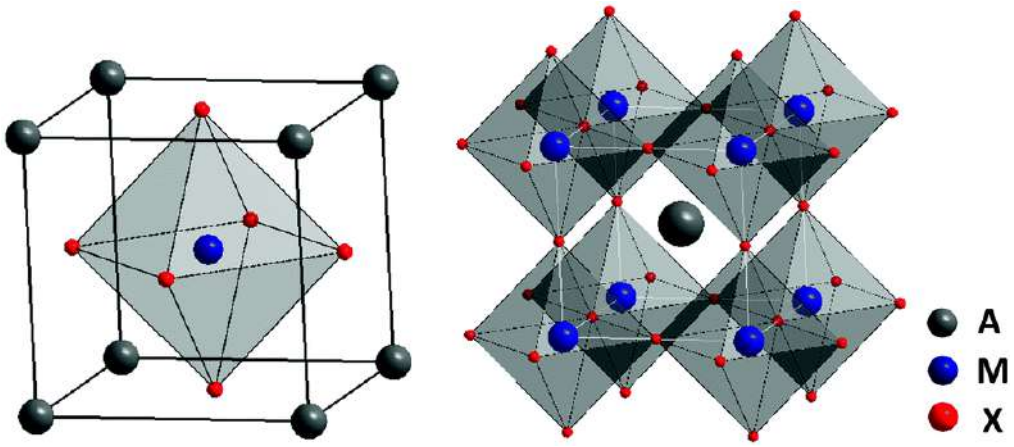

AMX_3

A : Organic Cation
M : Divalent metal cation
X : Halide anion

Inorg. Chem. Front., 2015, 2, 584-584

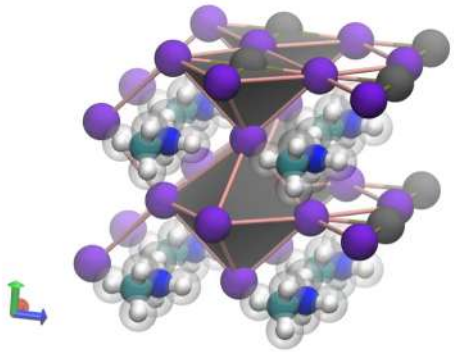

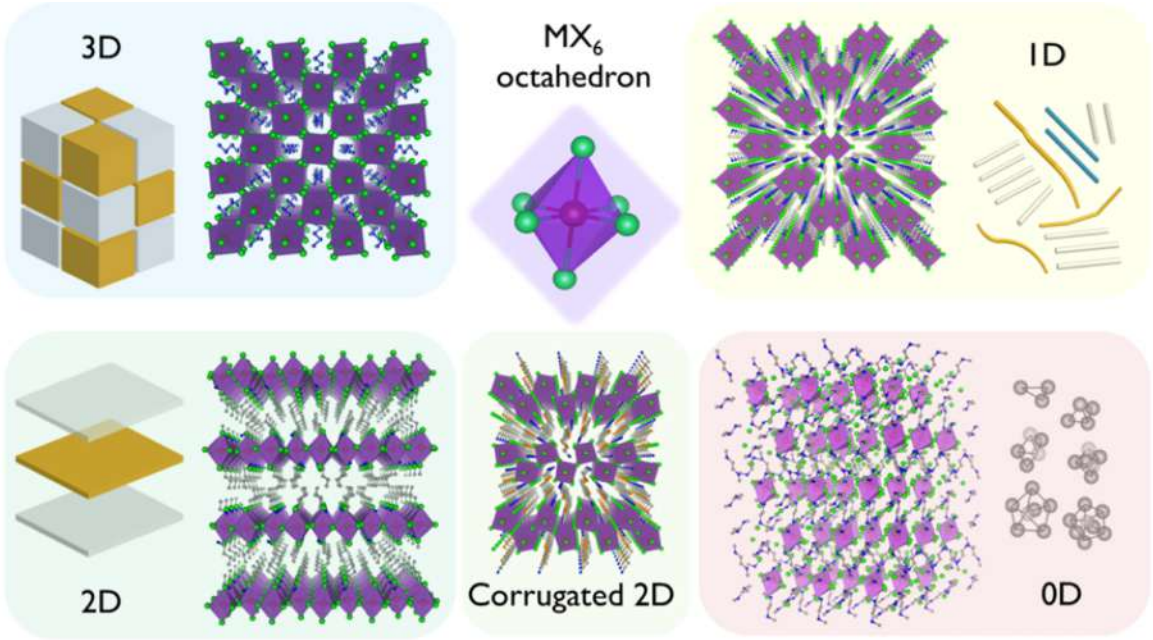

ACS Energy Lett. 2018, 3, 54−62

LETTER

doi:10.1038/nature18306

High-efficiency two-dimensional Ruddlesden–Popper perovskite solar cells

Hsinhan Tsai[1,2*], Wanyi Nie[1*], Jean-Christophe Blancon[1], Constantinos C. Stoumpos[3,4,5], Reza Asadpour[6], Boris Harutyunyan[4,5], Amanda J. Neukirch[1], Rafael Verduzco[2,7], Jared J. Crochet[1], Sergei Tretiak[1], Laurent Pedesseau[8], Jacky Even[8], Muhammad A. Alam[6], Gautam Gupta[1], Jun Lou[2], Pulickel M. Ajayan[2], Michael J. Bedzyk[4,5], Mercouri G. Kanatzidis[3,4,5] & Aditya D. Mohite[1]

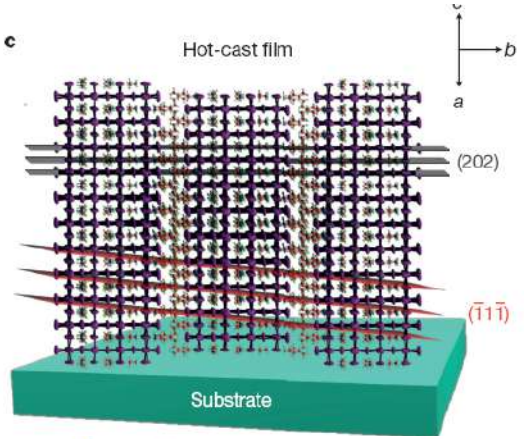

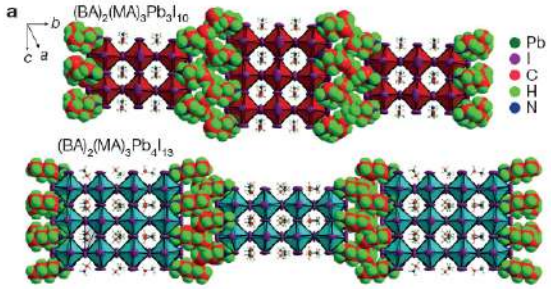

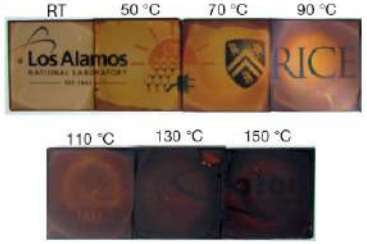

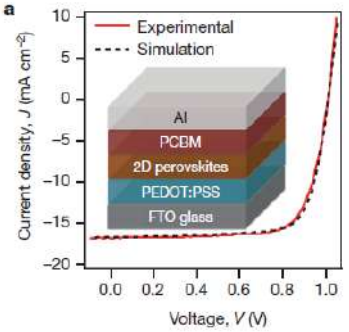

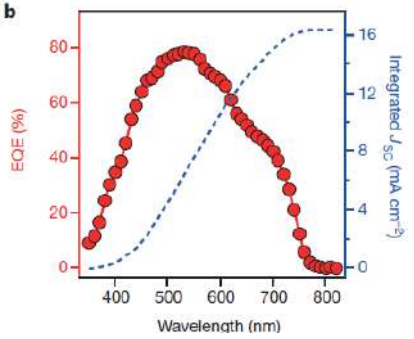

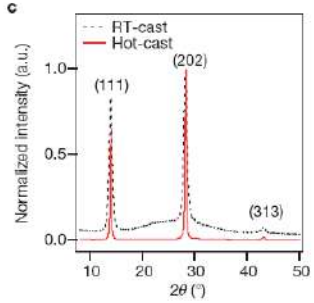

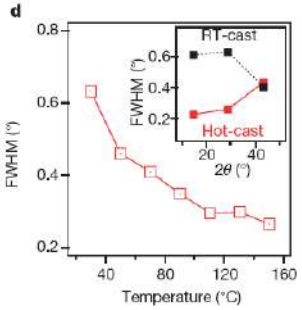

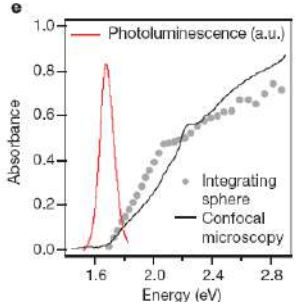

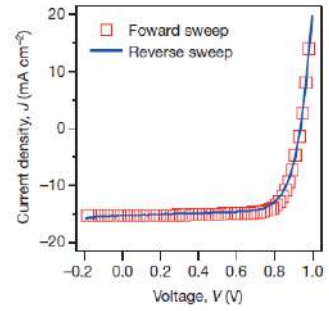

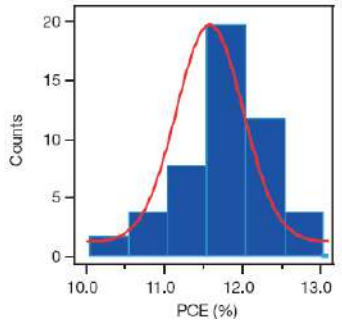

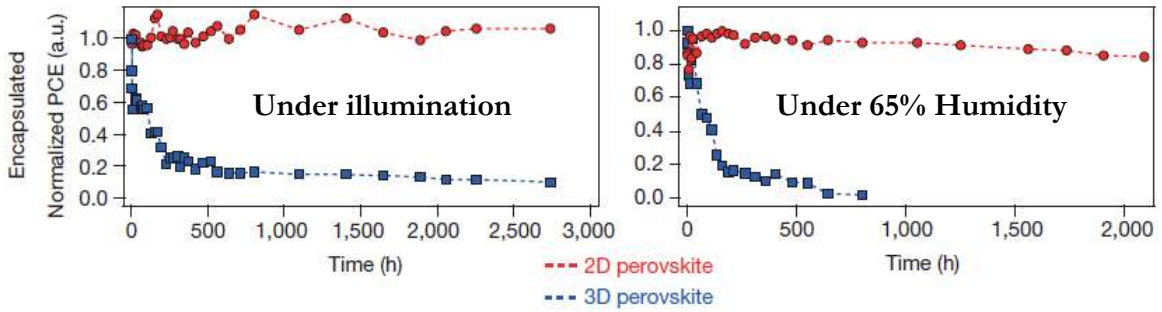

https://phys.org/news/2018-04-perovskite-solar-cells-efficient.html

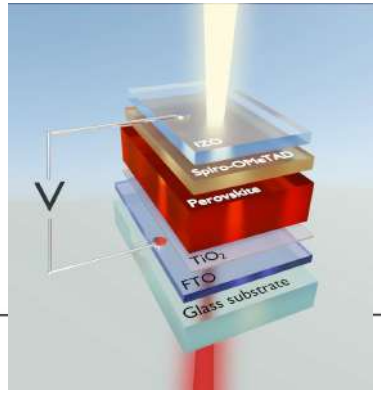

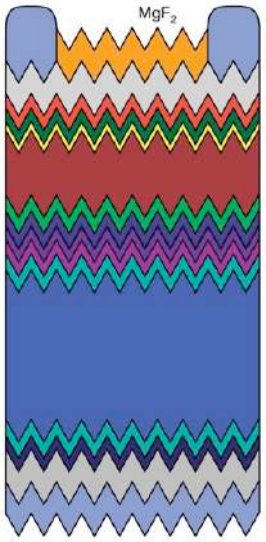

PCE = 25.2%

Best Research-Cell Efficiencies

NREL Transforming ENERGY

Multijunction Cells (2-terminal, monolithic)
LM = lattice matched
MM = metamorphic
IMM = inverted, metamorphic
- Three-junction (concentrator)
- Three-junction (non-concentrator)
- Two-junction (concentrator)
- Two-junction (non-concentrator)
- Four-junction or more (concentrator)
- Four-junction or more (non-concentrator)

Single-Junction GaAs
- Single crystal
- Concentrator
- Thin-film crystal

Crystalline Si Cells
- Single crystal (concentrator)
- Single crystal (non-concentrator)
- Multicrystalline
- Silicon heterostructures (HIT)
- Thin-film crystal

Thin-Film Technologies
- CIGS (concentrator)
- CIGS
- CdTe
- Amorphous Si:H (stabilized)

Emerging PV
- Dye-sensitized cells
- Perovskite cells
- Perovskite/Si tandem (monolithic)
- Organic cells
- Organic tandem cells
- Inorganic cells (CZTSSe)
- Quantum dot cells (various types)
- Perovskite/CIGS tandem (monolithic)

Cell Efficiency (%)

Variants of Perovskite Tandem Solar Cells

MY RESEARCH FOCUS

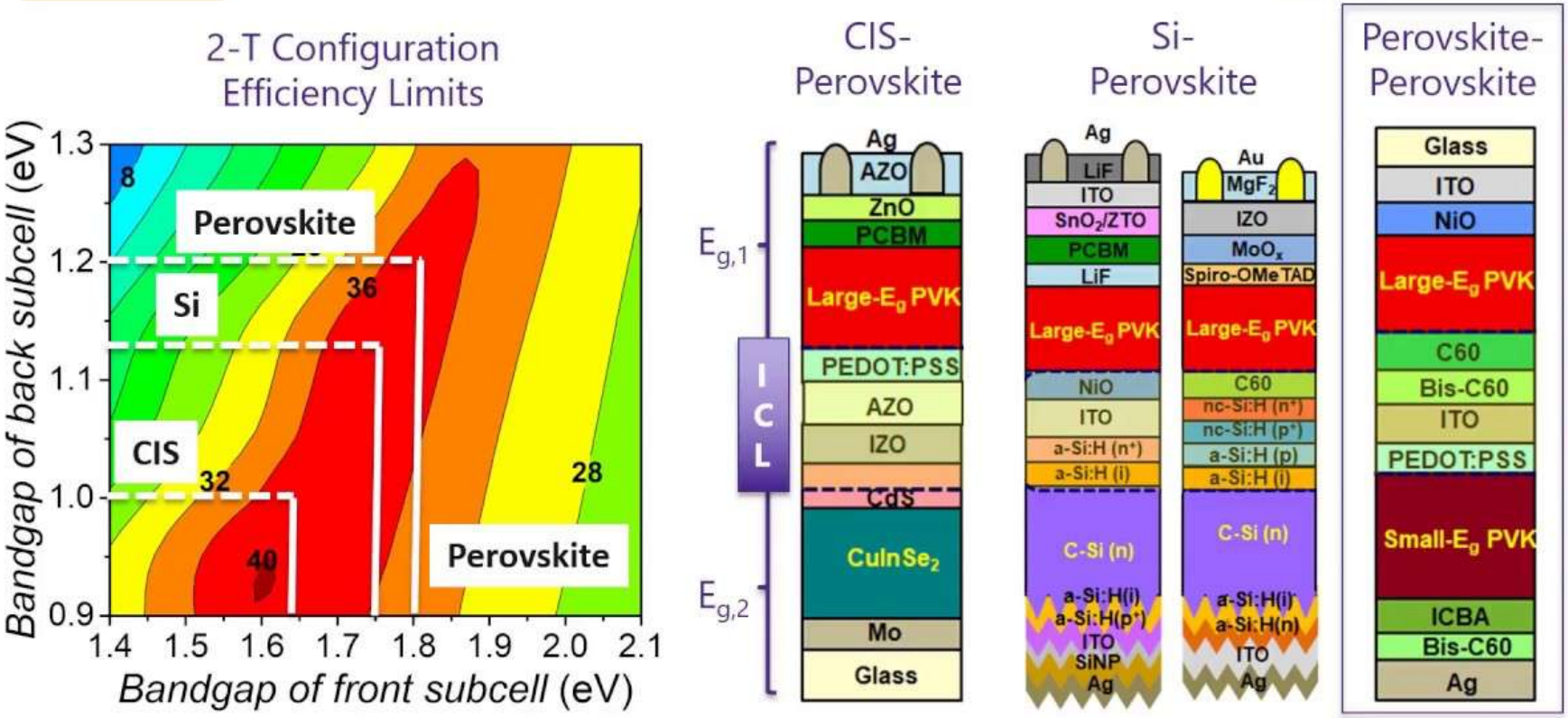

Rajagopal, Yang, & Jen et al., *Adv. Mater.* **2017**

Rajagopal, Yao, & Jen, *Adv. Mater.* **2018**

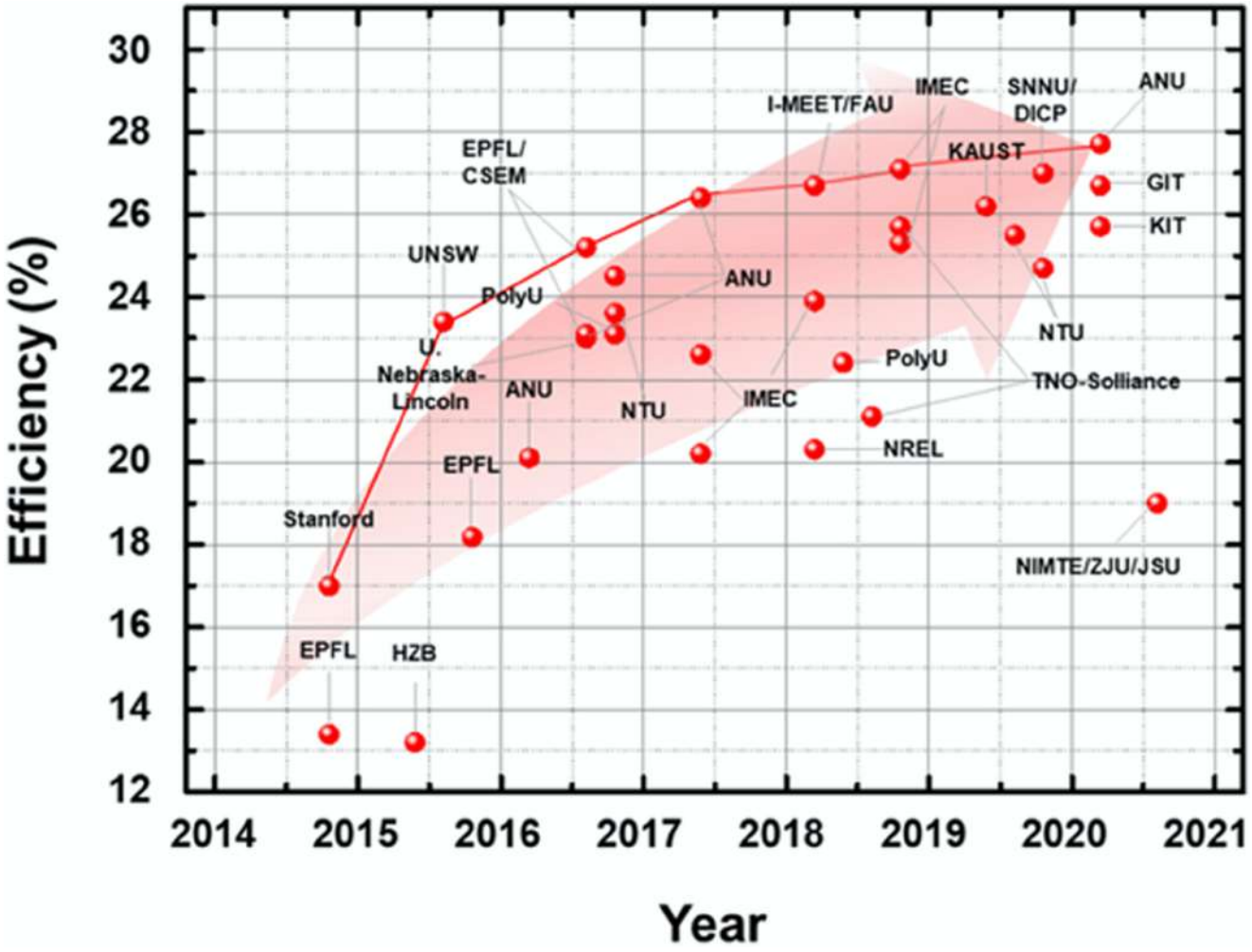

Choi and Coworkers, EcoMat DOI: 10.1002/eom2.12084 /eom2.12084

Solar Cells

Batteries

Super-capacitors

Organic/Inorganic Hybrids

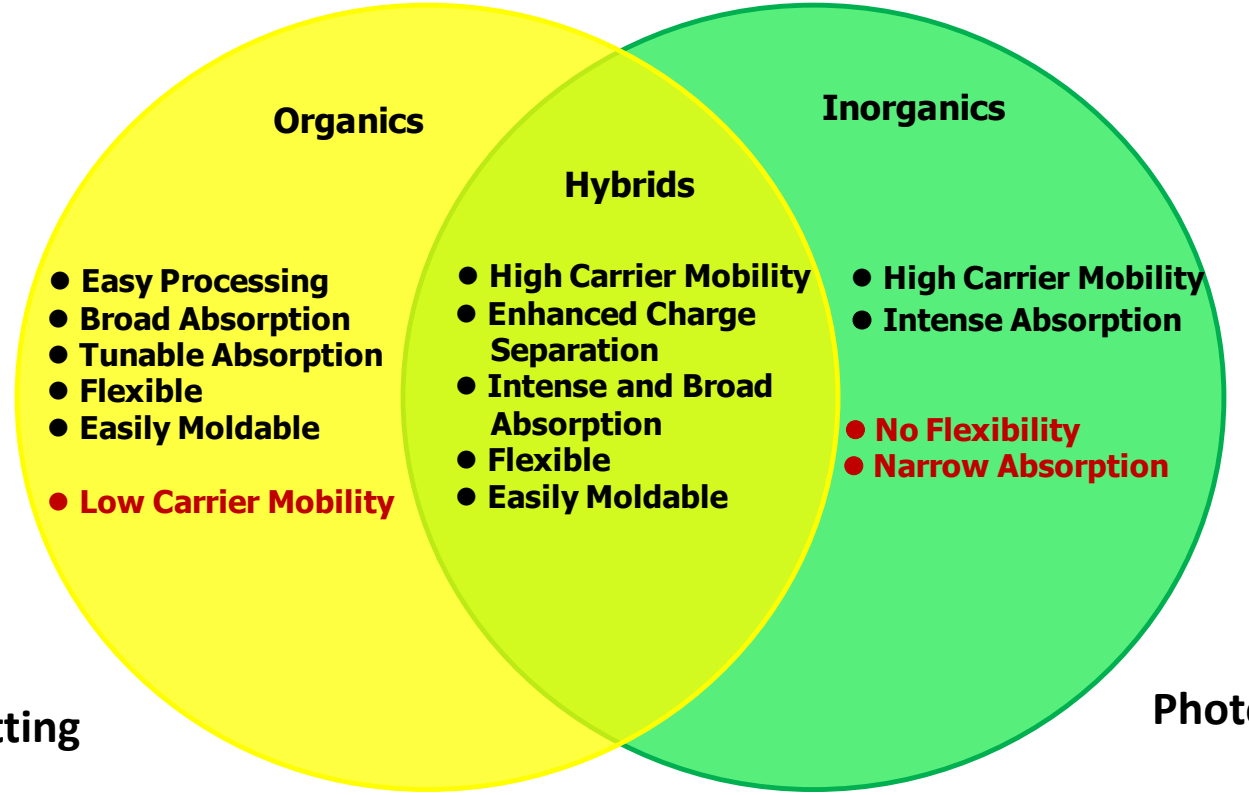

Fuel Cells

LEDs

Water splitting

Photo-catalysis

Superhydrophobic / dust resistant surfaces

Emerging Research Directions

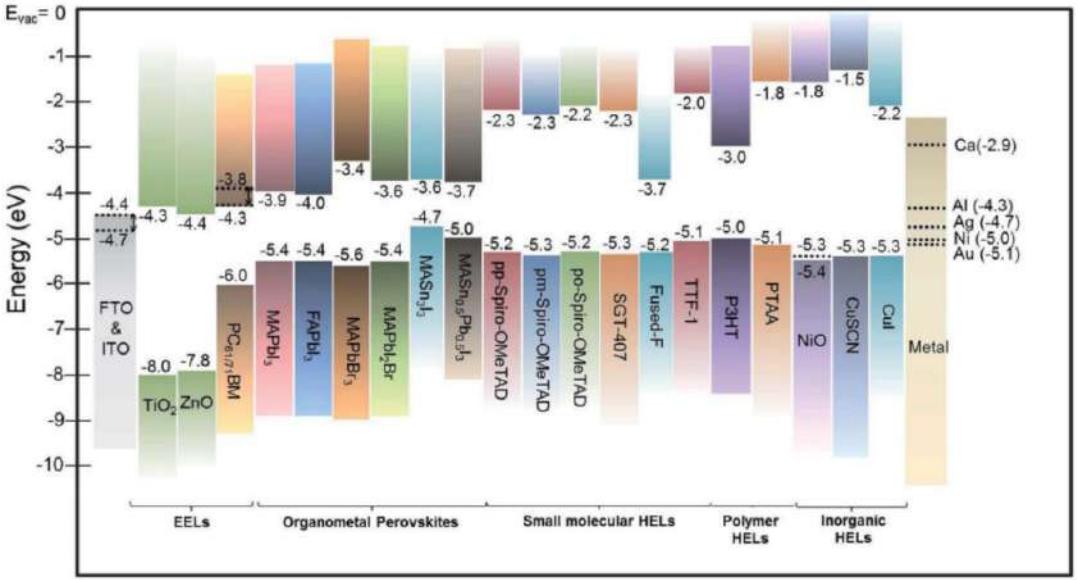

ACS Nano, 2016, 11, 9776–9786

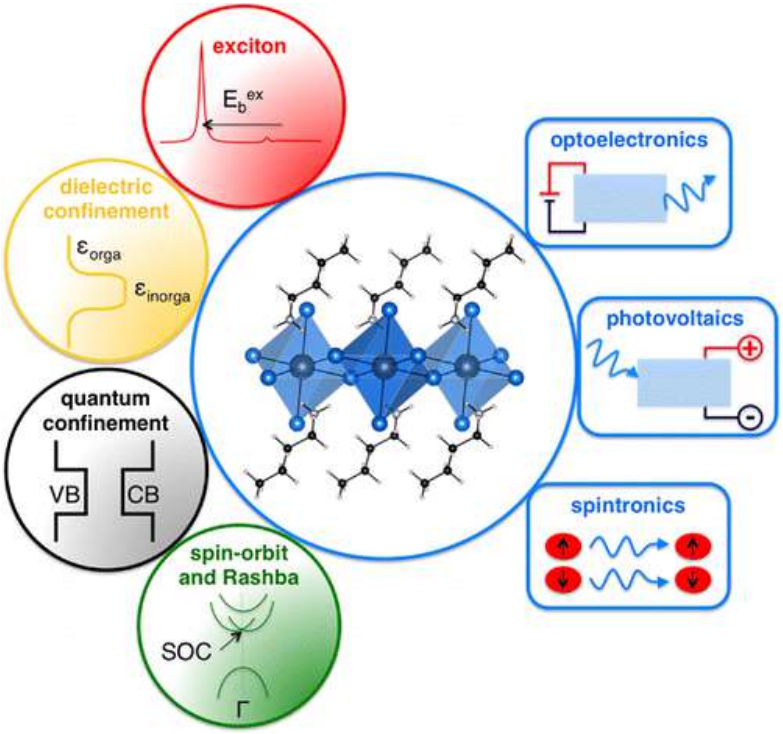

Energies 2016, 9(11), 861

Dye Sensitized Solar Cells & Perovskite Solar Cells

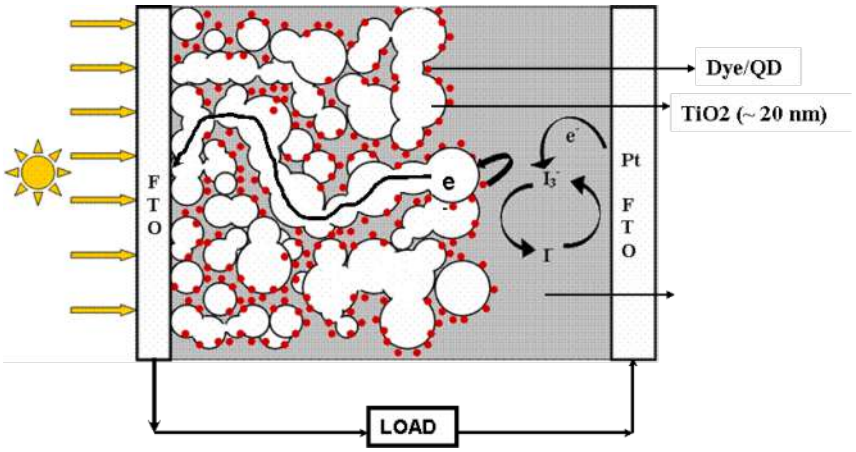

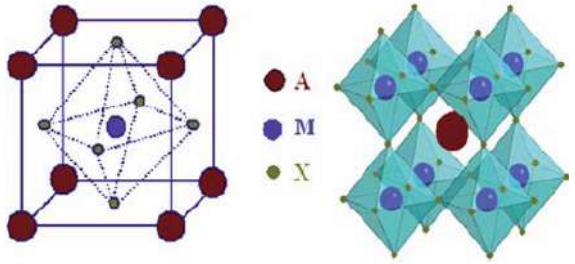

Champion Conversion Efficiency > 22%

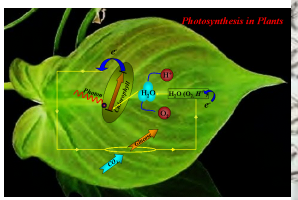

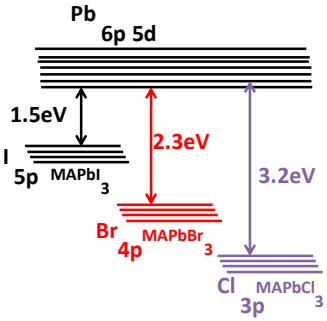

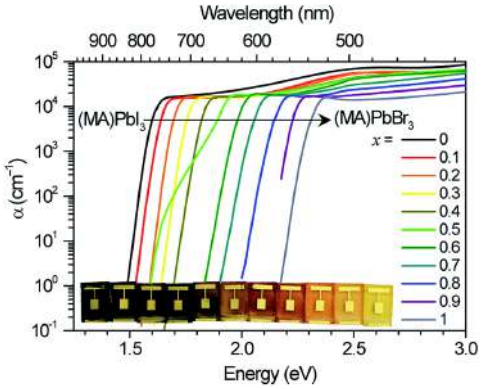

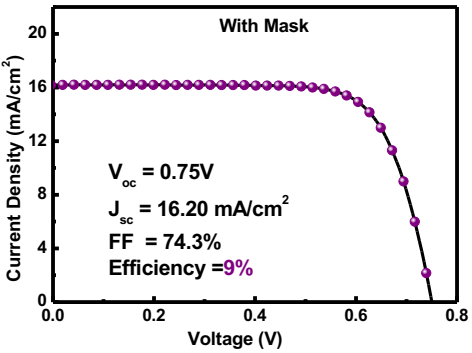

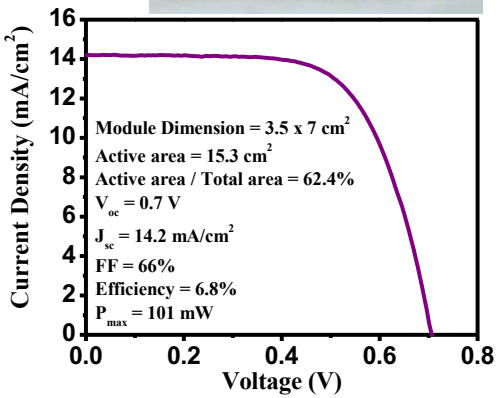

Devices are certified at IIT Bombay

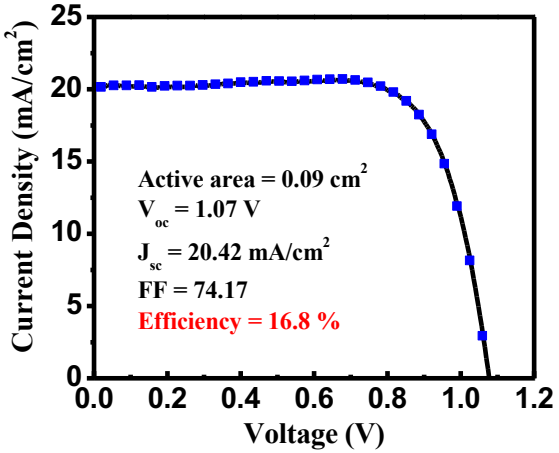

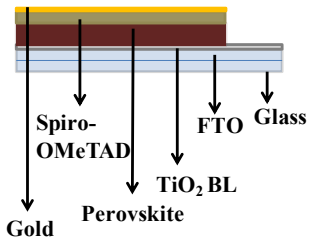

COMMUNICATION
Light Emitting Diodes
ADVANCED MATERIALS INTERFACES
www.advmatinterfaces.de

High Quality Hybrid Perovskite Semiconductor Thin Films with Remarkably Enhanced Luminescence and Defect Suppression via Quaternary Alkyl Ammonium Salt Based Treatment

Rounak Naphade, Baodan Zhao, Johannes M. Richter, Edward Booker, Shrreya Krishnamurthy, Richard H. Friend, Aditya Sadhanala, and Satishchandra Ogale**

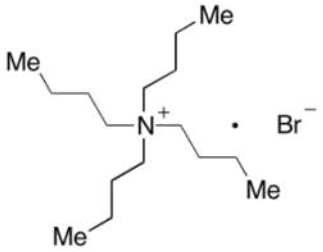

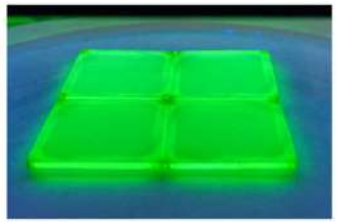

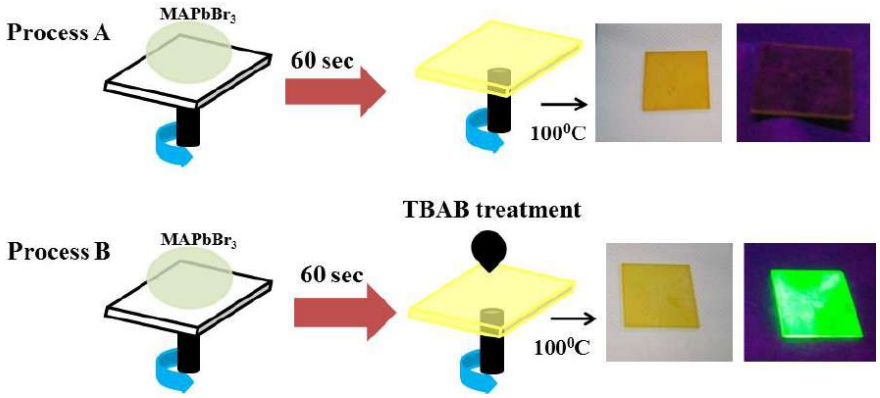

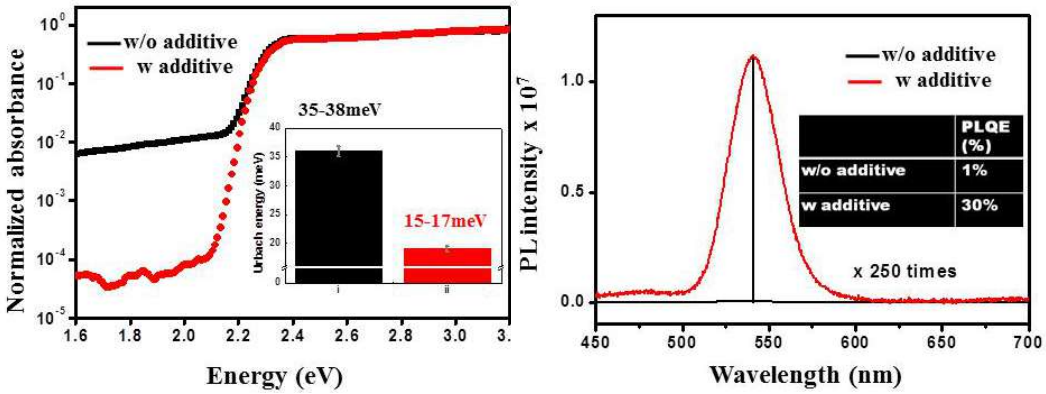

Adv. Mater. Interfaces 2017, 4, 1700562

Additive Mediated Solvent Engineering

Few drops of 0.1 m tetrabutylammonium bromide (TBAB) solution in chloroform
Short annealing step of 5 min at 100 °C

TBAB
Tetra Butyl Ammonium Bromide

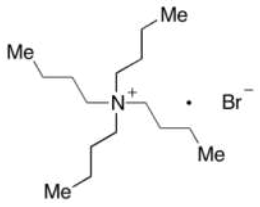

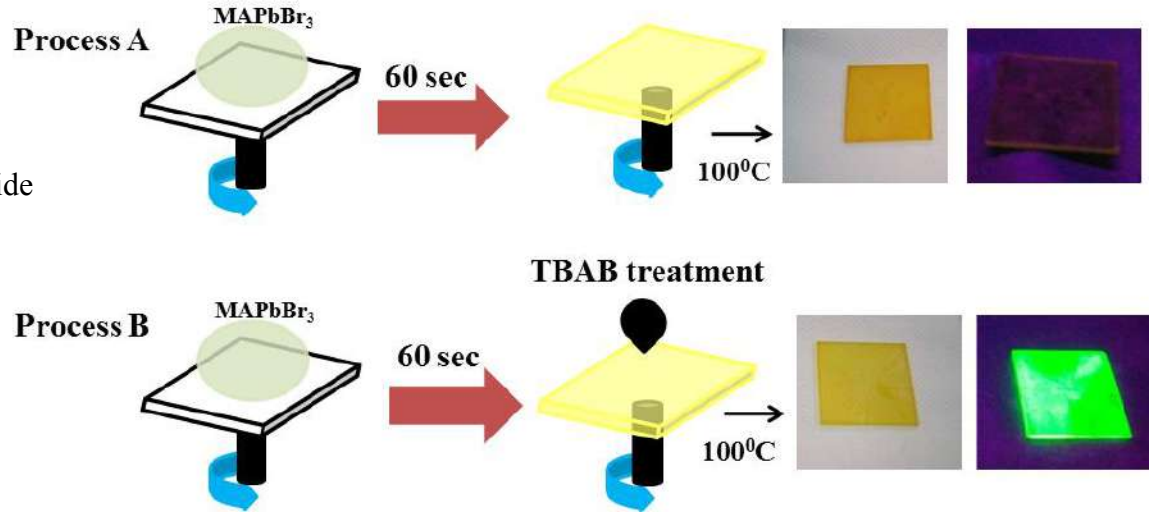

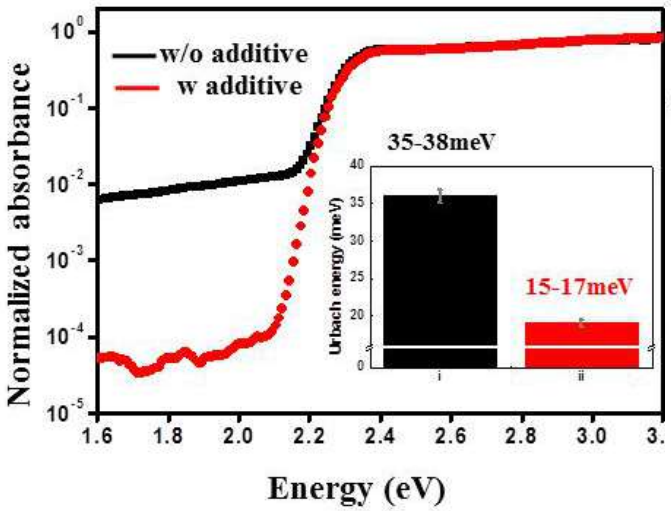

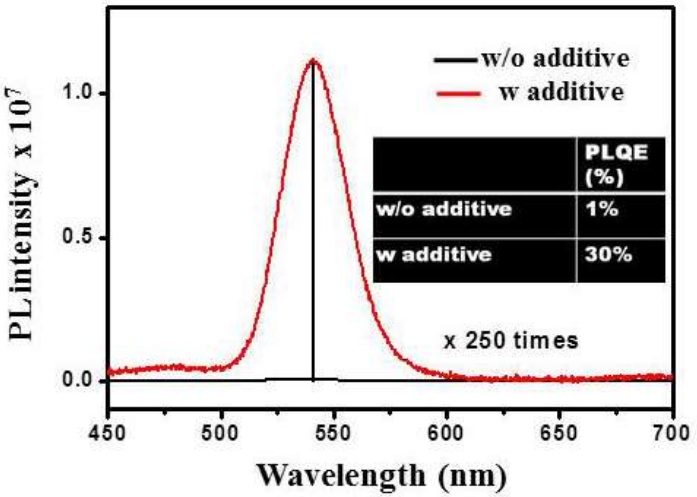

PL life time 407 nm, 1 micro-J/cm²

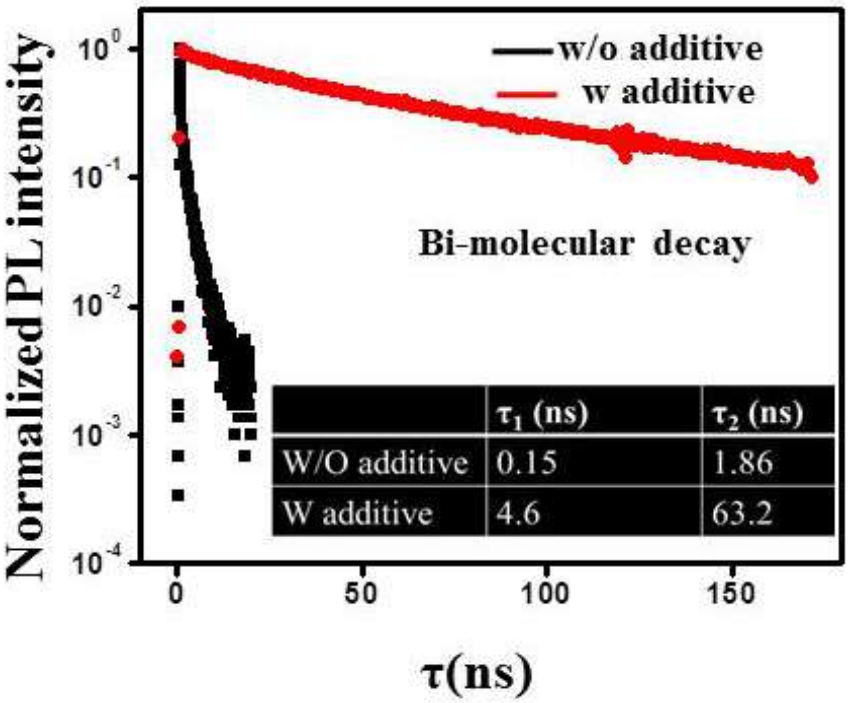

	τ_1 (ns)	τ_2 (ns)
W/O additive	0.15	1.86
W additive	4.6	63.2

Temperature stability

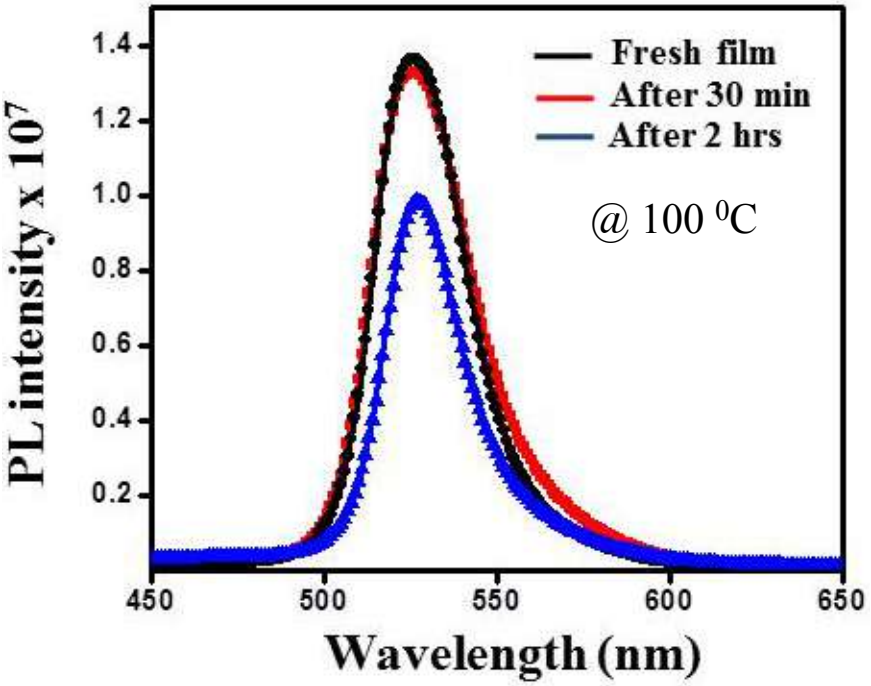

PLQE = K_r/ (K_r + K_{nr})

K_r: Radiative Recombination Rate Constant

K_{nr}: Non-Radiative Recombination Rate Constant

Films	Radiative rates (K_r)	Non-radiative rates (K_{nr})
w/o additive	5 * 10^5 s^{-1}	4.95 * 10^7 s^{-1}
W additive	1.88 * 10^6 s^{-1}	4.38 * 10^6 s^{-1}

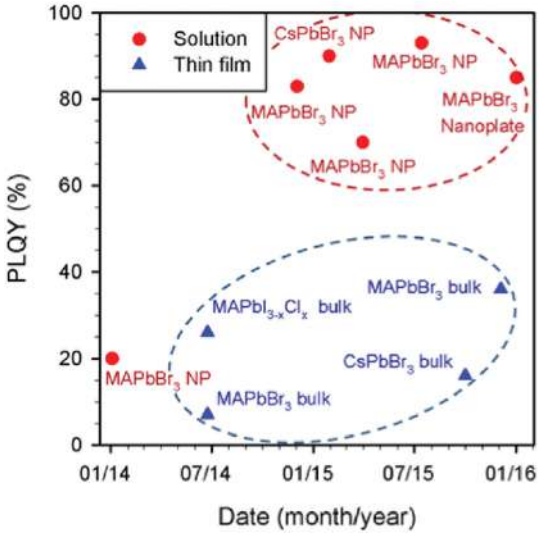

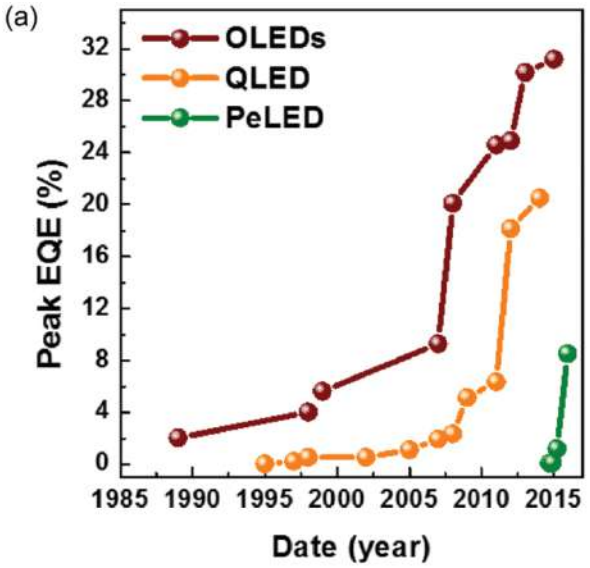

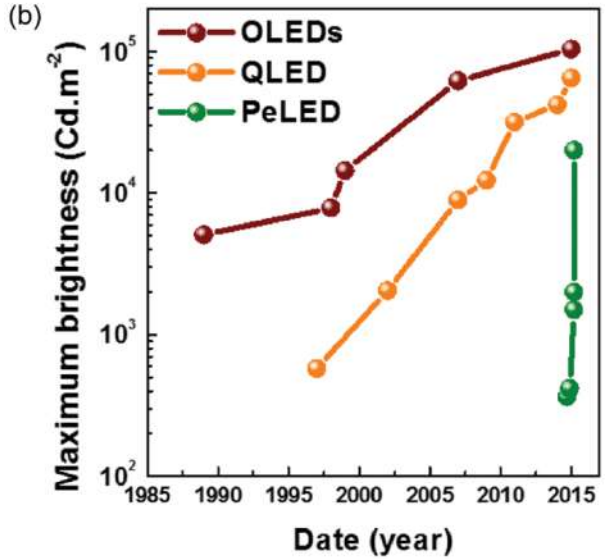

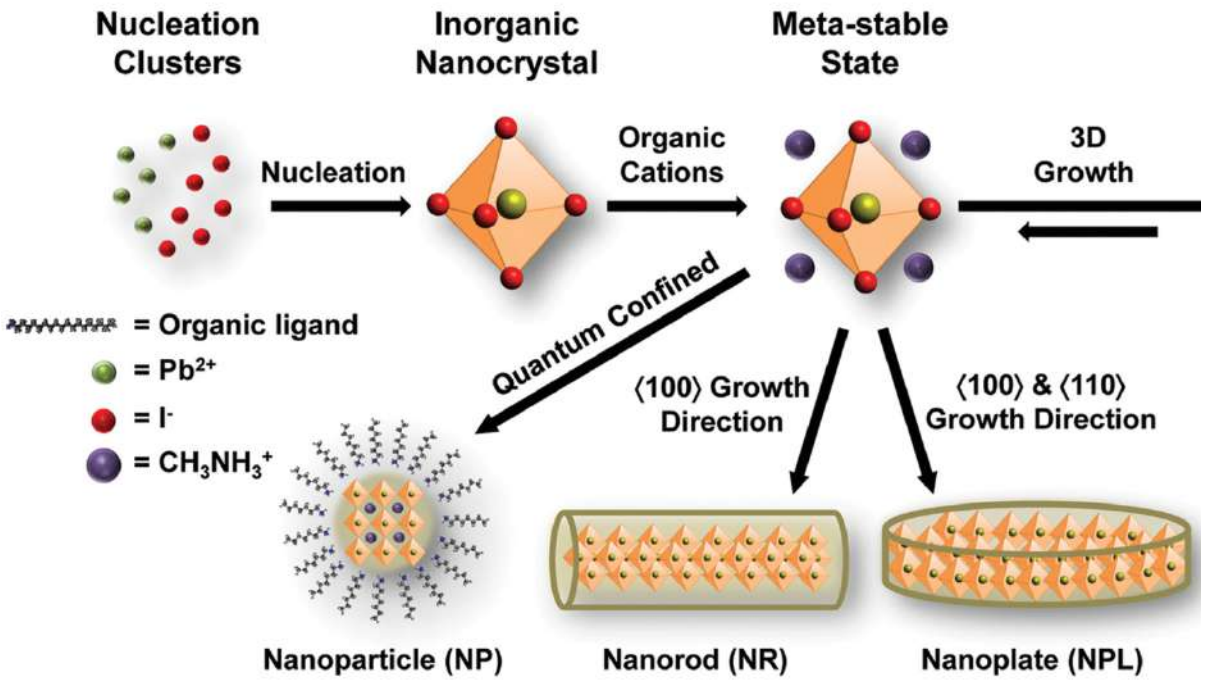

Adv. Mater. **2016**, *28*, 6804–6834

LED Measurements

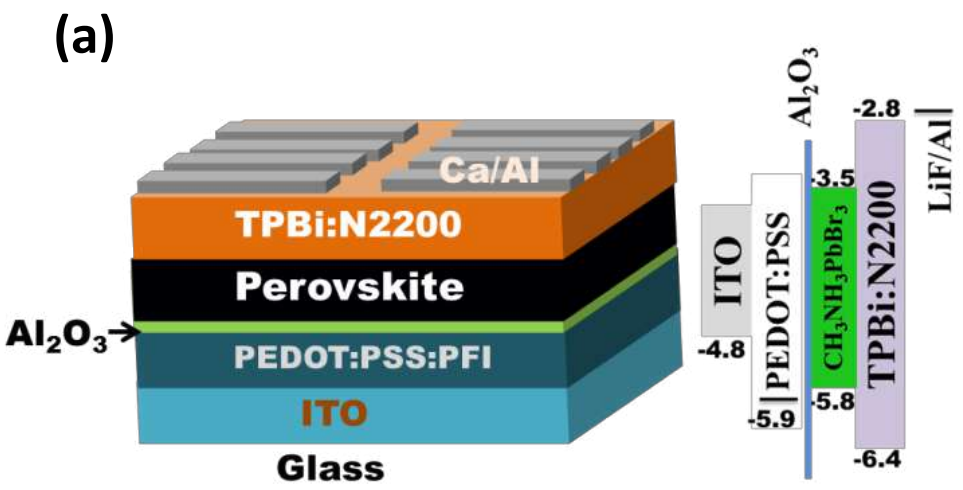

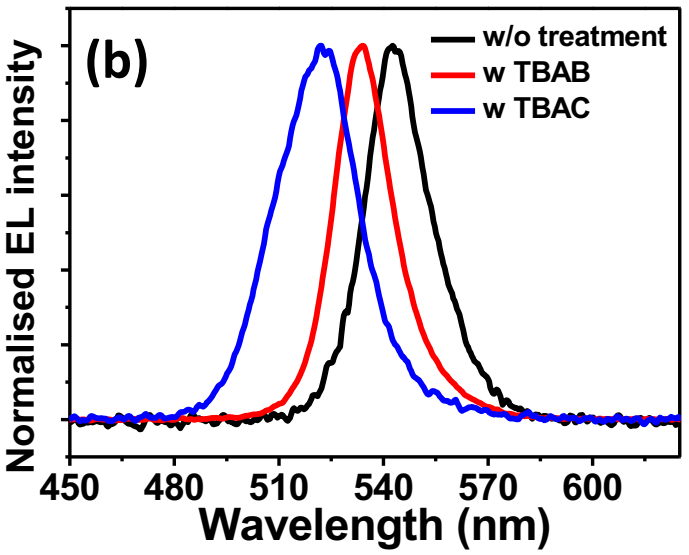

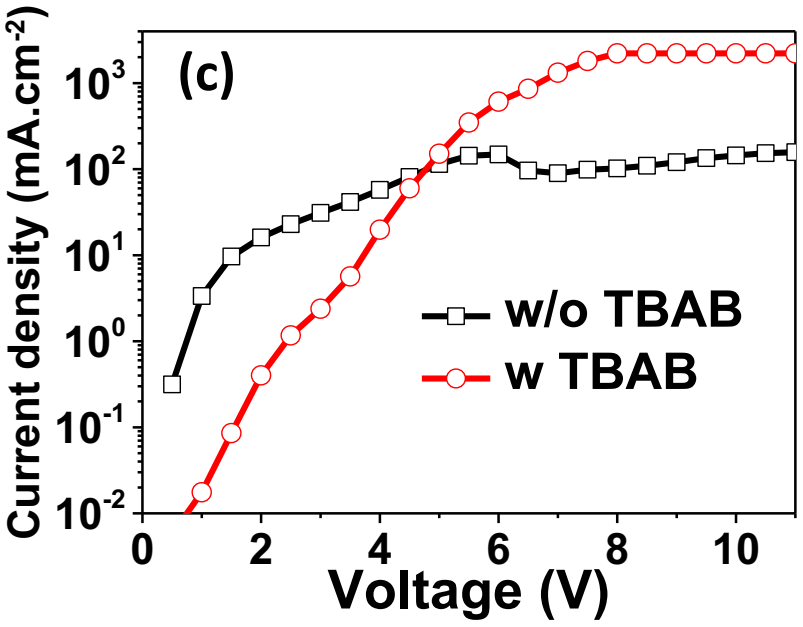

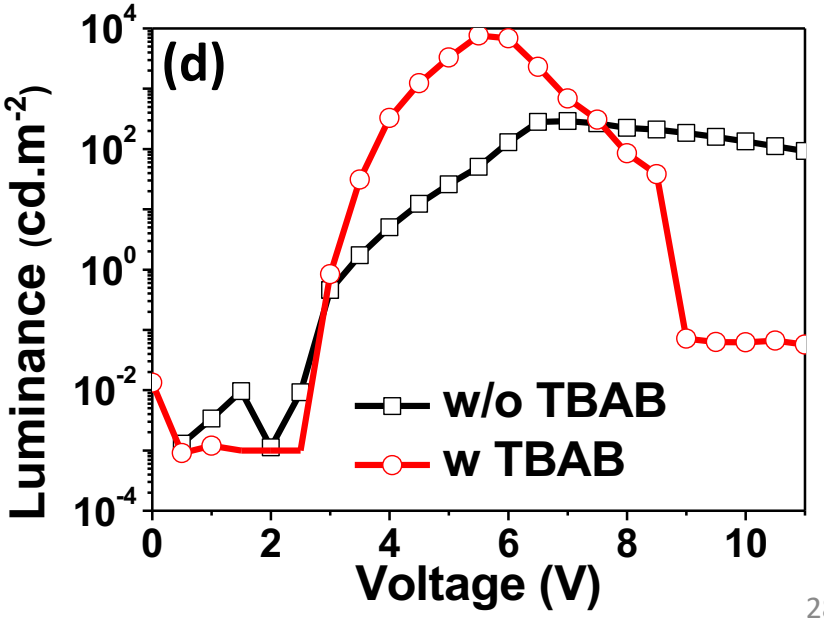

APL MATERIALS 6, 086107 (2018)

Quaternary alkylammonium salt incorporated 2D/3D mixed halide perovskite with highly enhanced photoluminescence and arrested iodide/bromide phase segregation

Prachi Kour, Mallu Chenna Reddy, Rounak Naphade,
and Satishchandra Ogale[a]

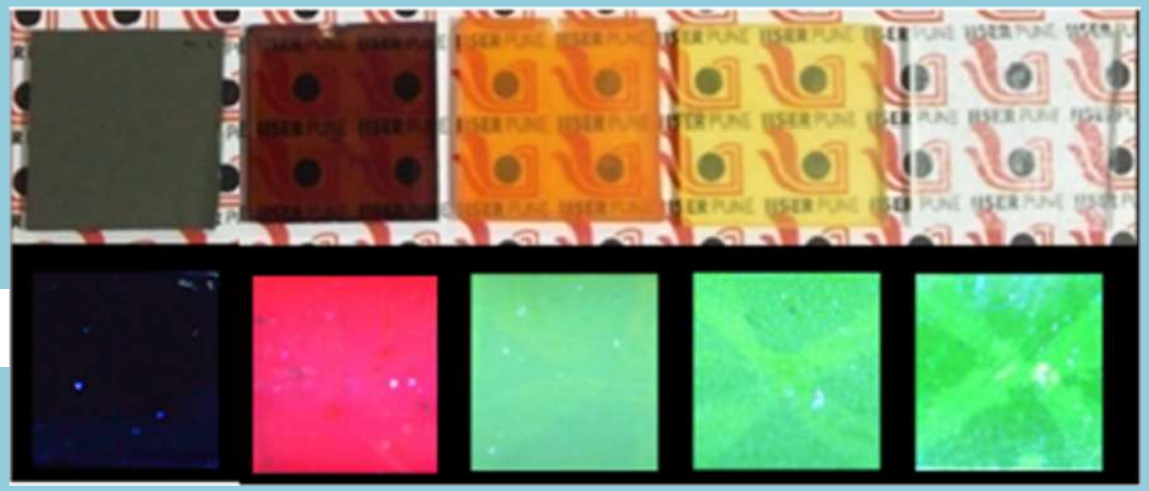

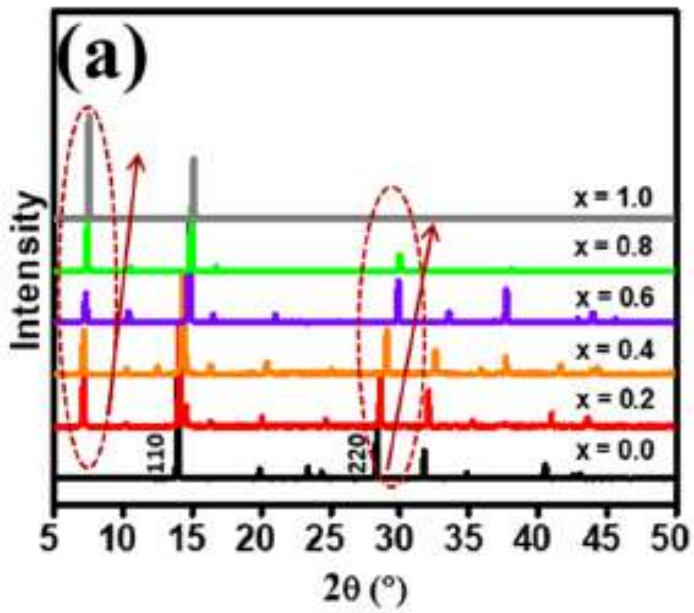
(a)
Intensity
x = 1.0
x = 0.8
x = 0.6
x = 0.4
x = 0.2
x = 0.0
110
220
5 10 15 20 25 30 35 40 45 50
2θ (°)

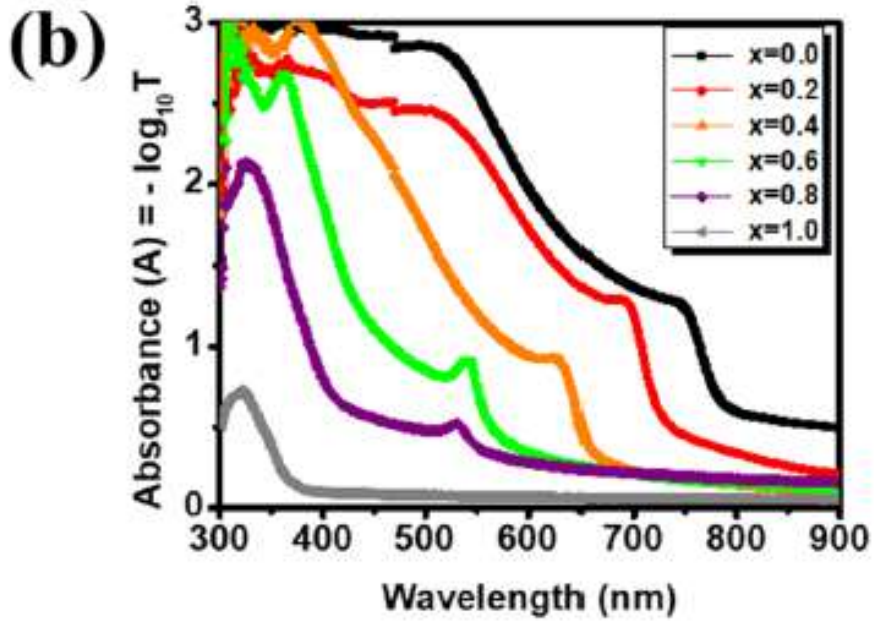
(b)
Absorbance (A) = - log10T
x=0.0
x=0.2
x=0.4
x=0.6
x=0.8
x=1.0
0 1 2 3
300 400 500 600 700 800 900
Wavelength (nm)

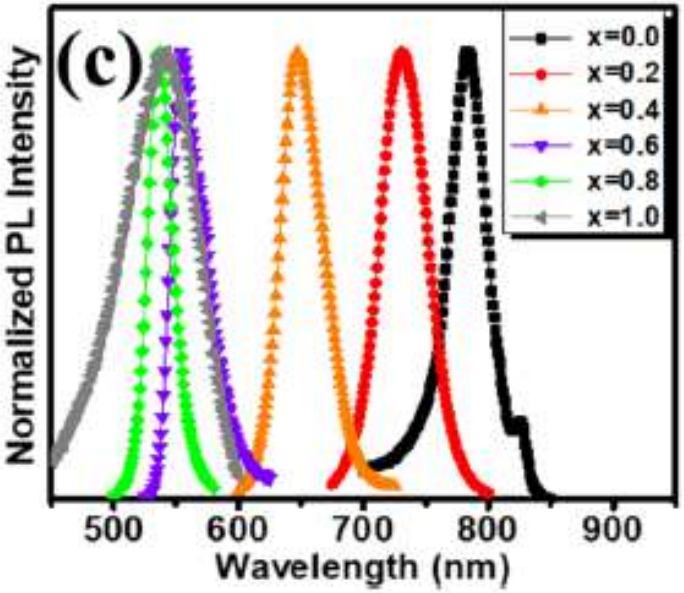
(c)
Normalized PL Intensity
x=0.0
x=0.2
x=0.4
x=0.6
x=0.8
x=1.0
500 600 700 800 900
Wavelength (nm)

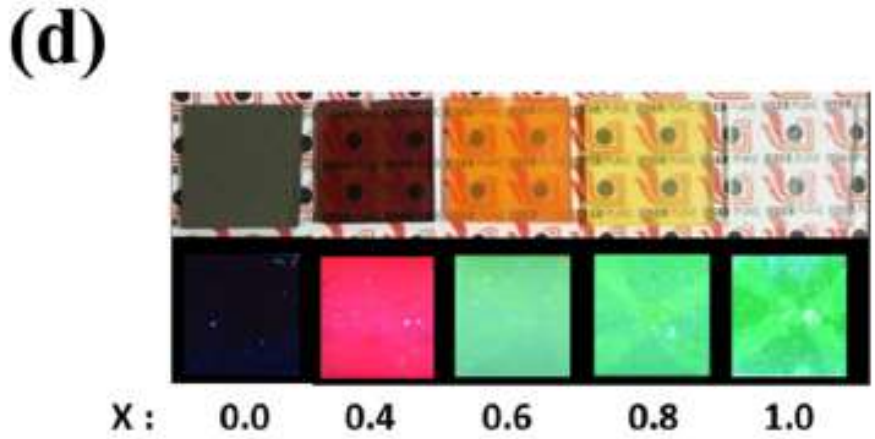
(d)
X : 0.0 0.4 0.6 0.8 1.0

Superior photo-stability, Carrier lifetime and PL

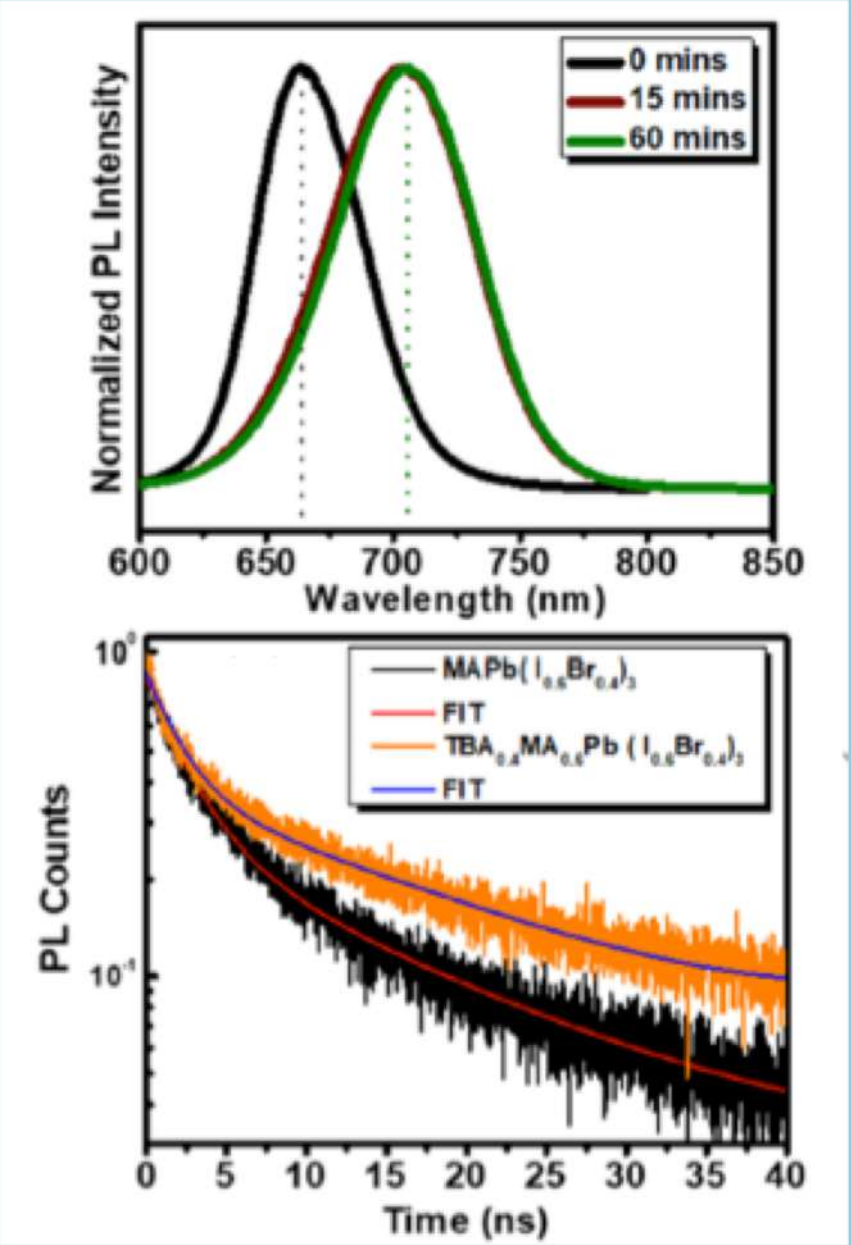

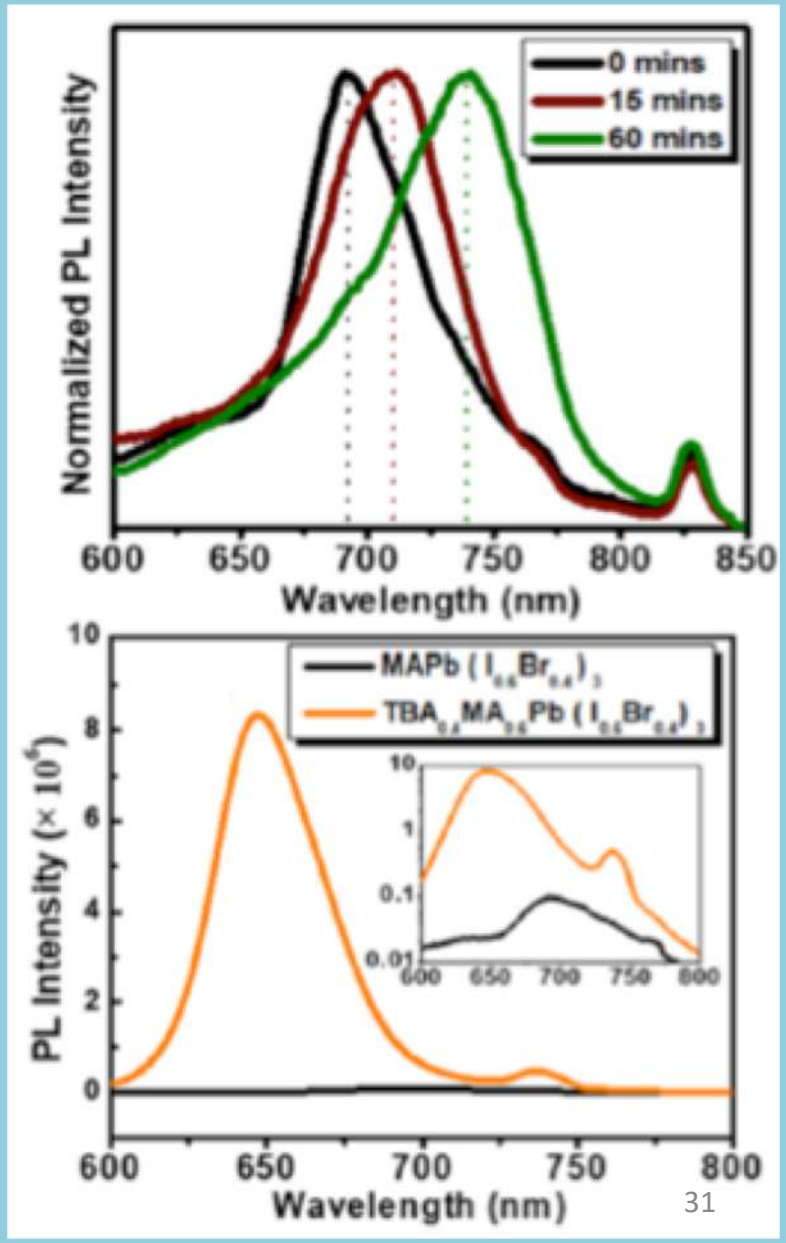

Low-temperature processing of optimally polymer-wrapped α-$CsPbI_3$ for self-powered flexible photo-detector application†

Umesh Bansode, Atikur Rahman* and Satishchandra Ogale *

α-$CsPbI_3$ is perhaps the most interesting candidate in this respect due to its significantly high thermal stability (> 300 C), and the right band gap of 1.73 eV, essential for tandem solar cells with silicon.

The processing temperature to form the cubic α-$CsPbI_3$ phase is > 300C. However, it is thermodynamically unstable at room temperature and gets converted to the yellow non-perovskite δ-phase (2.3 eV).

Unfortunately, the α-phase is also highly sensitive to moisture, getting converted to the δ form. Thus, it is a challenge to process the α-phase at low temperature and disallow its phase transformation at room temperature.

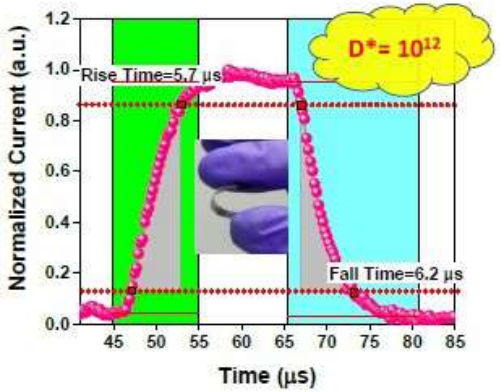

Polyvinylpyrrolidone (PVP) Wrapping

B. Li et al. *Nat. Commun.* 2018, **9**, 1076

Journal of Materials Chemistry C

Cite this: *J. Mater. Chem. C*, 2019, 7, 6986

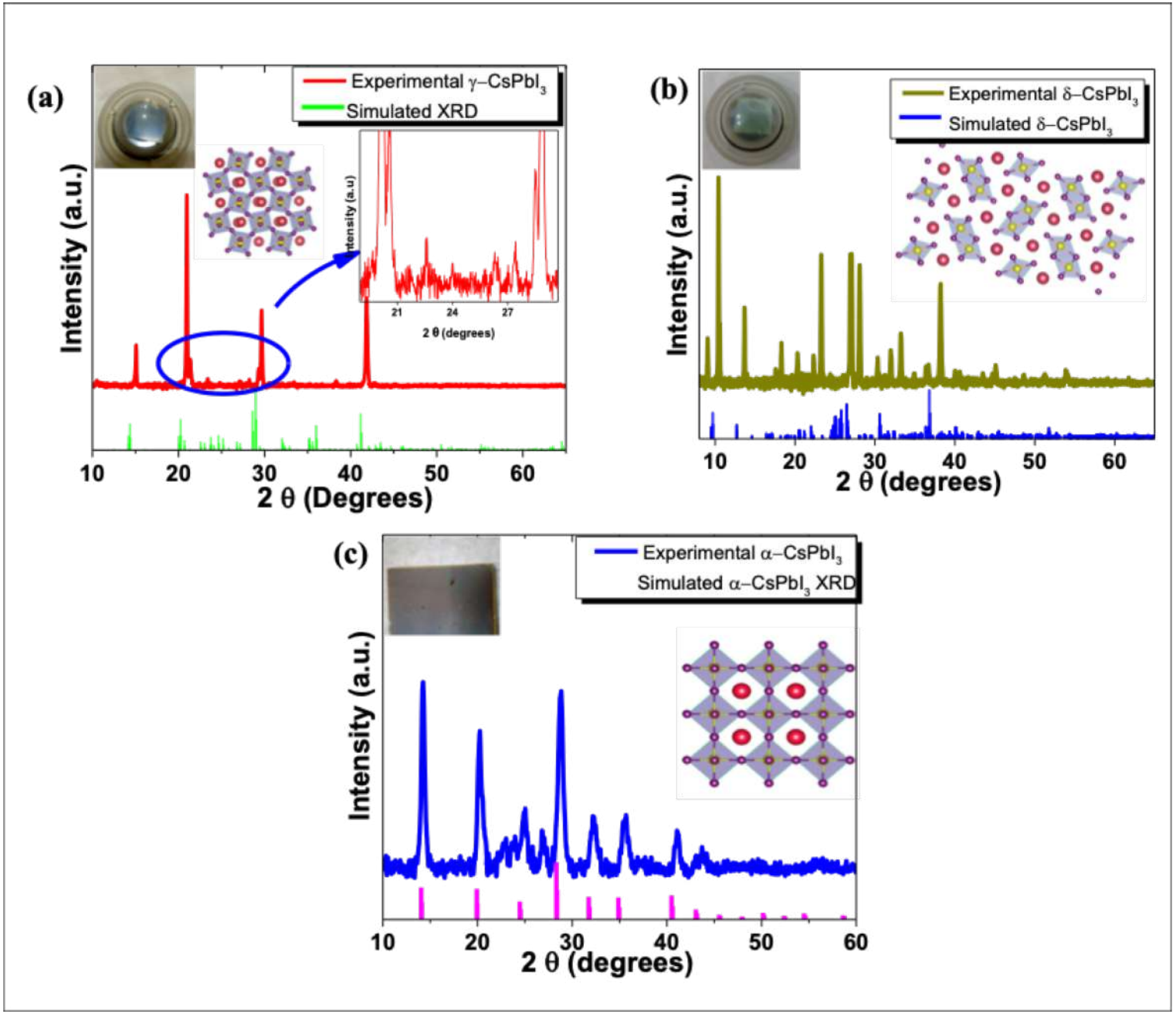
(a)
Experimental γ–CsPbI3
Simulated XRD
Intensity (a.u.)
2 θ (Degrees)
(b)
Experimental δ–CsPbI3
Simulated δ–CsPbI3
Intensity (a.u.)
2 θ (degrees)
(c)
Experimental α–CsPbI3
Simulated α–CsPbI3 XRD
Intensity (a.u.)
2 θ (degrees)

(a)

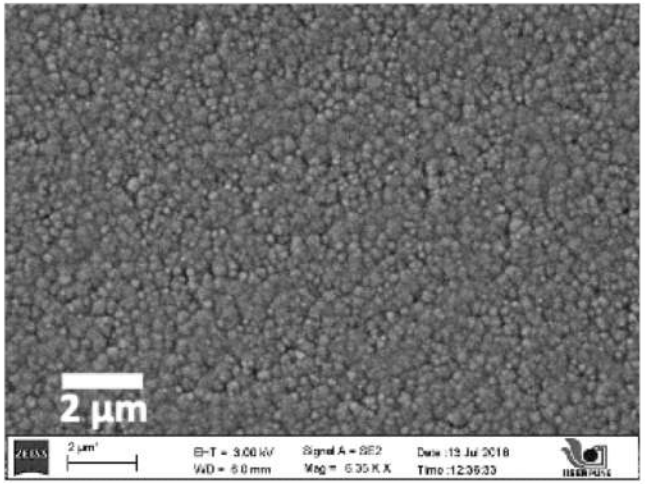

(b)

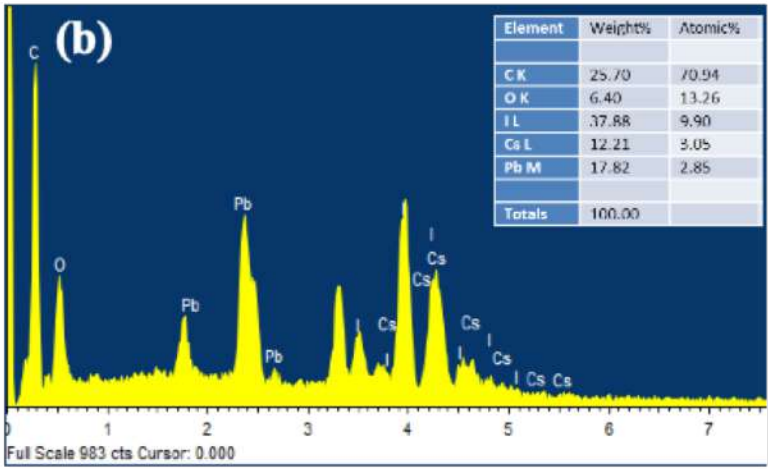

Element	Weight%	Atomic%
C K	25.70	70.94
O K	6.40	13.26
I L	37.88	9.90
Cs L	12.21	3.05
Pb M	17.82	2.85
Totals	100.00	

(c)

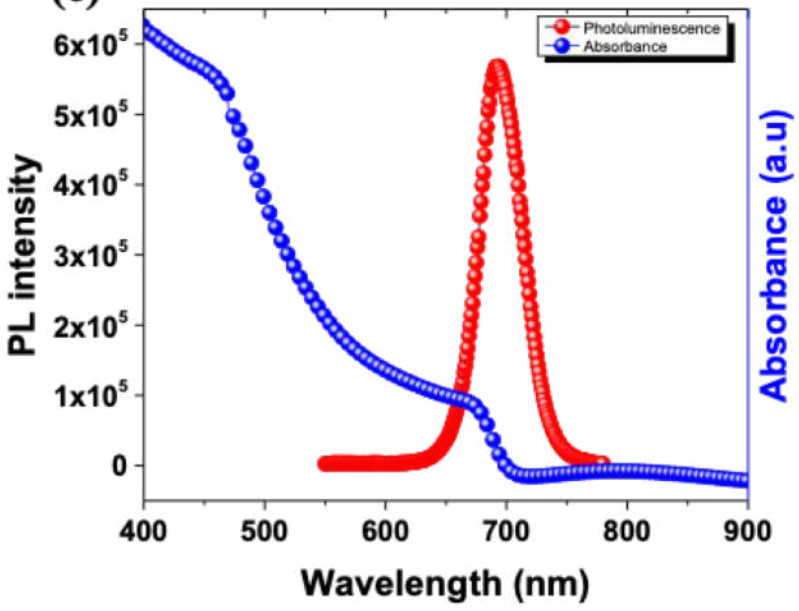

(d)

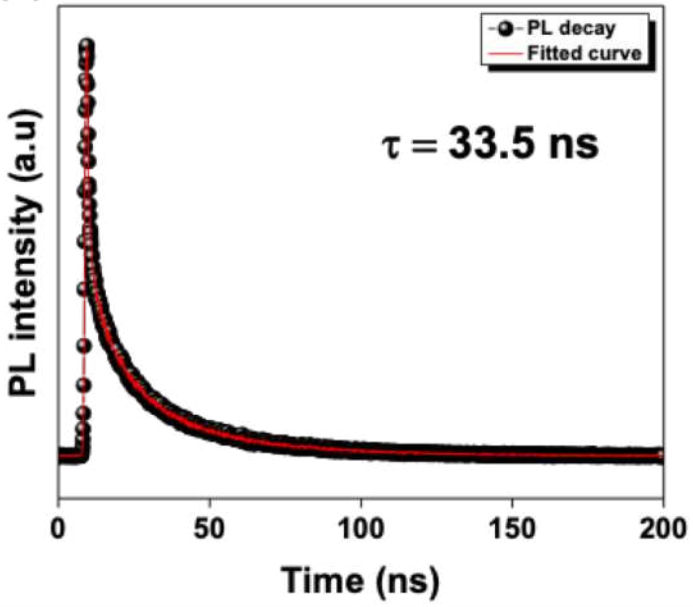

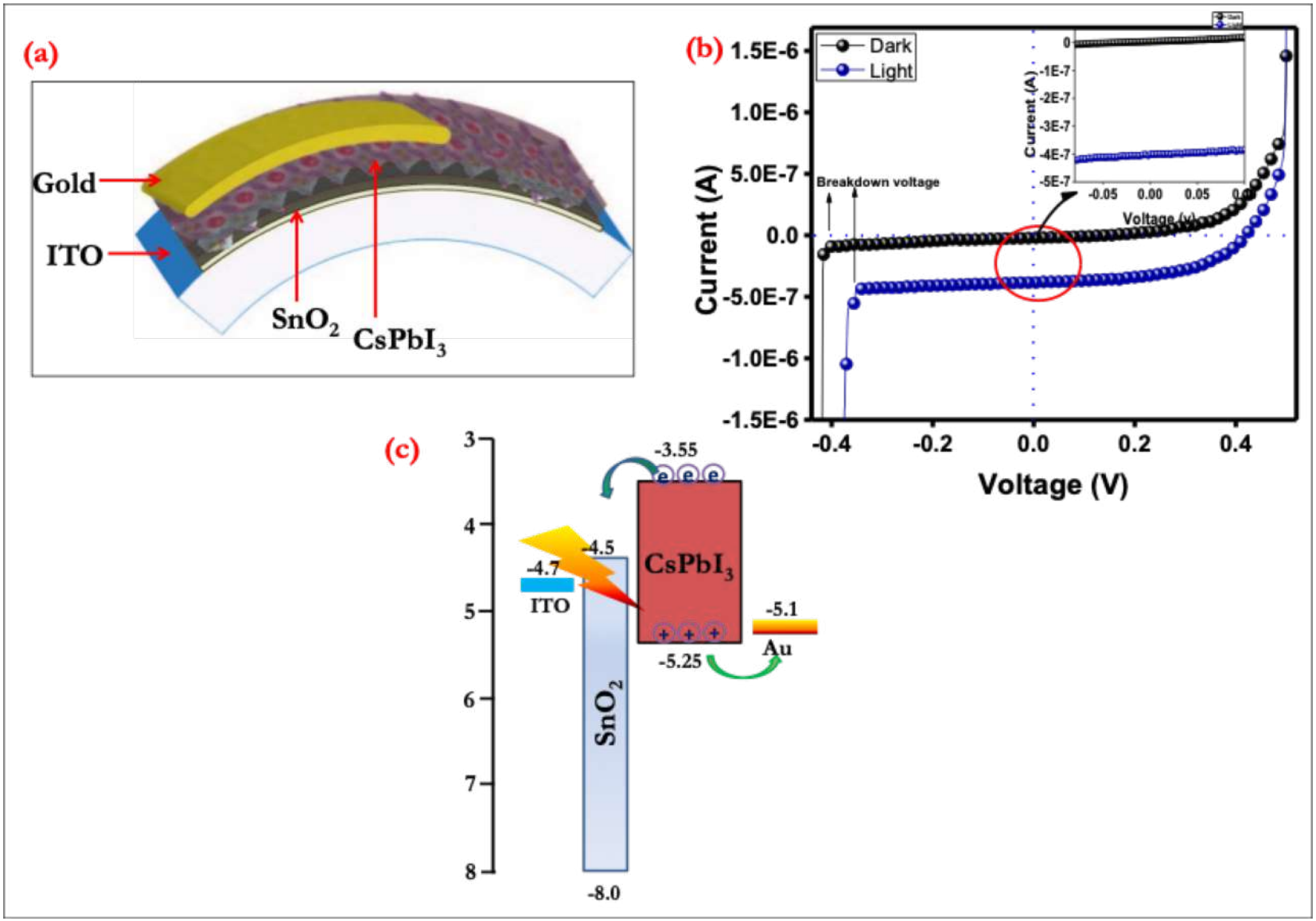
(a)
Gold
ITO
SnO2
CsPbI3
(b)
Dark
Light
Breakdown voltage
Current (A)
Voltage (V)
1.5E-6
1.0E-6
5.0E-7
0.0
-5.0E-7
-1.0E-6
-1.5E-6
-0.4
-0.2
0.0
0.2
0.4
(c)
-3.55
-4.5
-4.7
ITO
CsPbI3
-5.1
Au
-5.25
SnO2
-8.0
3
4
5
6
7
8

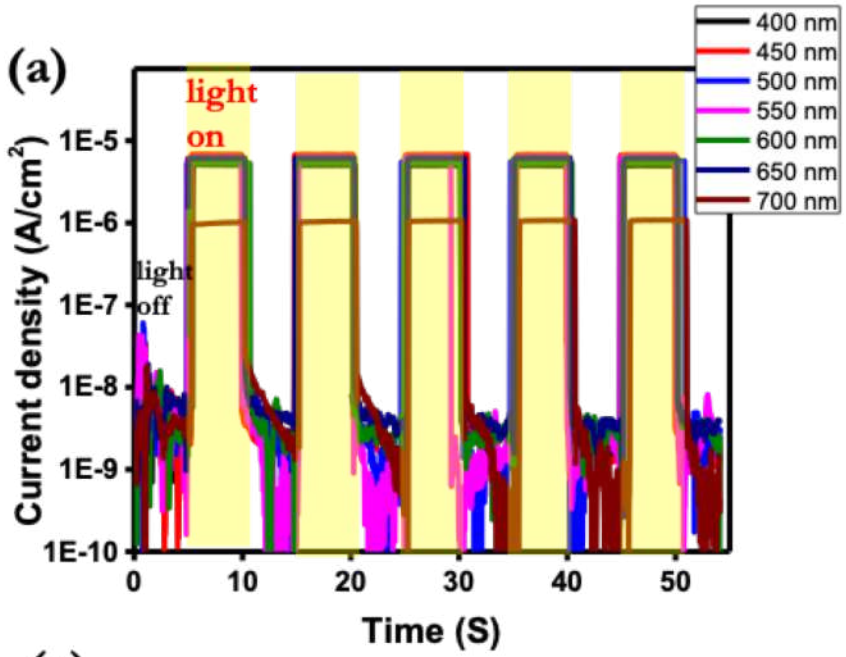
(a)
light on
light off
400 nm
450 nm
500 nm
550 nm
600 nm
650 nm
700 nm
Current density (A/cm2)
1E-5
1E-6
1E-7
1E-8
1E-9
1E-10
0
10
20
30
40
50
Time (S)

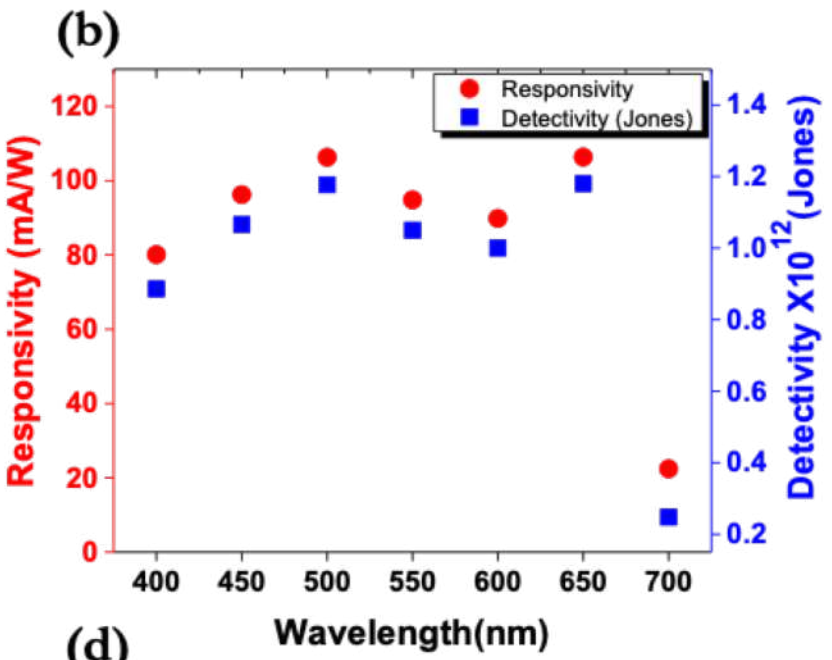
(b)
Responsivity
Detectivity (Jones)
Responsivity (mA/W)
Detectivity X10^12 (Jones)
120
100
80
60
40
20
0
1.4
1.2
1.0
0.8
0.6
0.4
0.2
400
450
500
550
600
650
700
Wavelength(nm)

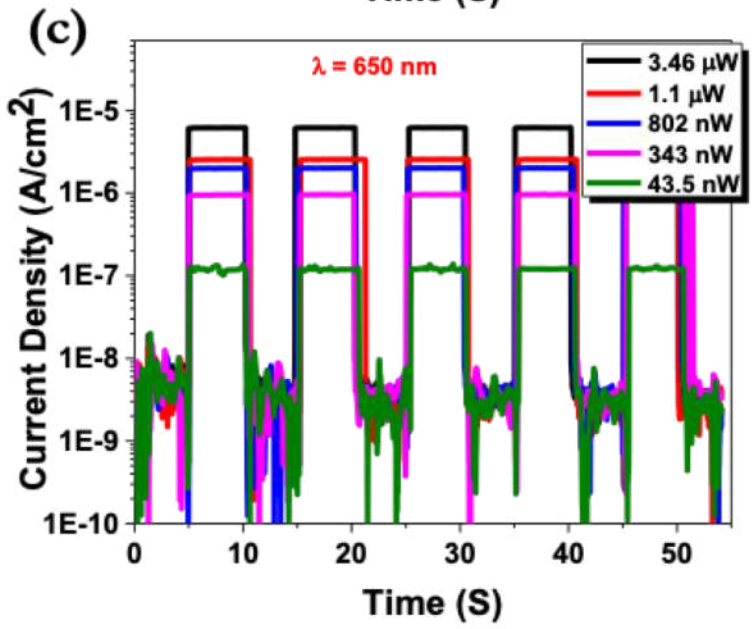
(c)
λ = 650 nm
3.46 μW
1.1 μW
802 nW
343 nW
43.5 nW
Current Density (A/cm2)
1E-5
1E-6
1E-7
1E-8
1E-9
1E-10
0
10
20
30
40
50
Time (S)

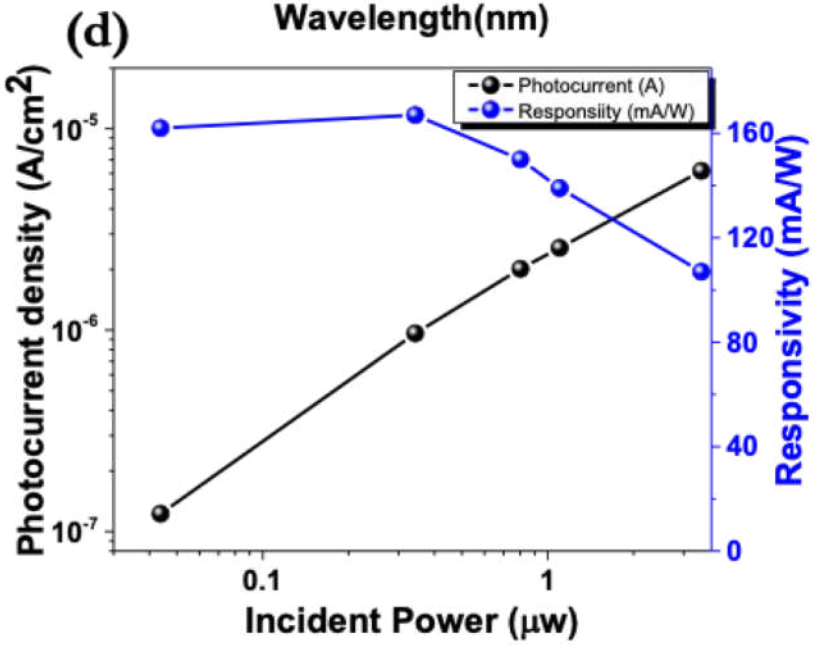
(d)
Photocurrent (A)
Responsiity (mA/W)
Photocurrent density (A/cm2)
10-5
10-6
10-7
160
120
80
40
0
Responsivity (mA/W)
0.1
1
Incident Power (μw)

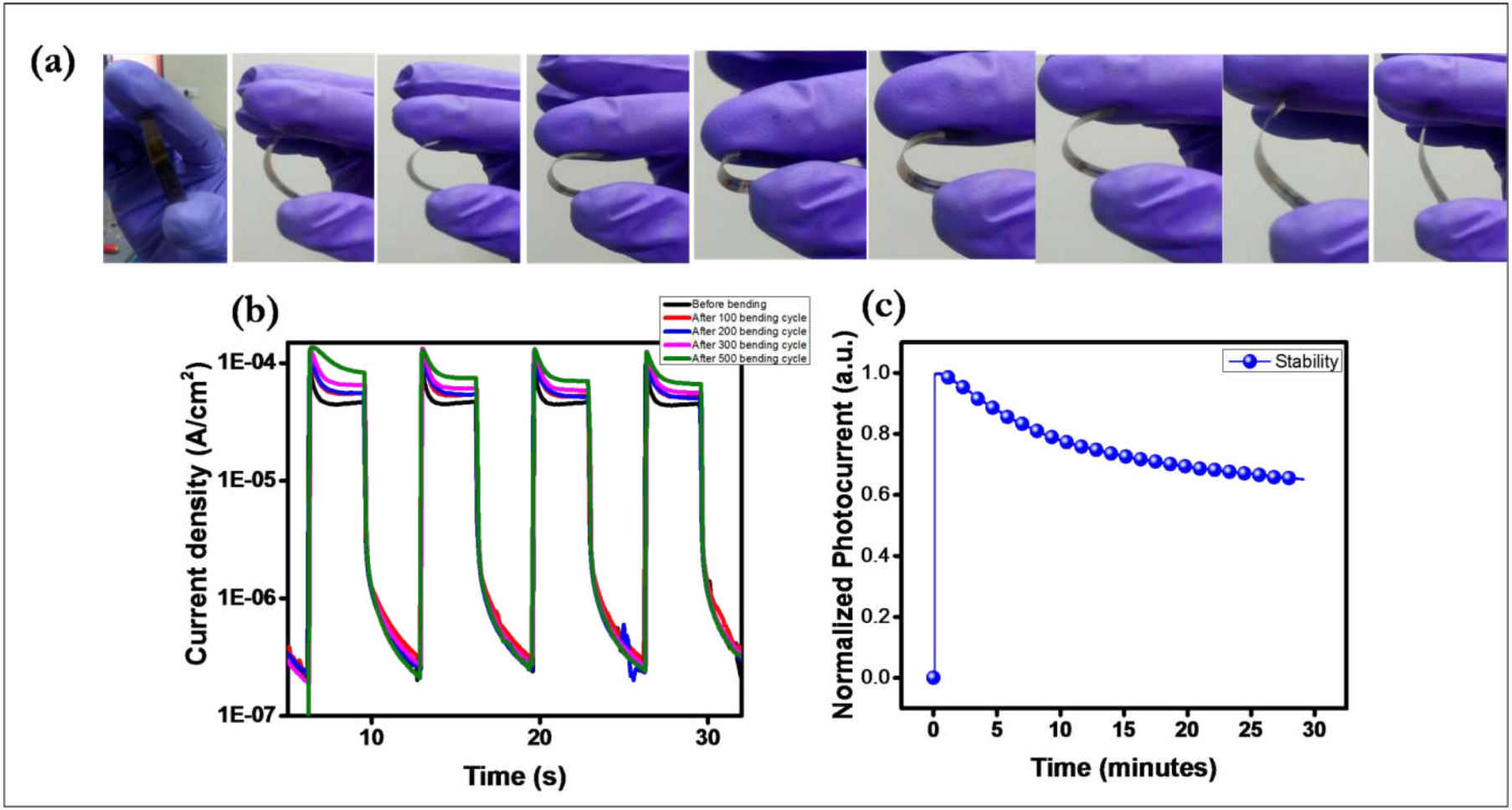
(a)
(b)
Before bending
After 100 bending cycle
After 200 bending cycle
After 300 bending cycle
After 500 bending cycle
Current density (A/cm²)
1E-04
1E-05
1E-06
1E-07
10
20
30
Time (s)
(c)
Stability
Normalized Photocurrent (a.u.)
1.0
0.8
0.6
0.4
0.2
0.0
0
5
10
15
20
25
30
Time (minutes)

Device	Flexible	Bias (V)	λ (nm)	R (A/W)	D* (Jones)	τ_r/ τ_f	Refs.
ITO/SnO_2/$CsPbI_3$/Au	Yes	0 V	400-700	>0.100	10^{12}	5.7/6.2 µs	This Work
Au/$CsPbI_3$/ Au	Yes	1 V	530	0.35	10^{10}	-	[68]
ITO/$CH_3NH_3PbI_3$/ITO	Yes	3 V	780	0.0367		100/100 ms	[60]
C/TiO_2/$MAPbI_3$/Spiro/ Au (#)	Yes	0 V	550	0.0169	10^{10}	200 /200 ms	[59]
ITO/$MAPbI_3$/ITO	Yes	1 V	400-760	81	10^{11}	230/280 µs	[67]
Au/PDOT:PSS/$MAPbI_3$/ PCBM/Al (#)	Yes	0 V	300-700	~100	-	4.1/3.3 µs	[58]
ITO/$CsPbBr_3$/ITO	Yes	10 V	442	0.64	-	19/24 µs	[57]
Carbon/TiO_2/$MAPbI_3$/ CuO/Cu_2O/Cu	Yes	0 V	350-850	0.56	10^{13}	<200/ <200 ms	[66]
Ni/GaN (NP)/Pt	Yes	0 V	400	0.03	10^{12}	100/100 ms	[62]
ZnO/Spiro-OMeTAD	Yes	0 V	365	$8X10^{-4}$	10^{9}	160/200ms	[61]
ITO/ZnO/$CsPbI_3$(NP) /P3HT/MoO_3/Ag (#)	No	0.5V	400-700		10^{12}	-	[70]
Au/$CsPbI_3$/Au	No	2 V	405	2.9 X 10^3	10^{13}	50/150 µs	[69]
ITO/SnO_2/$CsPbBr_3$/ Spiro/ Au (#)	No	0	465	0.172	10^{12}	140/120 µs	[65]
PDOT:PSS/ $(FASnI_3)_{0.6}(MAPbI_3)_{0.4}$/ C_{60}PCB/Al (#)	No	0.2 V	300-1000	0.4	10^{12}	6.9/9.1 µs	[64]
Au/$CsPbI_3$(NP)/Au	No	3 V	425-655	-	-	24/29 ms	[63]

IISER PUNE

CENTRE FOR ENERGY SCIENCE

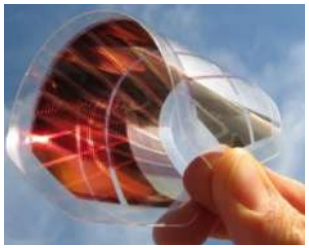

THE JOURNAL OF PHYSICAL CHEMISTRY C

Article

Cite This: J. Phys. Chem. C 2018, 122, 4802−4808

pubs.acs.org/JPCC

Flex-Mode Mechatronic Functionality of Lead Iodide Hybrid Perovskite Systems

Aniruddha Basu, Prachi Kour, Swati Parmar, Rounak Naphade,* and Satishchandra Ogale*

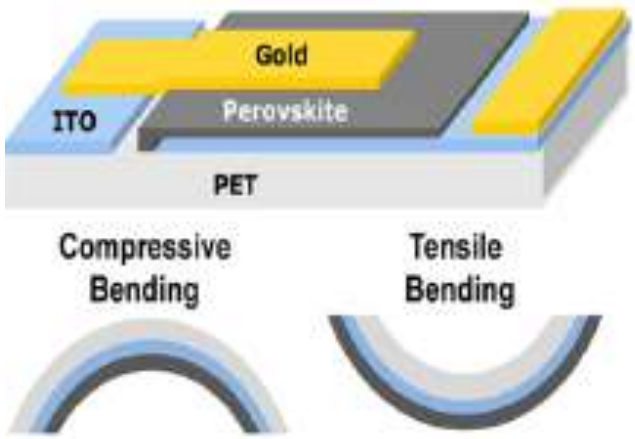

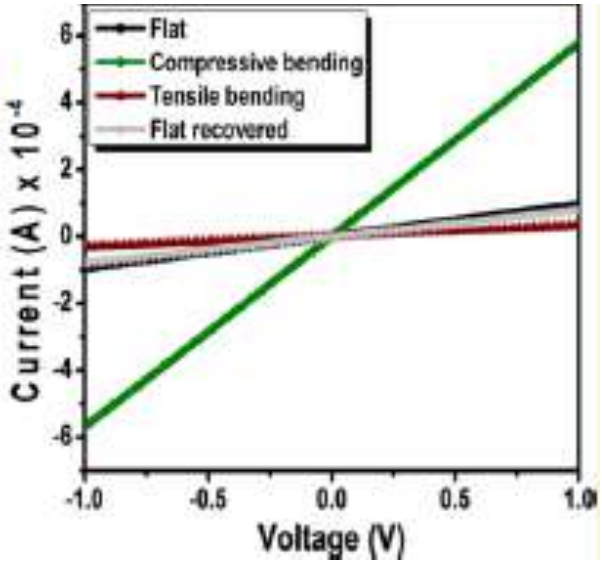

J. Phys. Chem. C 2018, 122, 4802−4808

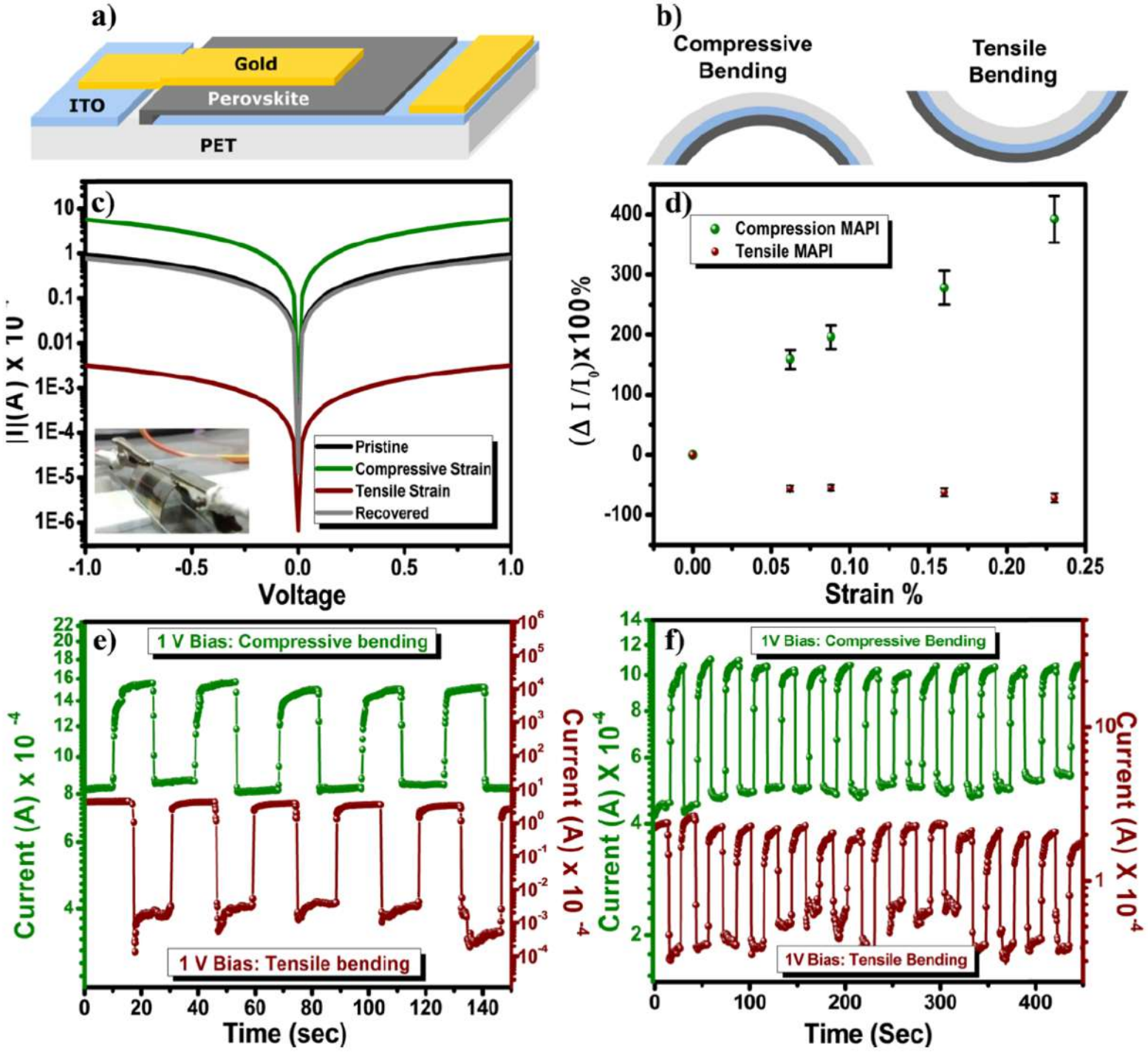
a)
Gold
Perovskite
ITO
PET
b)
Compressive Bending
Tensile Bending
c)
|I|(A) x 10
Pristine
Compressive Strain
Tensile Strain
Recovered
Voltage
d)
Compression MAPI
Tensile MAPI
(Δ I /I0)x100%
Strain %
e)
1 V Bias: Compressive bending
1 V Bias: Tensile bending
Current (A) x 10 -4
Time (sec)
f)
1V Bias: Compressive Bending
1V Bias: Tensile Bending
Current (A) X 10 -4
Time (Sec)

Device Characteristics for large grain $MAPbI_3$ film

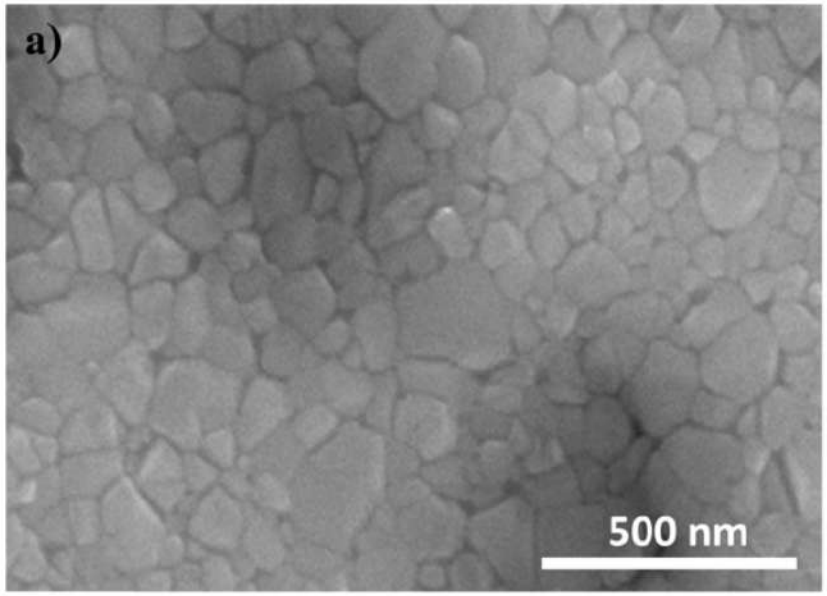

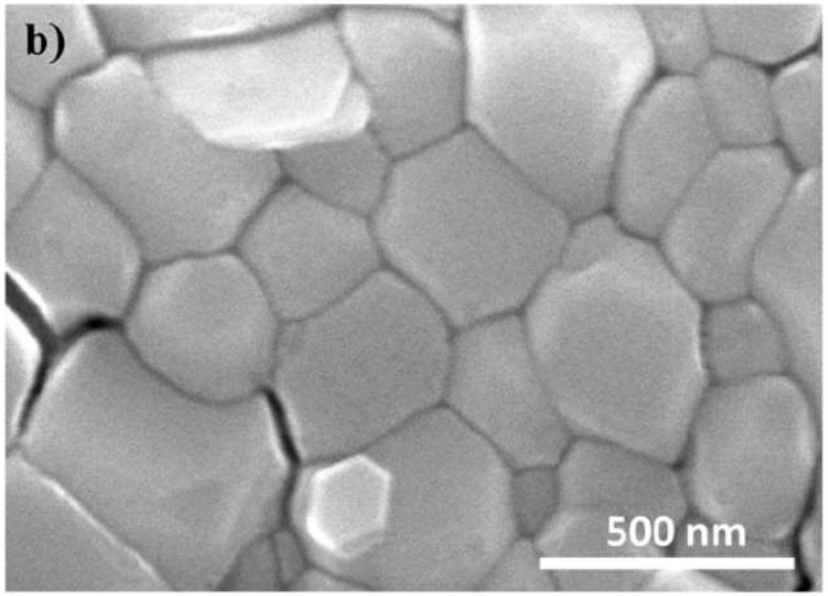

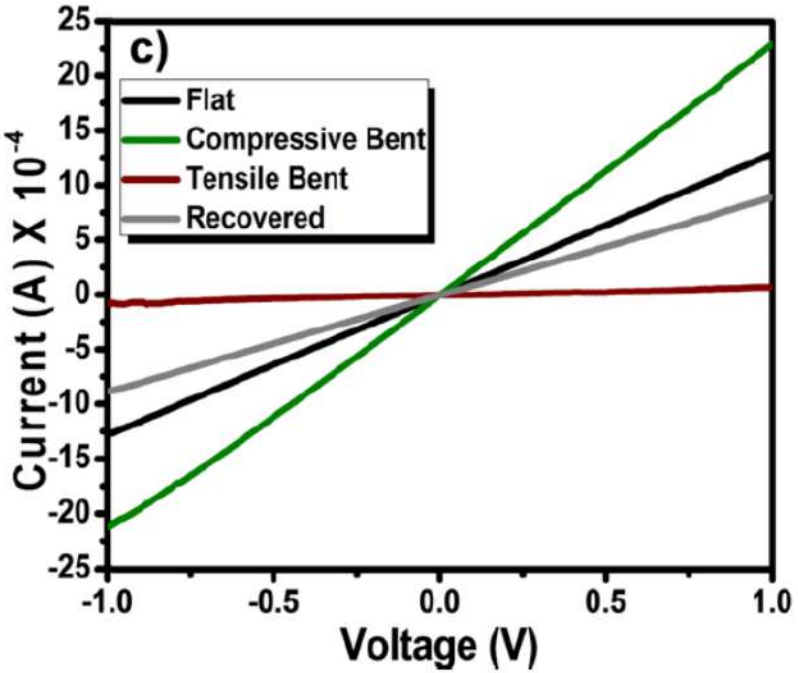

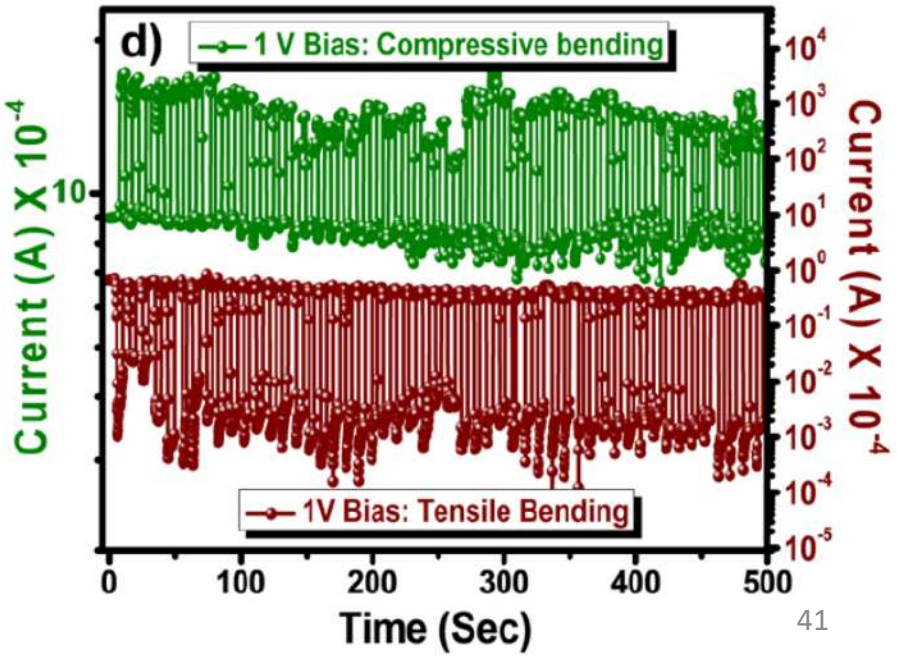

Material Characterization

XRD

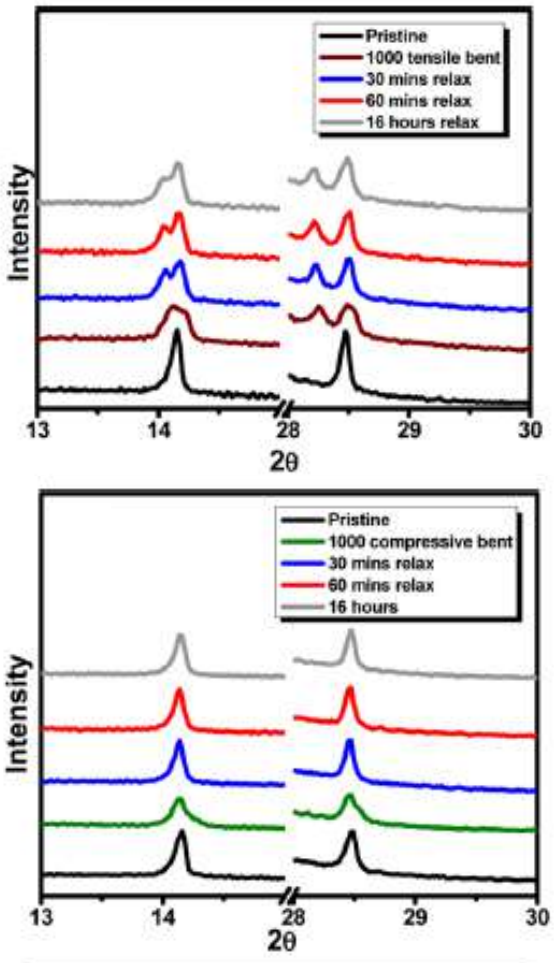

Raman

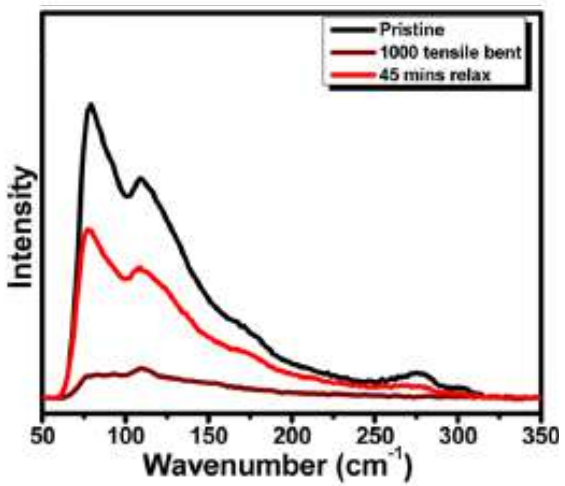

PL

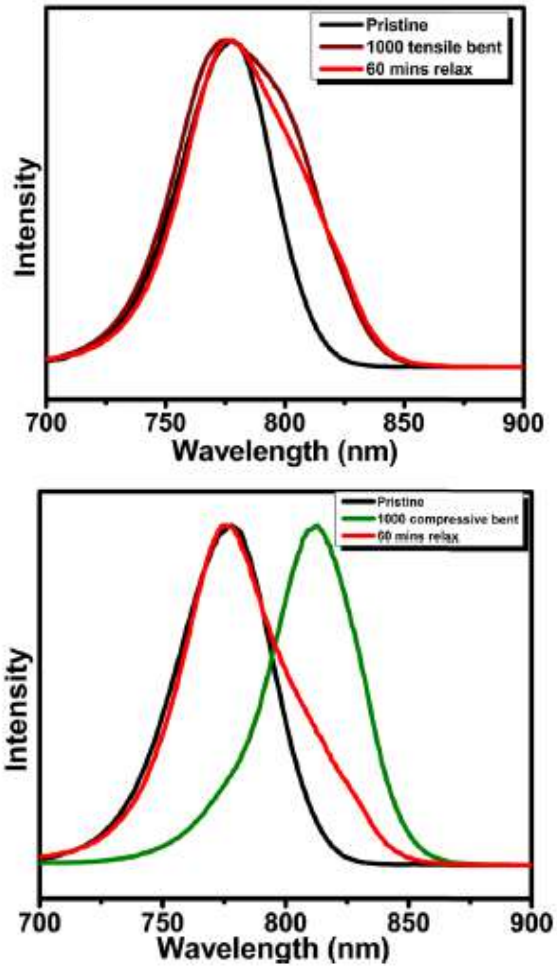

Molecular Ion Substitution at Anion Site

$CH_3NH_3PbI_{(3-x)}(BF_4)_x$: molecular ion substituted hybrid perovskite†

Chem. Comm., 2014, 50, 9741

Satyawan Nagane,*[ab] Umesh Bansode,[ab] Onkar Game,[ab] Shraddha Chhatre[ab] and Satishchandra Ogale*[ab]

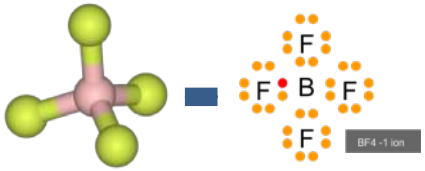

Strategy to incorporate electron withdrawing "fluorine" within the perovskite structure

- **It is difficult to have fluorine in hybrid perovskite structure.**
- **Incorporation of fluorine via organic precursor is difficult because of its small ionic radius.**
- **Incorporation of Fluorine via molecular ion (BF_4^-) is possible because of its nearly same ionic radius as of Iodine.**
- **Ionic radius of BF_4^- : 0.218 nm Ionic radius of I^- : 0.220nm Ionic radius of F^- : 0.136nm**

$CH_3NH_3BF_4$ prepared using methyl amine and tetrafluoroboric acid solutions

Perovskite synthesis protocol

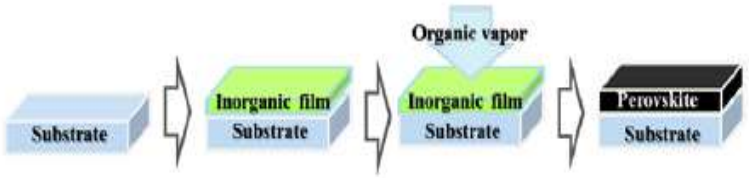

Yang Yang and coworkers J. Am. Chem. Soc. 2014, 136, 622−625

Perovskite synthesis

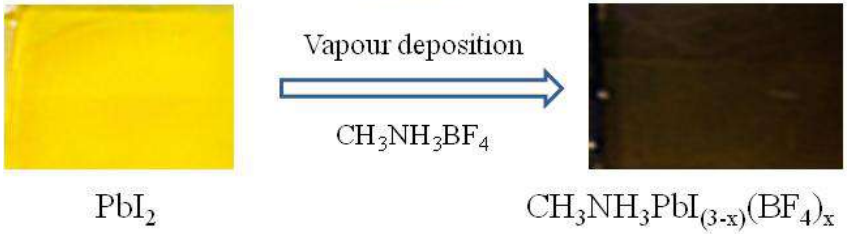

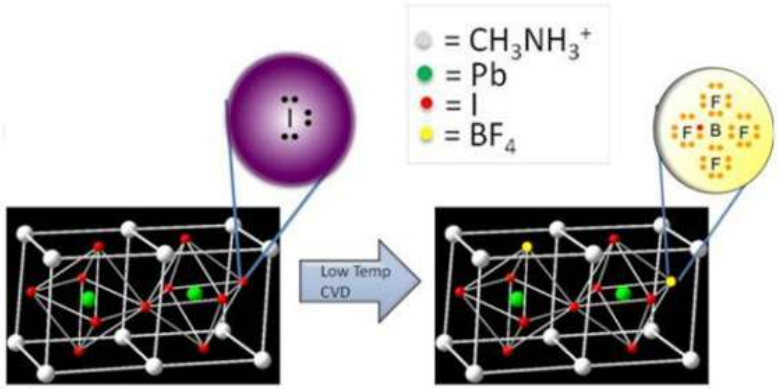

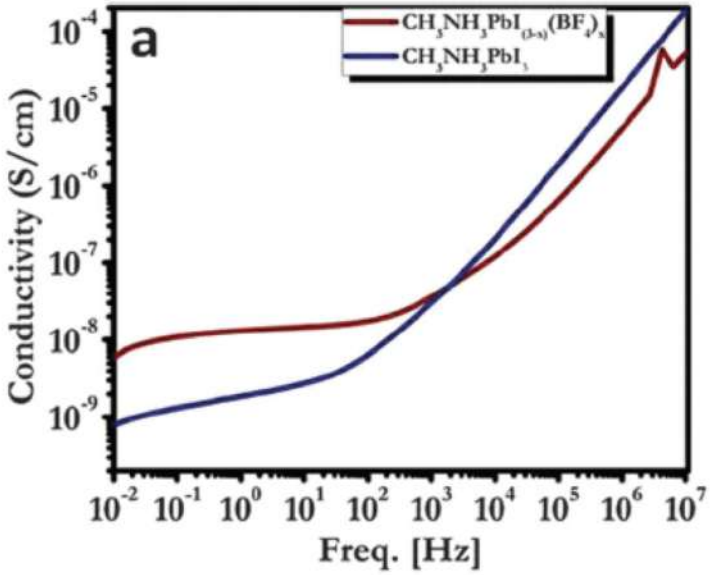

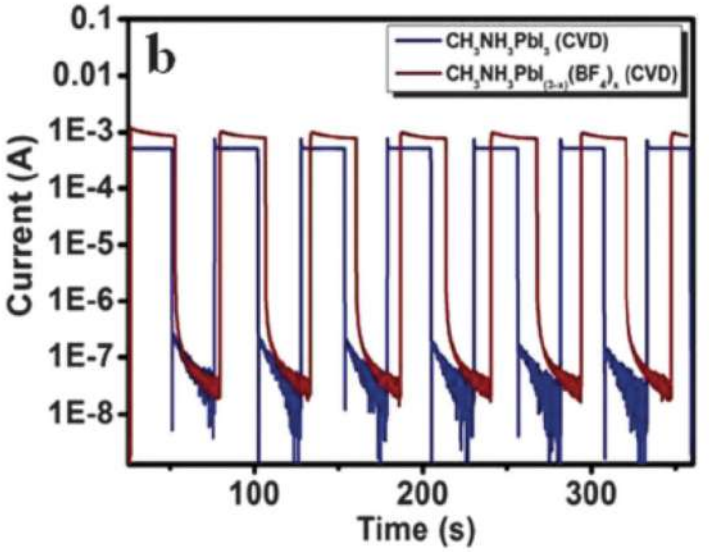

THE JOURNAL OF PHYSICAL CHEMISTRY Letters

Letter

pubs.acs.org/JPCL

$CH_3NH_3Pb(BF_4)_3$ and $(C_4H_9NH_3)_2Pb(BF_4)_4$ Family of 3D and 2D Perovskites without and with Iodide and Bromide Ions Substitution

Satyawan Nagane*,†,‡ and Satishchandra Ogale*,‡,§

Methyl Ammonium tetrafluoro borate

70 ^{0}C

$Pb(OAc)_2$ (DMSO) + $CH_3NH_3BF_4$ (IPA) → $CH_3NH_3Pb(BF_4)_3$

$Pb(NO_3)_2$ (DMSO) + $CH_3NH_3BF_4$ (IPA) → $CH_3NH_3Pb(BF_4)_3$

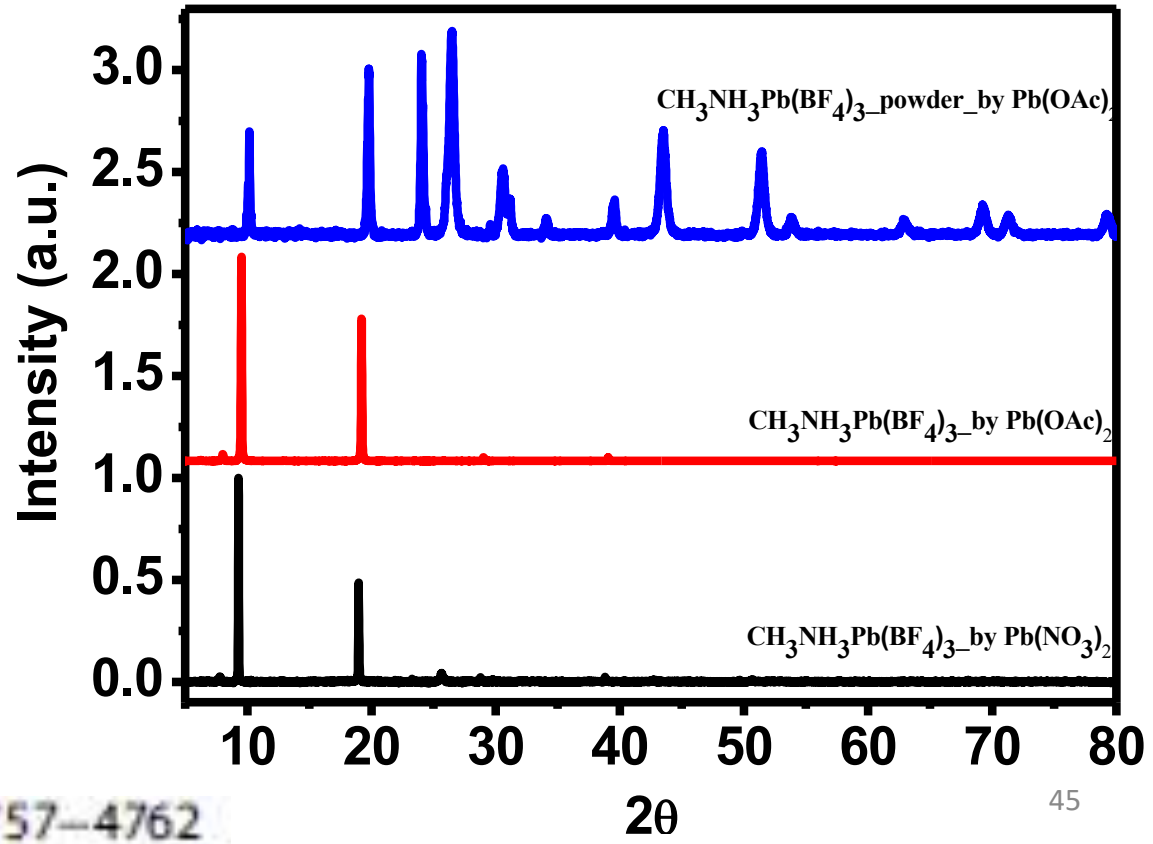

J. Phys. Chem. Lett. 2016, 7, 4757−4762

Butyl Ammonium tetrafluoro borate

70 ^{0}C

$Pb(OAc)_2/Pb(NO_3)_2 + C_4H_9NH_3BF_4$
(DMSO) (IPA)
$\downarrow$
$C_4H_9NH_3Pb(BF_4)_4$

$PbBr_2 + C_4H_9NH_3BF_4$
(DMF) (IPA)
$\downarrow$
$C_4H_9NH_3PbBr_{(4-x)}(BF_4)_x$

$PbI_2 + C_4H_9NH_3BF_4$
(DMF) (IPA)
$\downarrow$
$C_4H_9NH_3PbI_{(4-x)}(BF_4)_x$

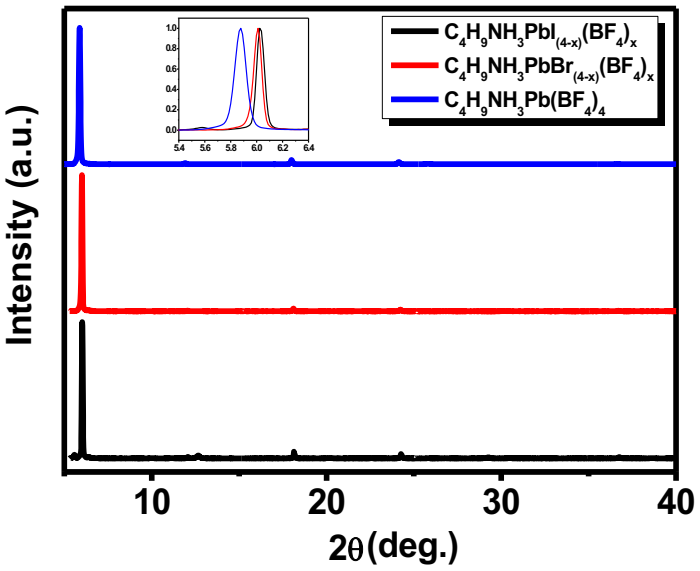

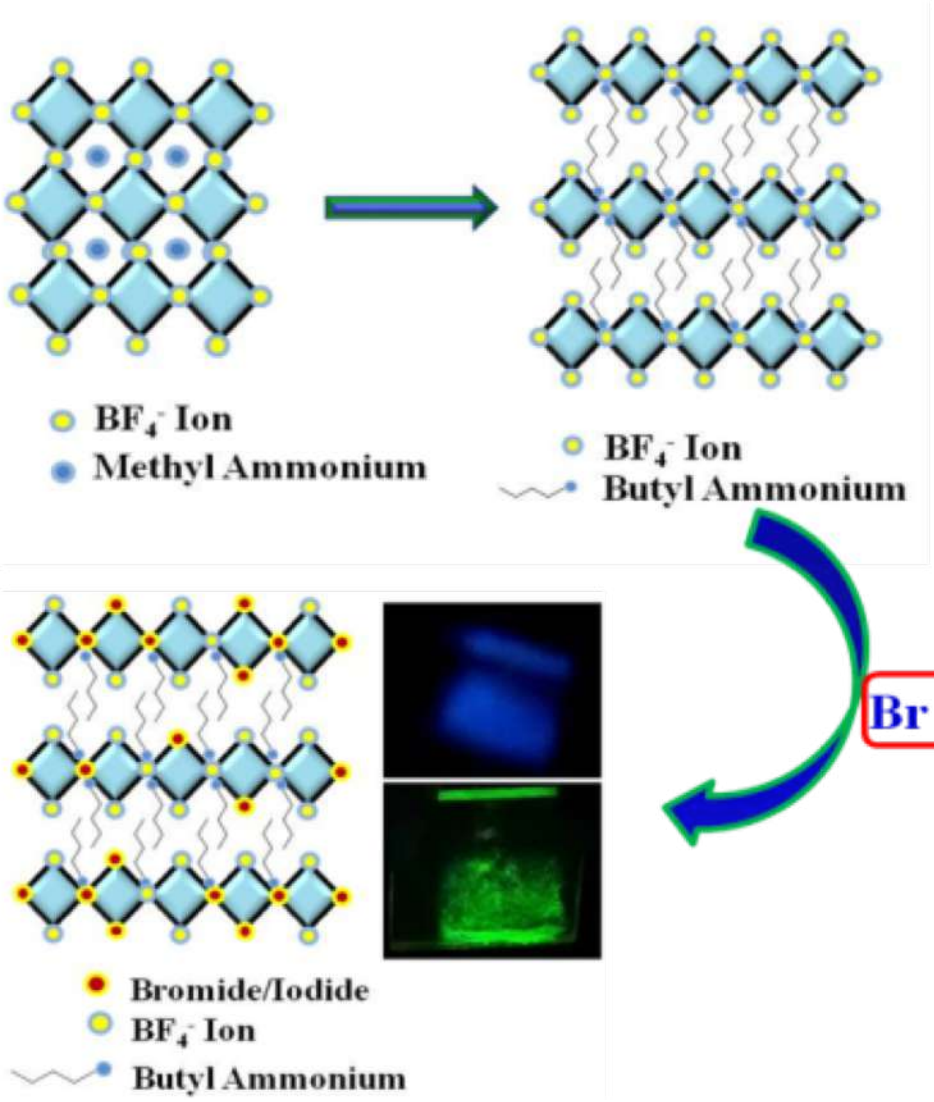

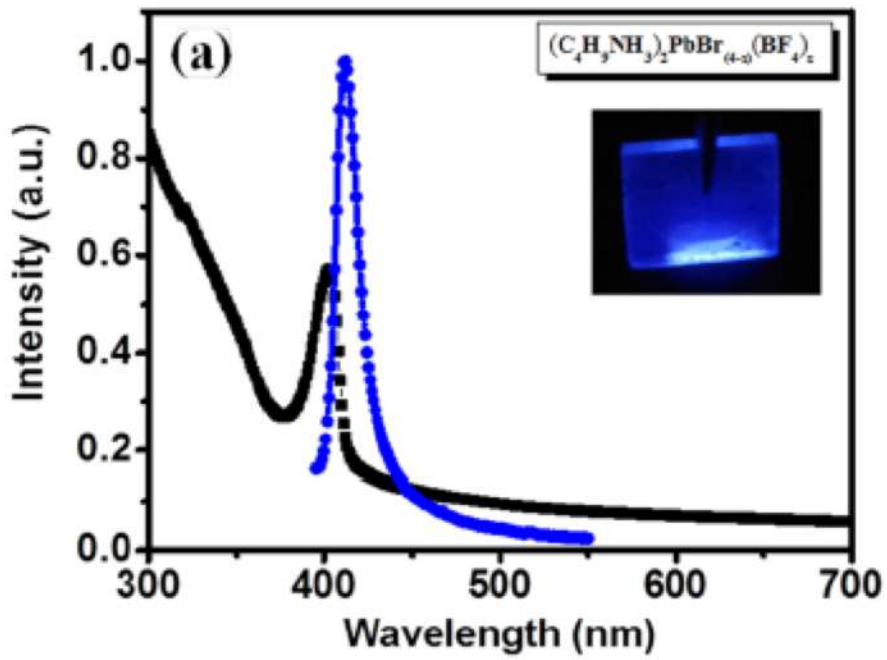
(a)
$(C_4H_9NH_3)_2PbBr_{(4-x)}(BF_4)_x$
Intensity (a.u.)
Wavelength (nm)

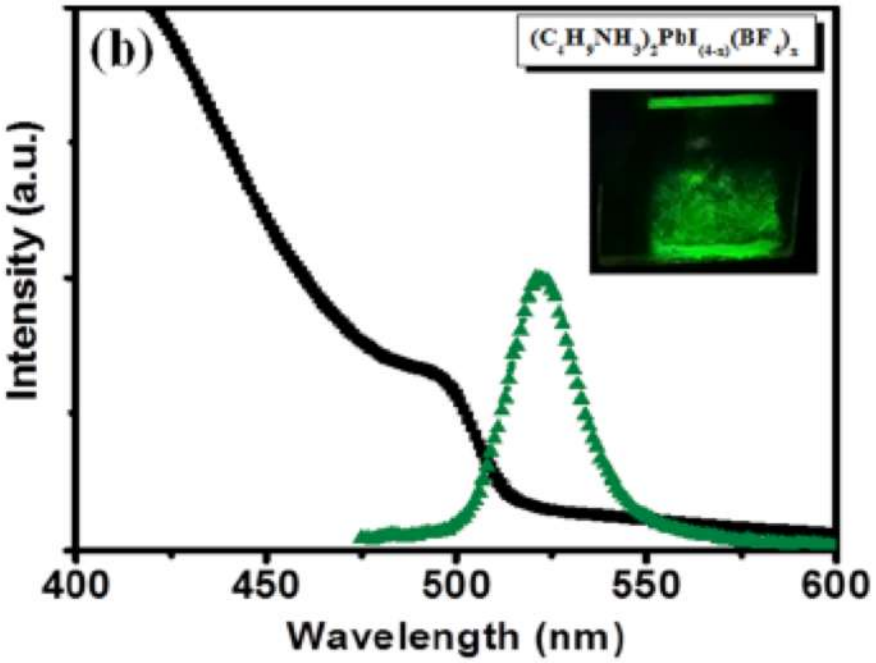
(b)
$(C_4H_9NH_3)_2PbI_{(4-x)}(BF_4)_x$
Intensity (a.u.)
Wavelength (nm)

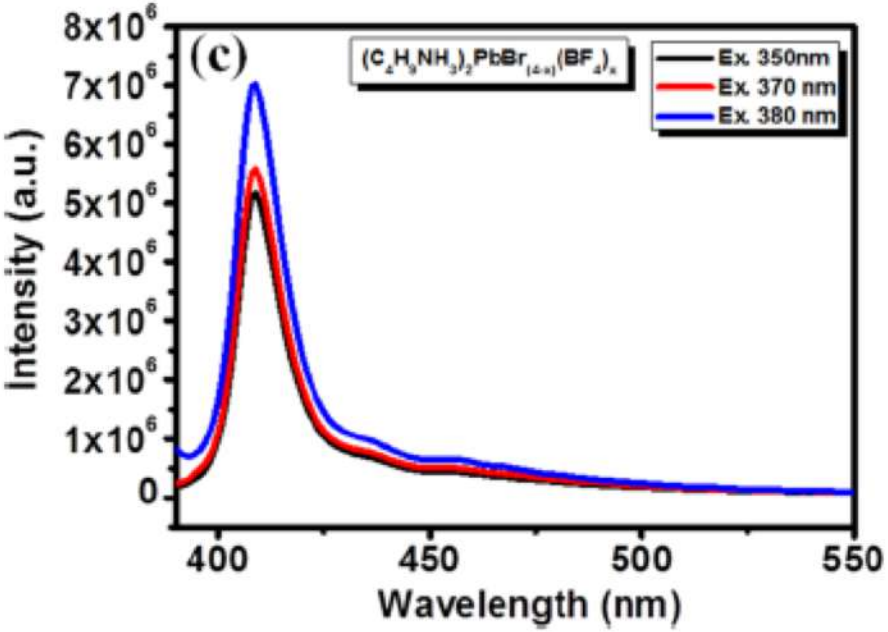
(c)
$(C_4H_9NH_3)_2PbBr_{(4-x)}(BF_4)_x$
Ex. 350nm
Ex. 370 nm
Ex. 380 nm
Intensity (a.u.)
Wavelength (nm)

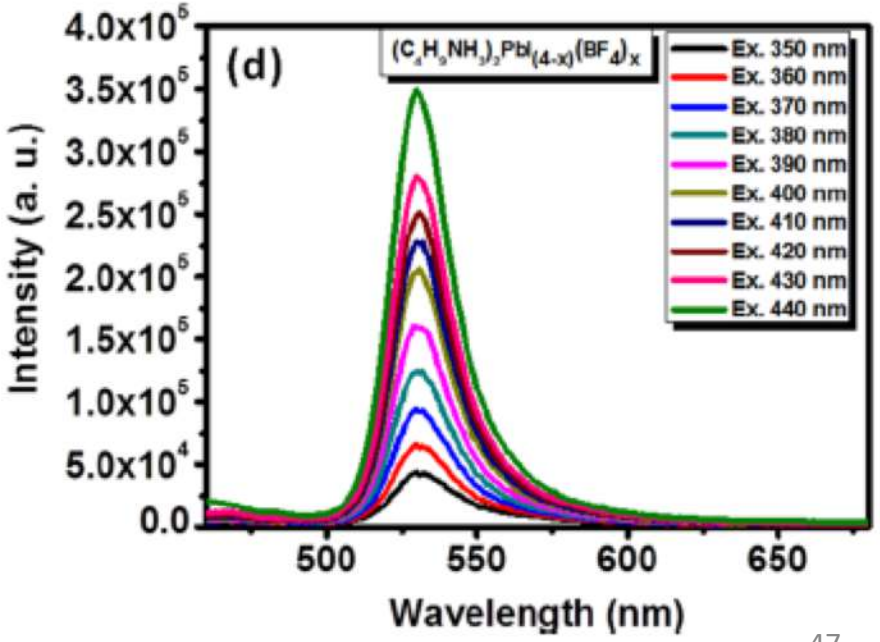
(d)
$(C_4H_9NH_3)_2PbI_{(4-x)}(BF_4)_x$
Ex. 350 nm
Ex. 360 nm
Ex. 370 nm
Ex. 380 nm
Ex. 390 nm
Ex. 400 nm
Ex. 410 nm
Ex. 420 nm
Ex. 430 nm
Ex. 440 nm
Intensity (a. u.)
Wavelength (nm)

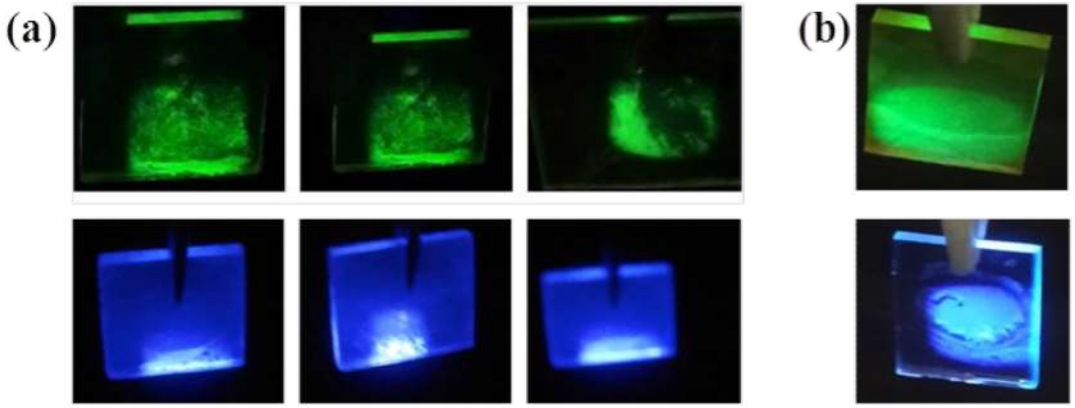
(a)
(b)

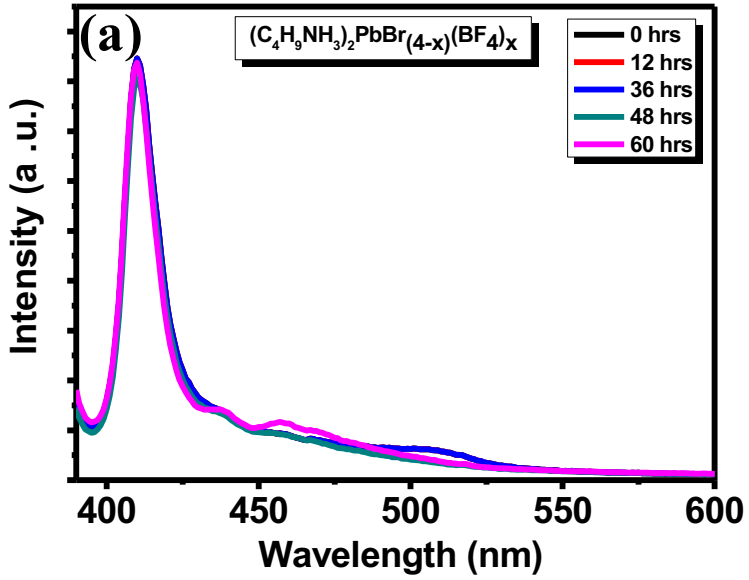
(a)
$(C_4H_9NH_3)_2PbBr_{(4-x)}(BF_4)_x$
0 hrs
12 hrs
36 hrs
48 hrs
60 hrs
Intensity (a .u.)
400
450
500
550
600
Wavelength (nm)

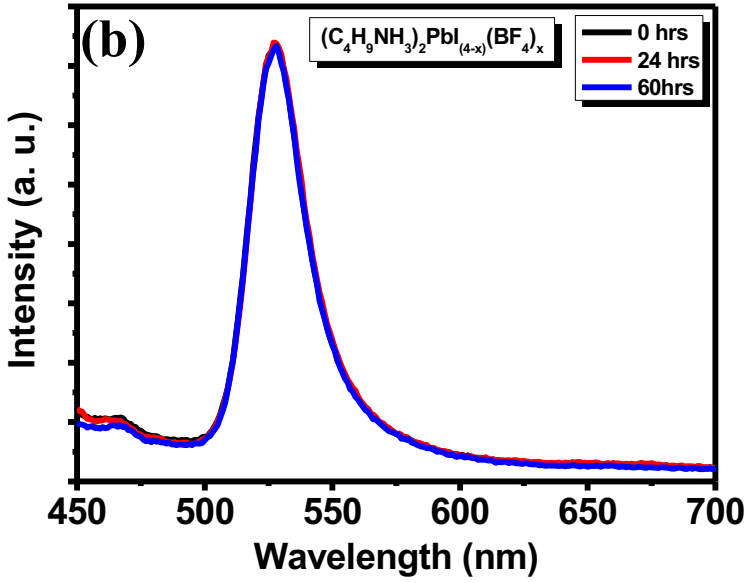
(b)
$(C_4H_9NH_3)_2PbI_{(4-x)}(BF_4)_x$
0 hrs
24 hrs
60hrs
Intensity (a. u.)
450
500
550
600
650
700
Wavelength (nm)

Broadband Luminescence

White LEDs

JACS
JOURNAL OF THE AMERICAN CHEMICAL SOCIETY

Communication

Self-Assembly of Broadband White-Light Emitters

Emma R. Dohner.[†] Eric T. Hoke.[‡] and Hemamala I. Karunadasa*,[†]

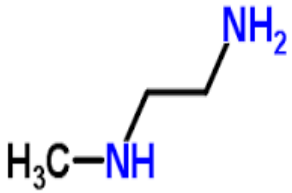

N-methylethane-1,2-diammine(N-MEDA)

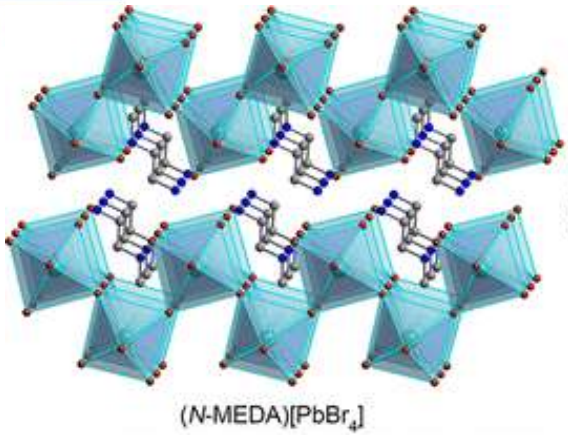

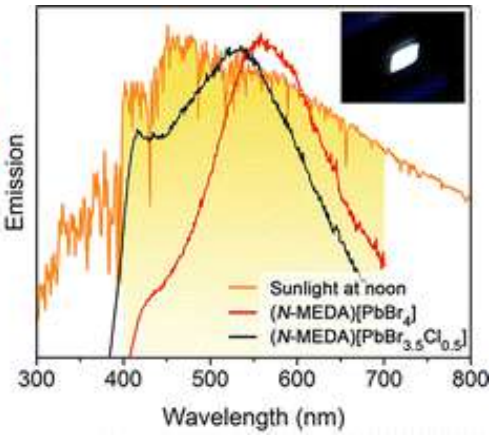

Ref. *J. Am. Chem. Soc.*, **2014**, *136* (5), pp 1718–1721

JACS
JOURNAL OF THE AMERICAN CHEMICAL SOCIETY

Communication

pubs.acs.org/JACS

Intrinsic White-Light Emission from Layered Hybrid Perovskite

Emma R. Dohner,[†] Adam Jaffe,[†] Liam R. Bradshaw,[§] and Hemamala I. Karunadasa*,[†]

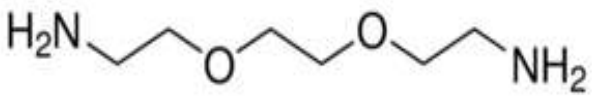

2,2′-(Ethylenedioxy) bis(ethylammine) [EDBE]

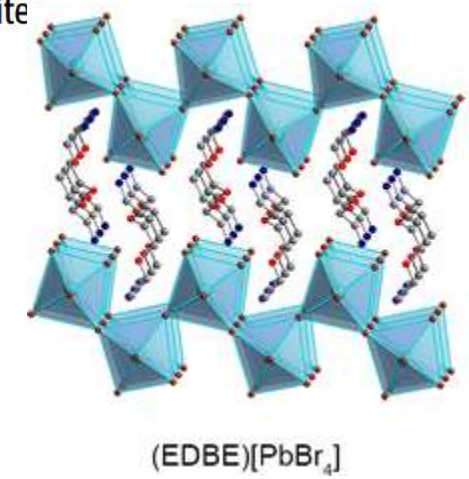

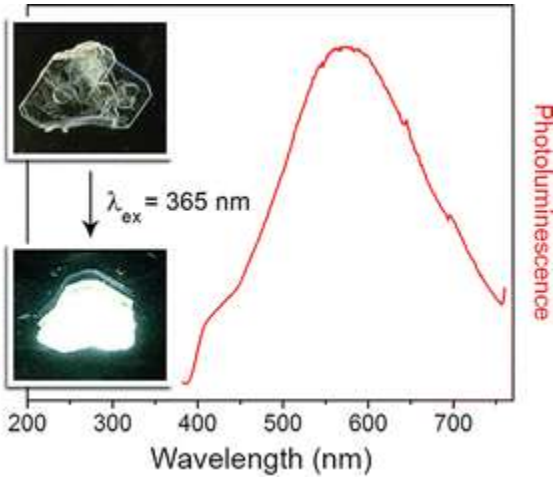

Ref. *J. Am. Chem. Soc.*, **2014**, *136* (38), pp 13154–13157

From the journal:
Chemical Science

Structural origins of broadband emission from layered Pb–Br hybrid perovskites

Matthew D. Smith,[a] Adam Jaffe,[a] Emma R. Dohner,[a] Aaron M. Lindenberg[b] and Hemamala I. Karunadasa*[a]

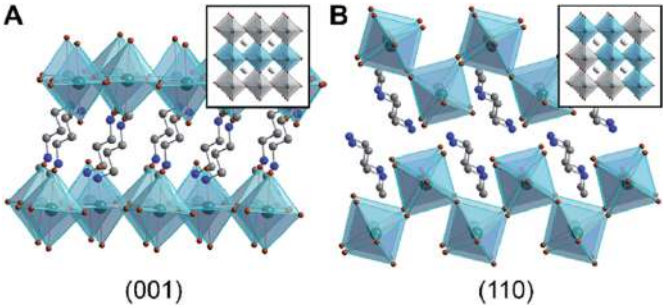

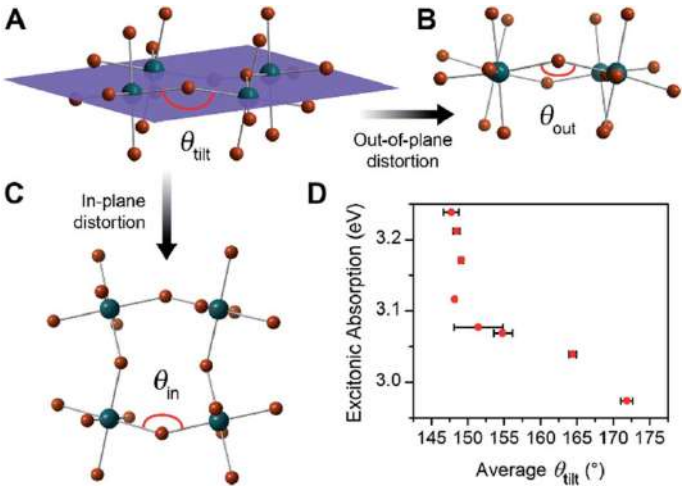

Ref. Chem. Sci., 2017,**8**, 4497-4504

J|A|C|S
JOURNAL OF THE AMERICAN CHEMICAL SOCIETY

White-light Emission and Structural Distortion in New Corrugated 2D Lead Bromide Perovskites

Lingling Mao, Yilei Wu, Constantinos C. Stoumpos, Michael R. Wasielewski, and Mercouri G. Kanatzidis

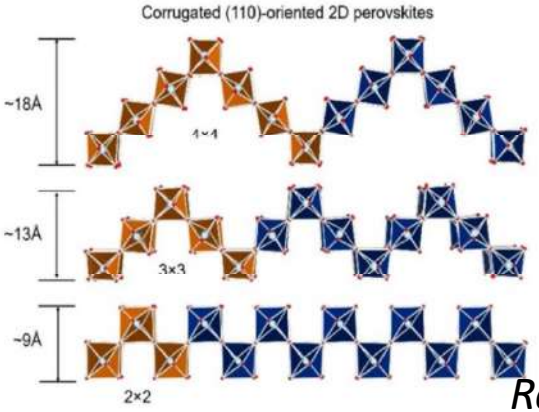

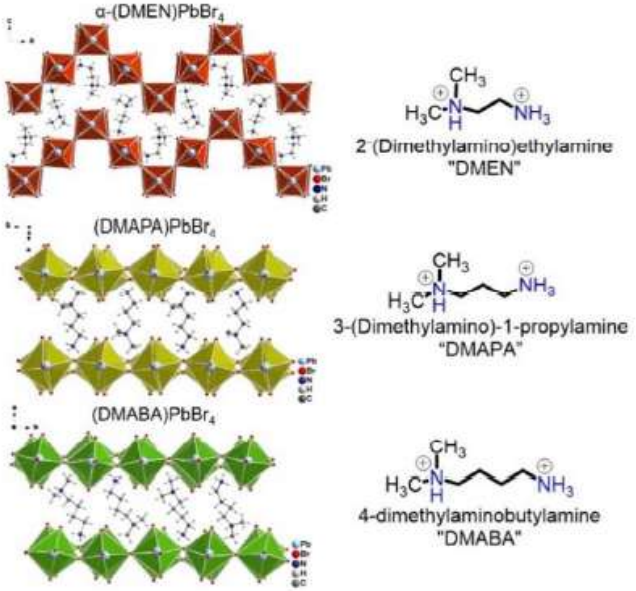

Ref. J. Am. Chem. Soc., **2017**, *139* (14), pp 5210–5215

FULL PAPER
Hybrid Perovskites
ADVANCED OPTICAL MATERIALS
www.advopticalmat.de

Molecular and Self-Trapped Excitonic Contributions to the Broadband Luminescence in Diamine-Based Low-Dimensional Hybrid Perovskite Systems

Shrreya Krishnamurthy, Rounak Naphade, Wasim J. Mir, Suresh Gosavi, Sudip Chakraborty, Ramanathan Vaidhyanathan,* and Satishchandra Ogale**

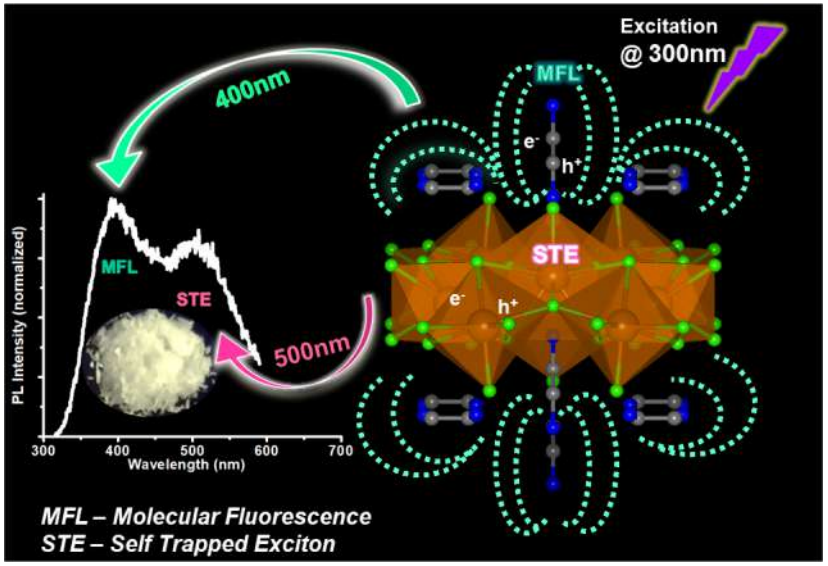

ADVANCED OPTICAL MATERIALS
Adv.Optical Mater. 2018,1800751

Structural Study (Single Crystal XRD)

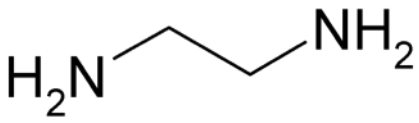

(a) System 1 : 1D ribbon perovskite [$P2_1/n$] – Ethylene diamine

$(H_3N\text{-}CH_2\text{-}CH_2\text{-}NH_3)_8(Pb_4Br_{18}) \cdot Br_6$

(b) System 2 : 2D twisted layered perovskite [*Pbcm*] - – Ethylene diamine

$(H_3N\text{-}CH_2\text{-}CH_2\text{-}NH_3)\ (Pb_2Cl_6)$

(c) System 3 : 0D dual octahedral perovskite [*Pnnm*] Piperazine

$(C_4N_2H_{12})_4(Pb_2Br_{11}) \cdot (Br)(H_2O)_4$

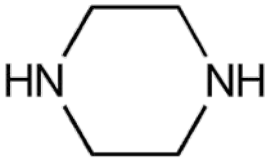

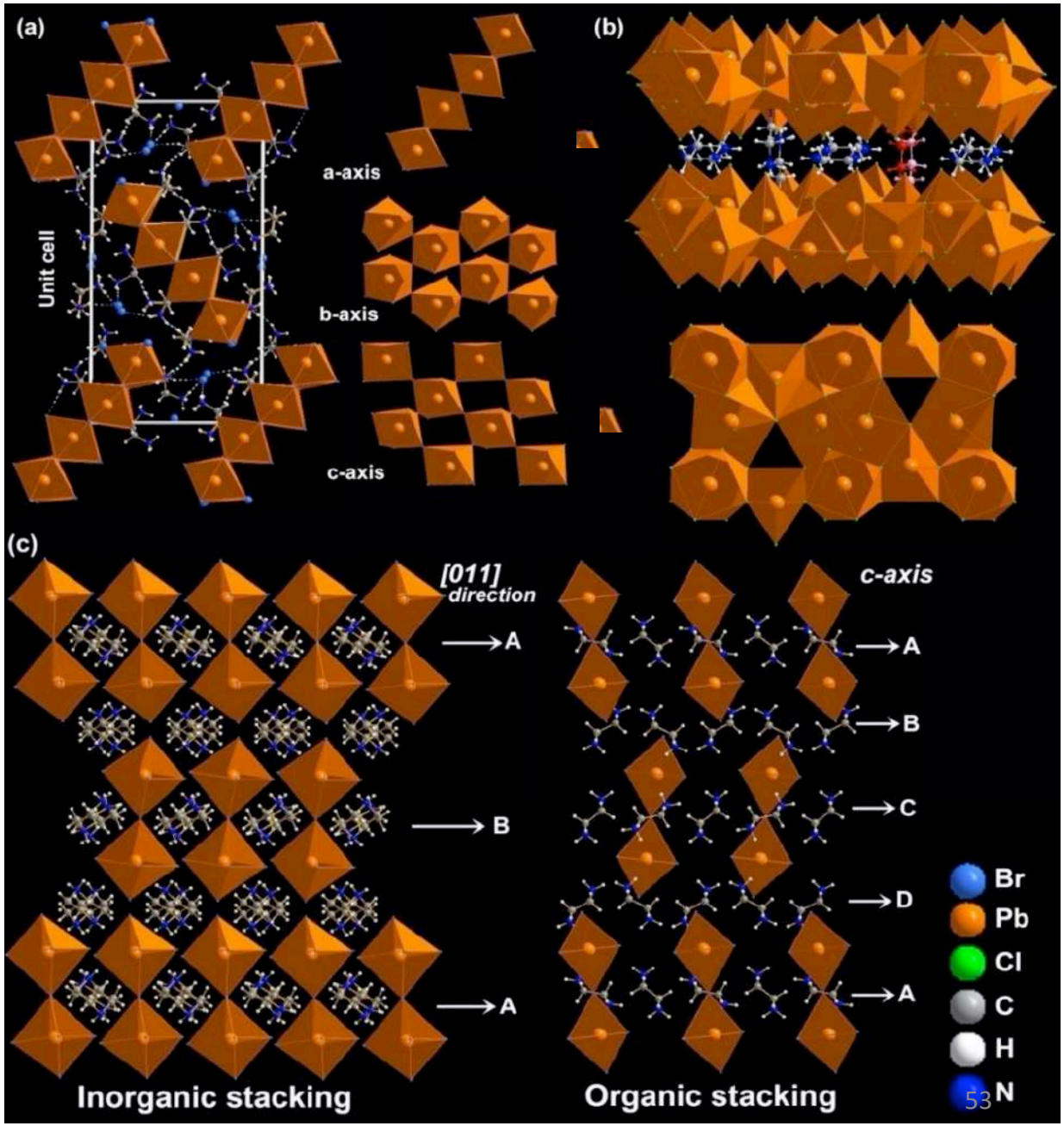

Photo-Physical measurements
(Diffused Reflectance Spectroscopy and Photoluminescence)

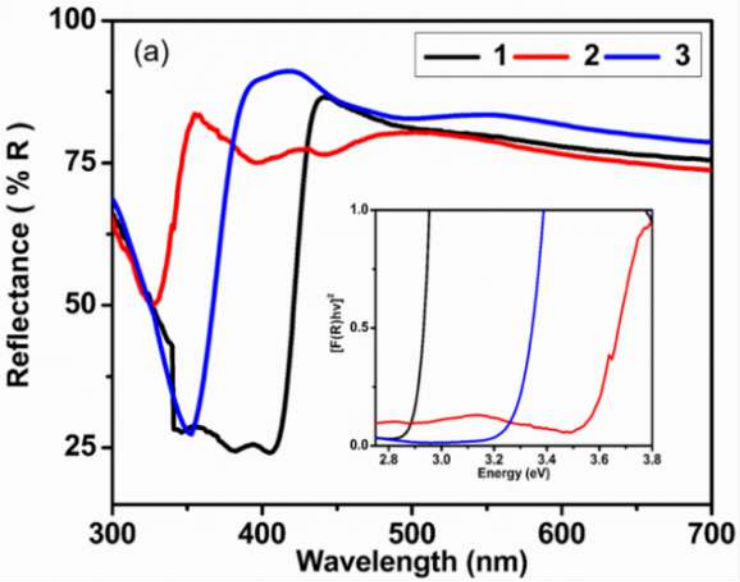

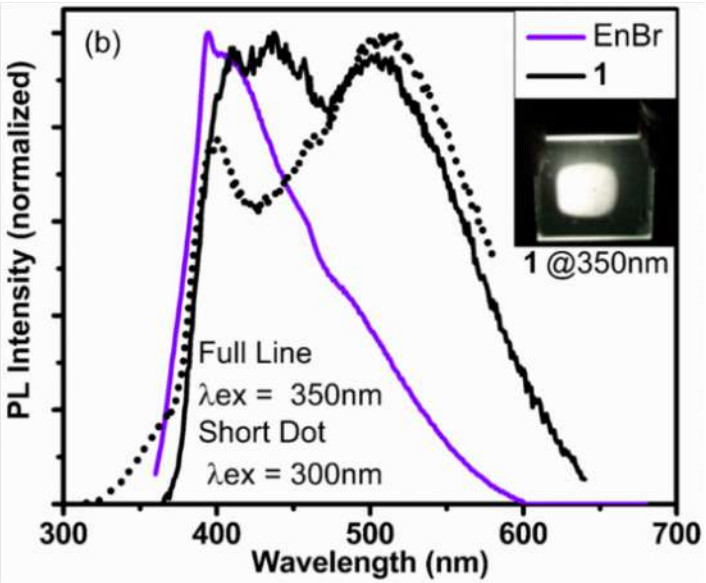

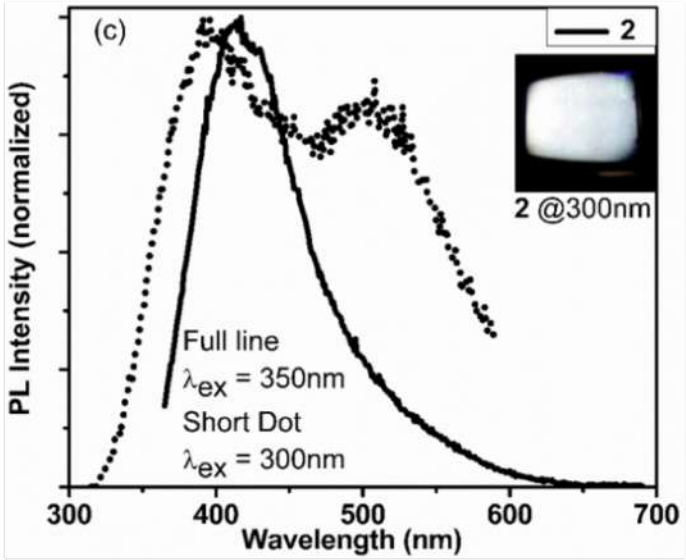

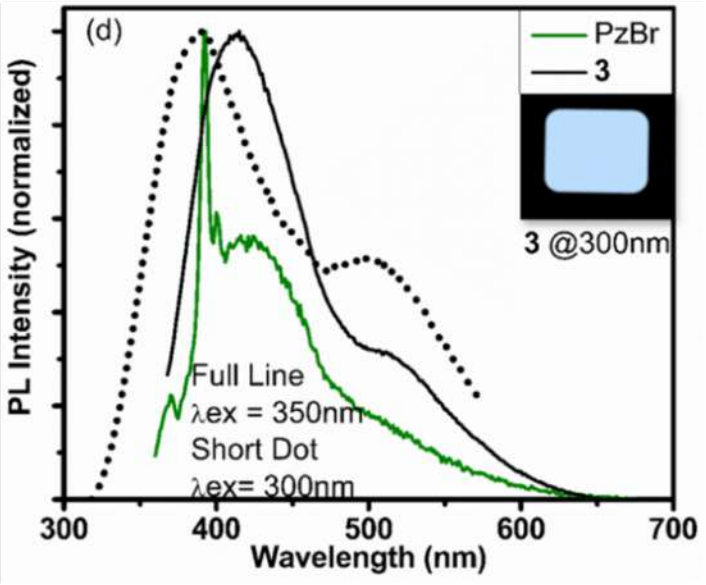

Raman Spectroscopy

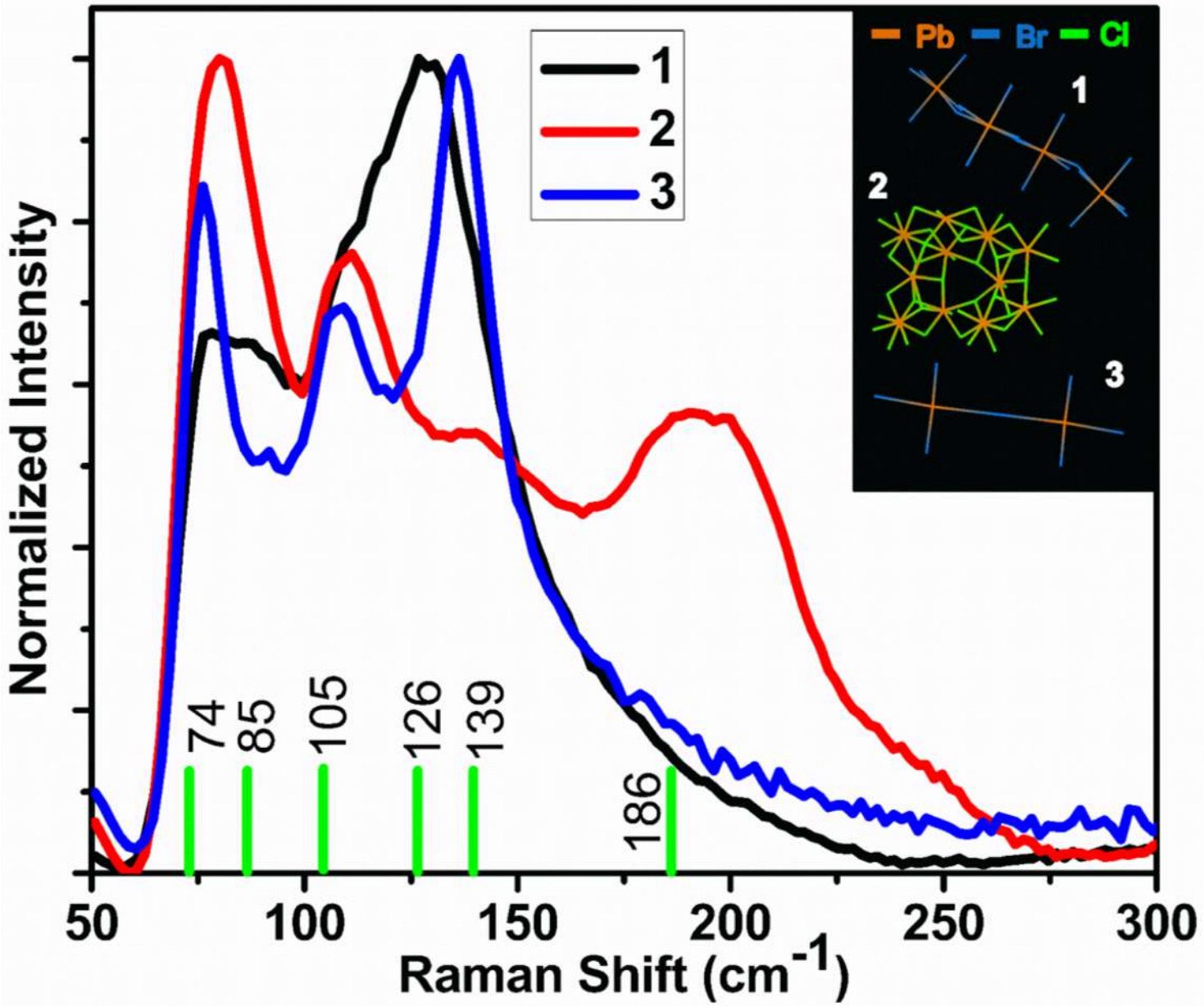

IISER PUNE

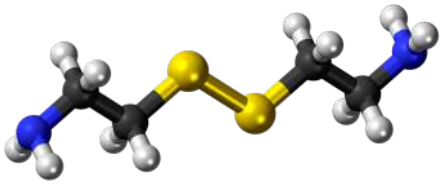

CENTRE FOR ENERGY SCIENCE

Cystamine-configured lead halide based 2D hybrid molecular crystals: Synthesis and photoluminescence systematics

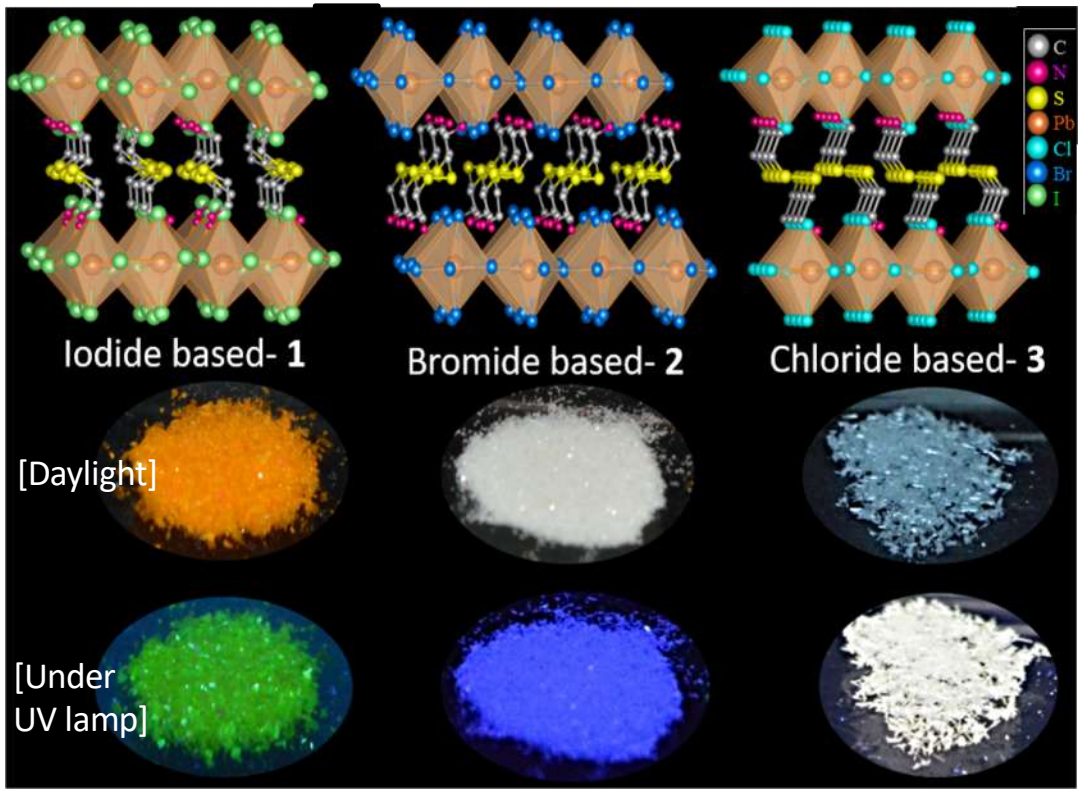

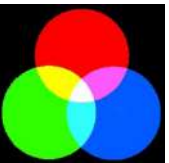

APL Materials 6, 114204 (2018)

Photo-Physical measurements

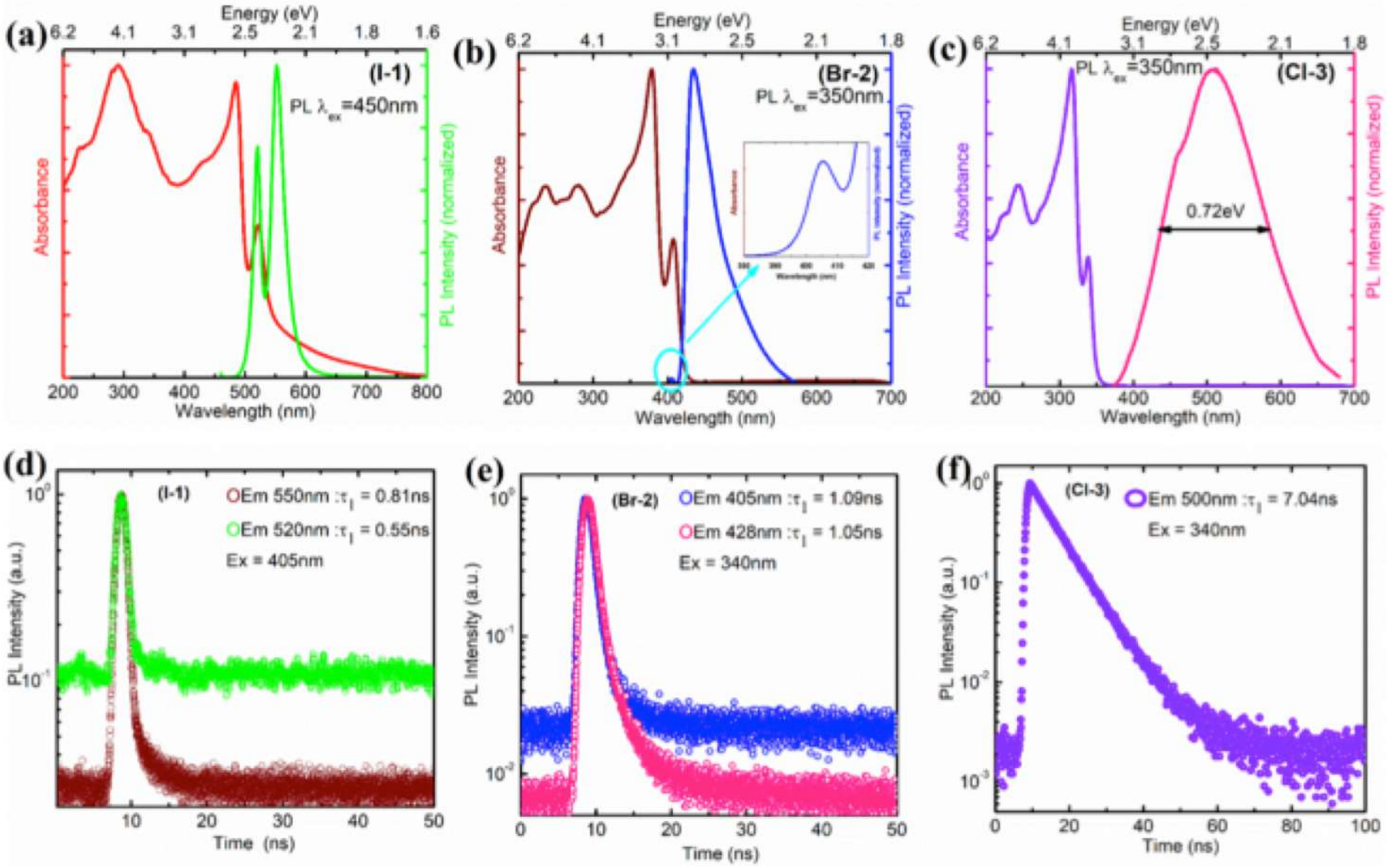

GDCh Communications Angewandte International Edition Chemie

Quantum Dots

International Edition: DOI: 10.1002/anie.201712608
German Edition: DOI: 10.1002/ange.201712608

Photoluminescence Quenching in Self-Assembled $CsPbBr_3$ Quantum Dots on Few-Layer Black Phosphorus Sheets

Subas Muduli, Padmini Pandey, Gayathri Devatha, Rohit Babar, Thripuranthaka M, Dushyant C. Kothari, Mukul Kabir, Pramod P. Pillai,* and Satishchandra Ogale**

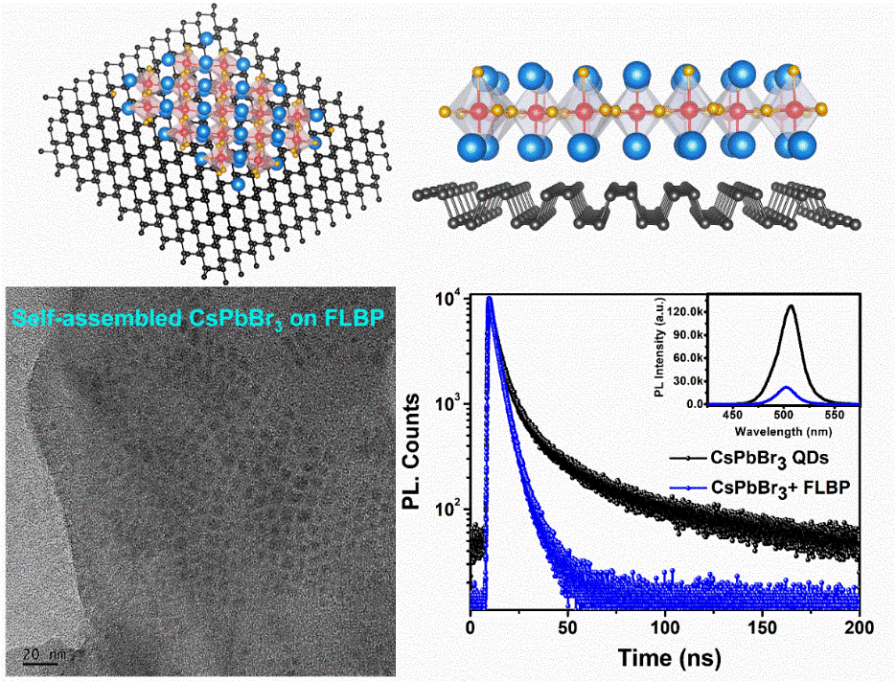






Angew. Chem. Int. Ed. 2018, 57, 7682

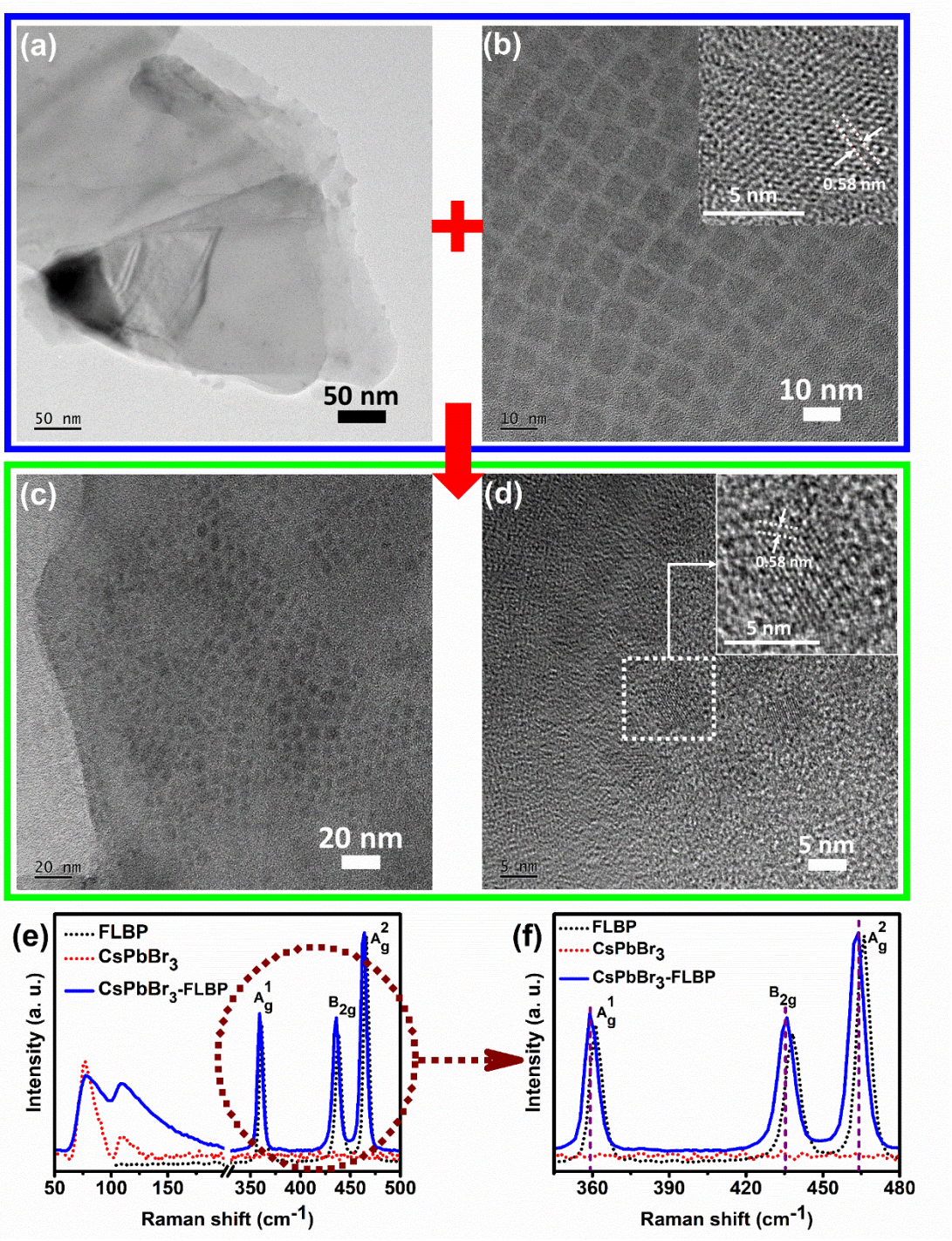
(a)
50 nm
50 nm
(b)
5 nm
0.58 nm
10 nm
10 nm
(c)
20 nm
20 nm
(d)
0.58 nm
5 nm
5 nm
5 nm
(e)
FLBP
CsPbBr3
CsPbBr3-FLBP
A1g
B2g
A2g
Intensity (a. u.)
50
100
150
350
400
450
500
Raman shift (cm-1)
(f)
FLBP
CsPbBr3
CsPbBr3-FLBP
A1g
B2g
A2g
Intensity (a. u.)
360
390
420
450
480
Raman shift (cm-1)

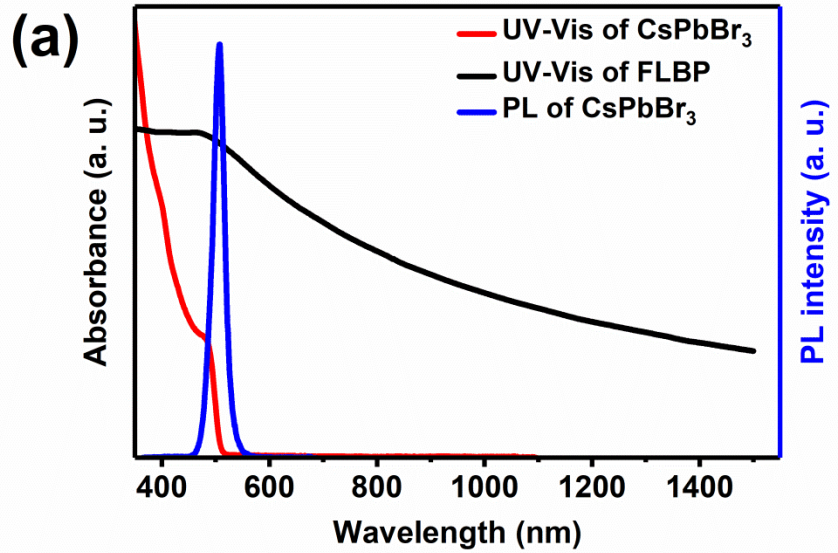
(a)
UV-Vis of CsPbBr3
UV-Vis of FLBP
PL of CsPbBr3
Absorbance (a. u.)
PL intensity (a. u.)
400
600
800
1000
1200
1400
Wavelength (nm)

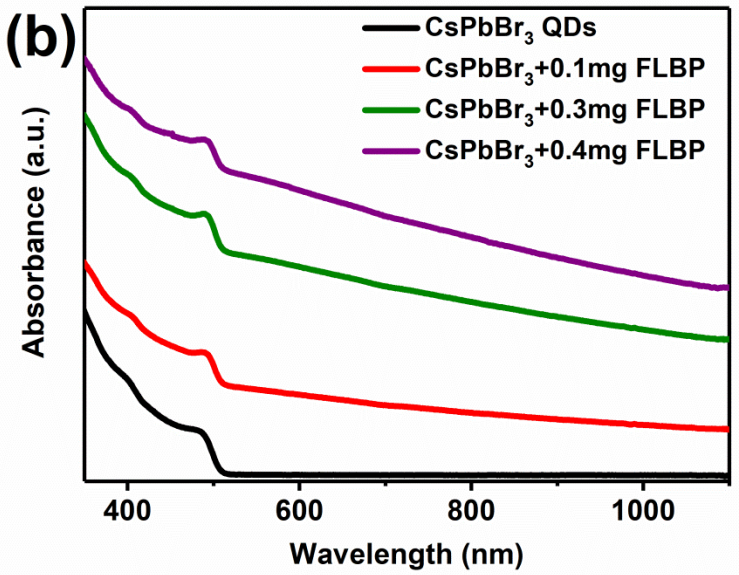
(b)
CsPbBr3 QDs
CsPbBr3+0.1mg FLBP
CsPbBr3+0.3mg FLBP
CsPbBr3+0.4mg FLBP
Absorbance (a.u.)
400
600
800
1000
Wavelength (nm)

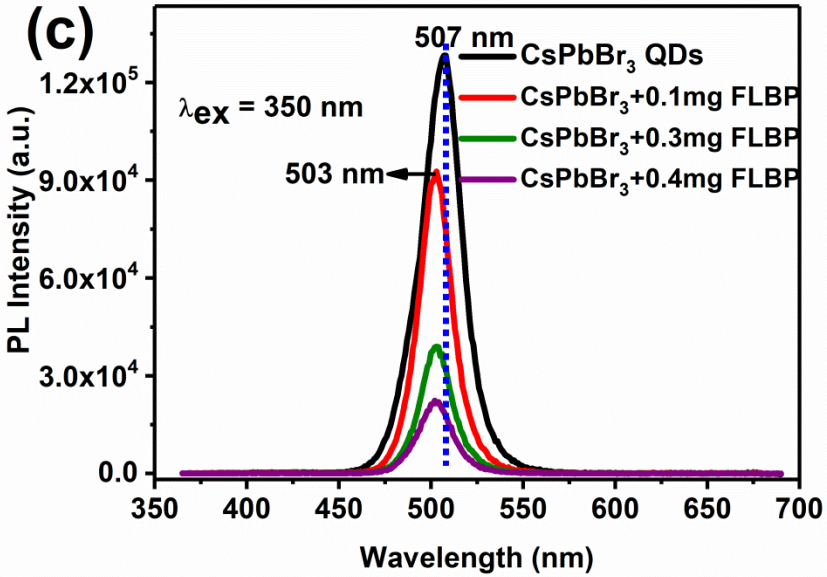
(c)
507 nm
CsPbBr3 QDs
λex = 350 nm
CsPbBr3+0.1mg FLBP
CsPbBr3+0.3mg FLBP
503 nm
CsPbBr3+0.4mg FLBP
PL Intensity (a.u.)
1.2x10^5
9.0x10^4
6.0x10^4
3.0x10^4
0.0
350
400
450
500
550
600
650
700
Wavelength (nm)

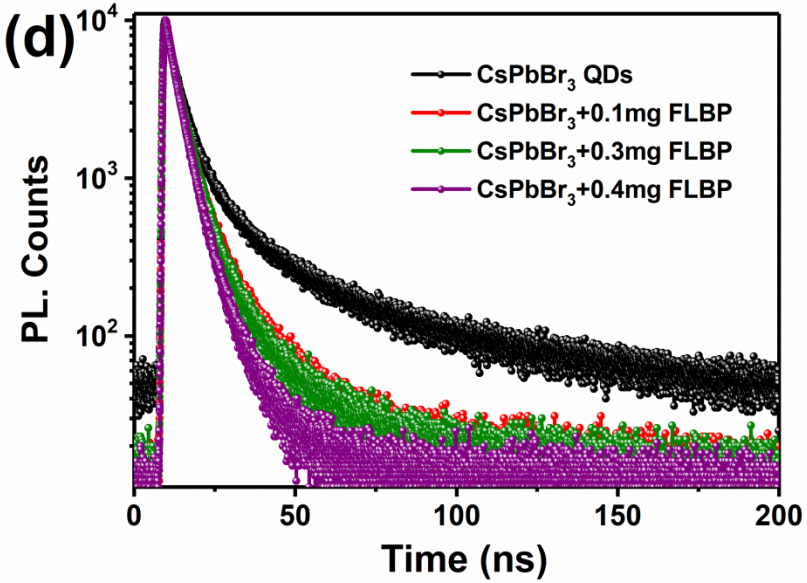
(d)
CsPbBr3 QDs
CsPbBr3+0.1mg FLBP
CsPbBr3+0.3mg FLBP
CsPbBr3+0.4mg FLBP
PL. Counts
10^4
10^3
10^2
0
50
100
150
200
Time (ns)

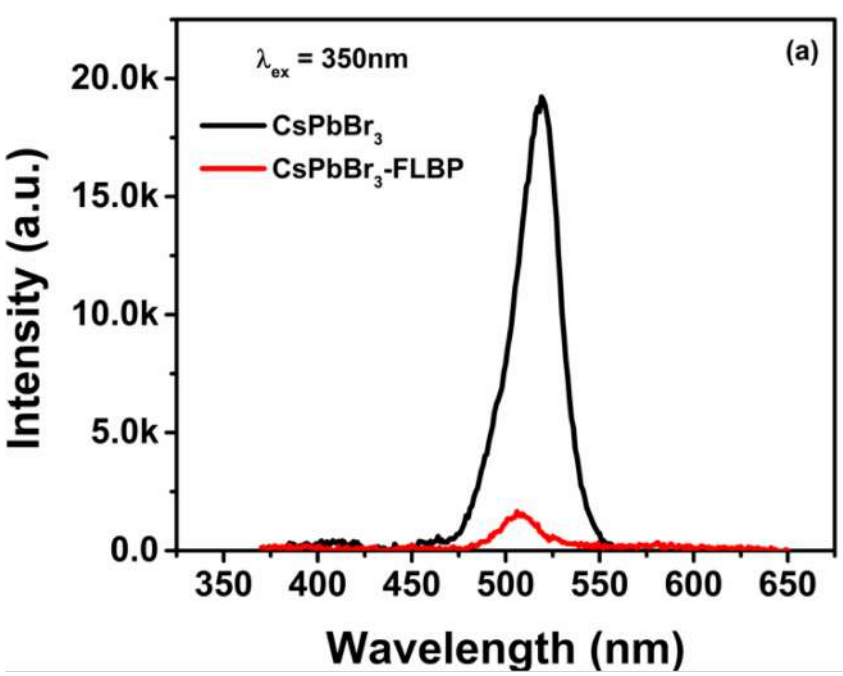
(a)
λex = 350nm
CsPbBr3
CsPbBr3-FLBP
Intensity (a.u.)
Wavelength (nm)

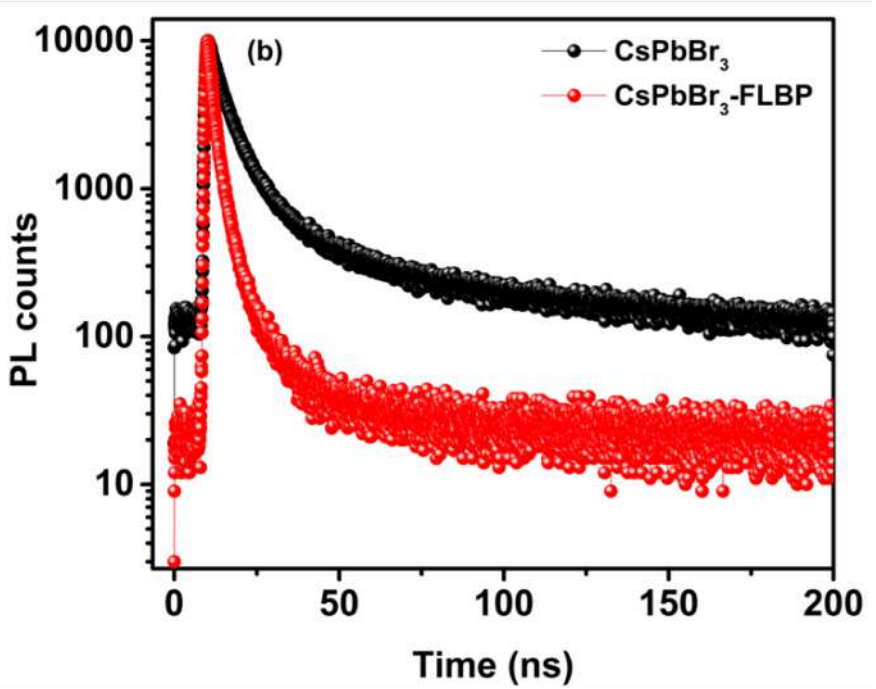
(b)
CsPbBr3
CsPbBr3-FLBP
PL counts
Time (ns)

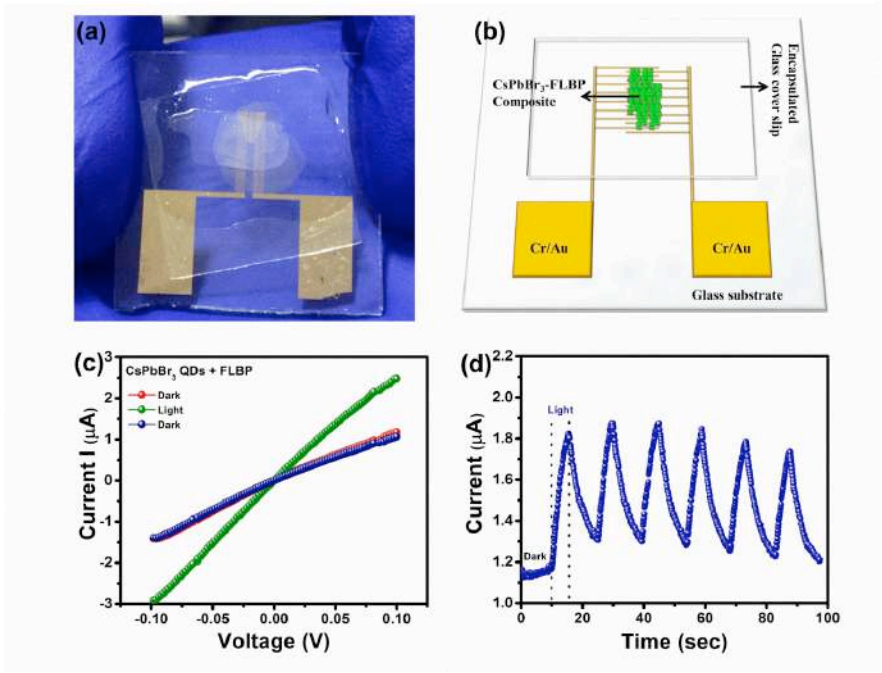
(a)
(b)
CsPbBr3-FLBP Composite
Encapsulated Glass cover-slip
Cr/Au
Cr/Au
Glass substrate
(c)
CsPbBr3 QDs + FLBP
Dark
Light
Dark
Current I (μA)
Voltage (V)
(d)
Light
Dark
Current (μA)
Time (sec)

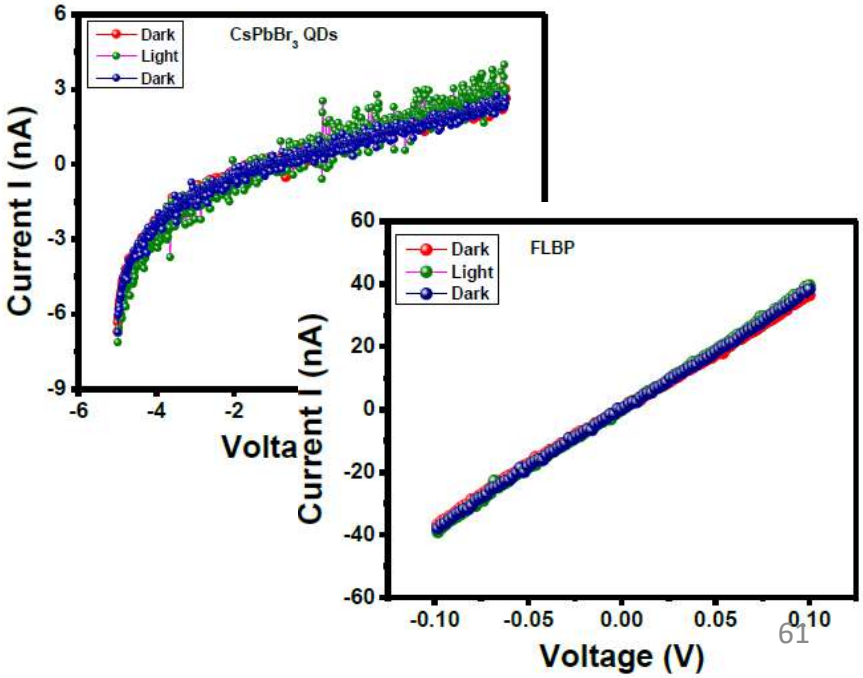
Dark
Light
Dark
CsPbBr3 QDs
Current I (nA)
Volta
FLBP
Dark
Light
Dark
Current I (nA)
Voltage (V)

$CsPbBr_3$–$Ti_3C_2T_x$ MXene QD/QD Heterojunction: Photoluminescence Quenching, Charge Transfer, and Cd Ion Sensing Application

Padmini Pandey, Arundhati Sengupta, Swati Parmar, Umesh Bansode, Suresh Gosavi, Abhishek Swarnkar, Subas Muduli,* Aditya D. Mohite,* and Satishchandra Ogale*

Cite This: *ACS Appl. Nano Mater.* 2020, 3, 3305–3314

Read Online

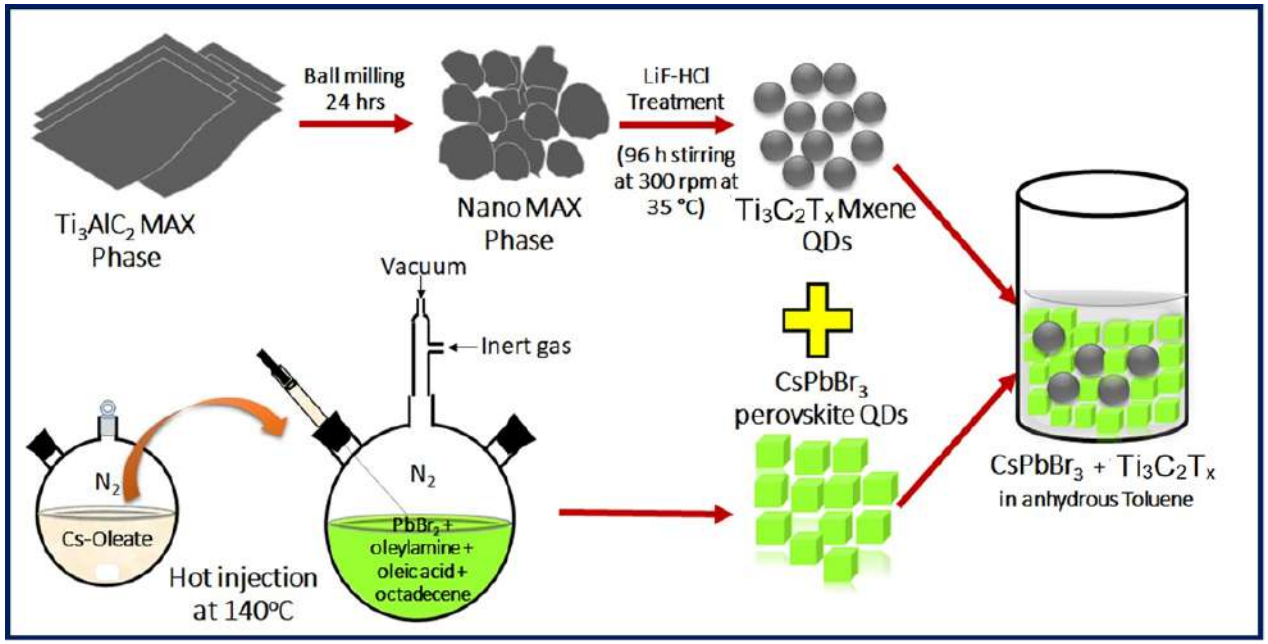

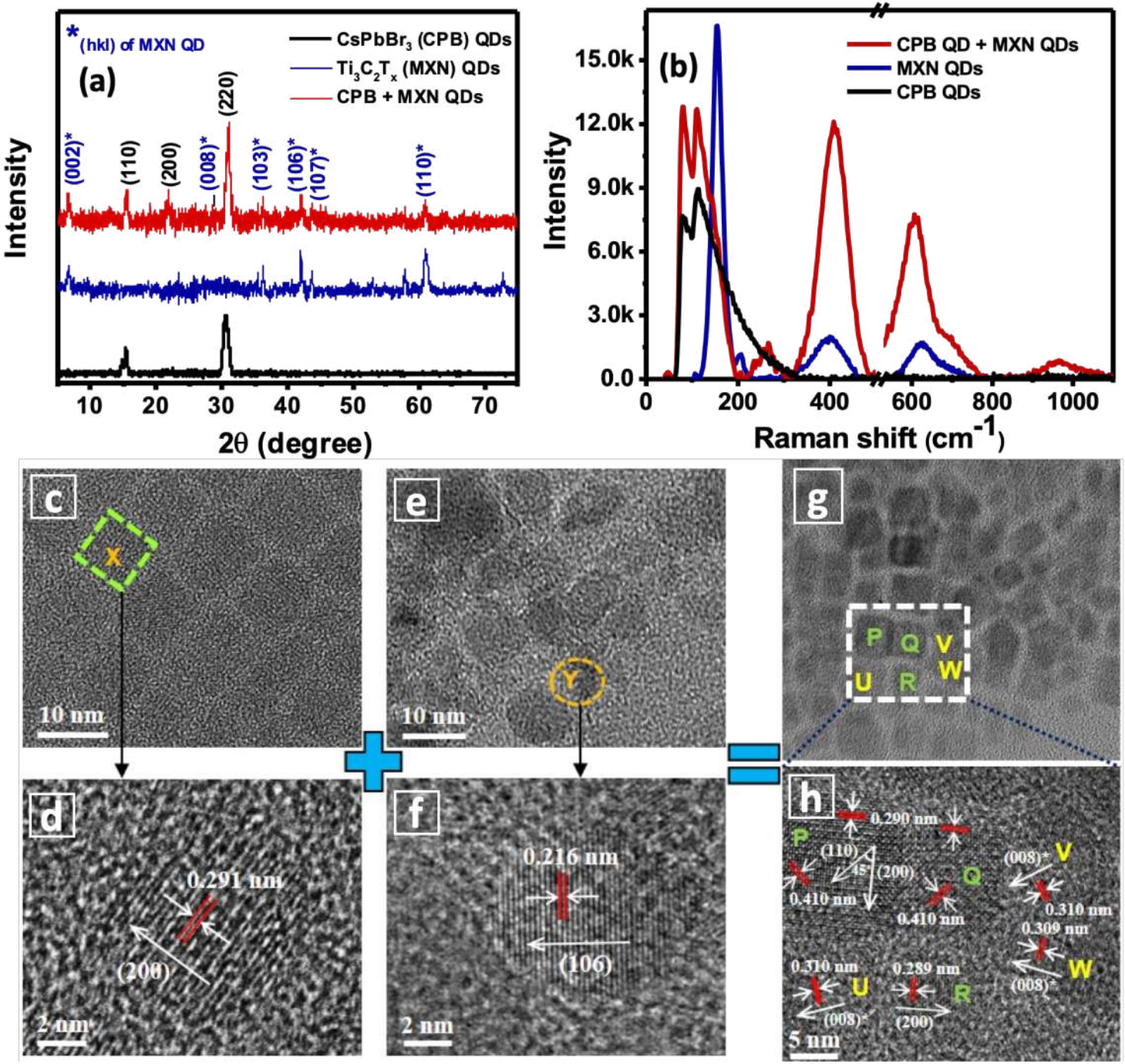
*(hkl) of MXN QD
CsPbBr3 (CPB) QDs
Ti3C2Tx (MXN) QDs
CPB + MXN QDs
(a)
(002)*
(110)
(200)
(008)*
(220)
(103)*
(106)*
(107)*
(110)*
Intensity
2θ (degree)
(b)
CPB QD + MXN QDs
MXN QDs
CPB QDs
Intensity
Raman shift (cm-1)
c
X
10 nm
d
0.291 nm
(200)
2 nm
e
Y
10 nm
f
0.216 nm
(106)
2 nm
g
P Q V
U R W
h
0.290 nm
P
(110)
45°
(200)
Q
0.410 nm
0.410 nm
(008)*
V
0.310 nm
0.309 nm
W
0.310 nm
U
0.289 nm
R
(008)*
(008)*
(200)
5 nm

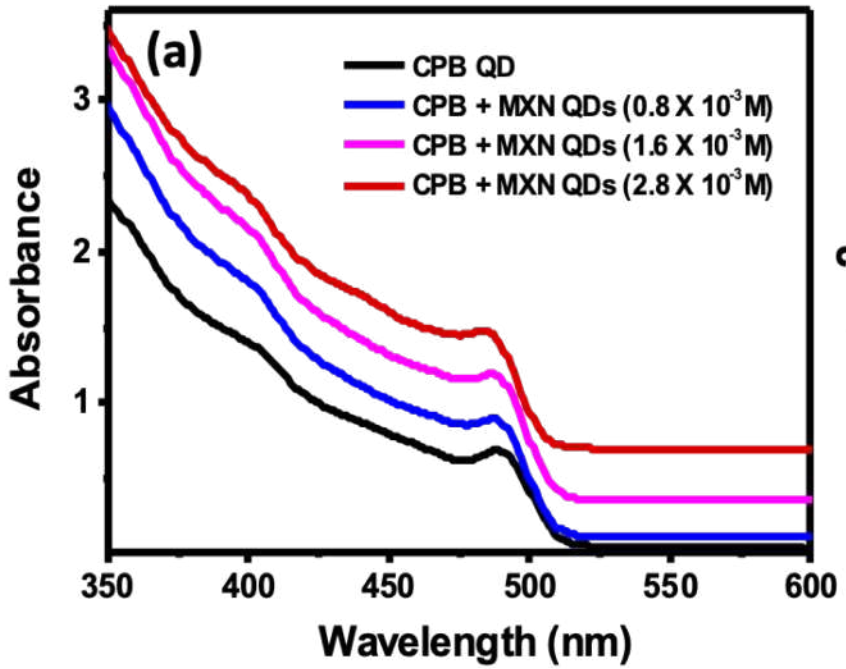
(a)
CPB QD
CPB + MXN QDs (0.8 X 10^{-3}M)
CPB + MXN QDs (1.6 X 10^{-3}M)
CPB + MXN QDs (2.8 X 10^{-3}M)
Absorbance
Wavelength (nm)

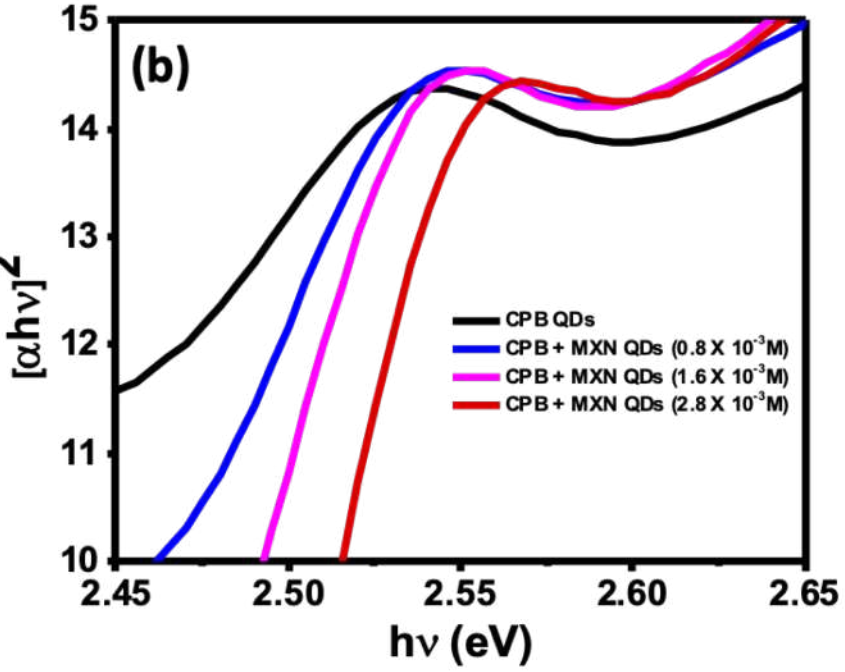
(b)
CPB QDs
CPB + MXN QDs (0.8 X 10^{-3}M)
CPB + MXN QDs (1.6 X 10^{-3}M)
CPB + MXN QDs (2.8 X 10^{-3}M)
$[\alpha h\nu]^2$
hν (eV)

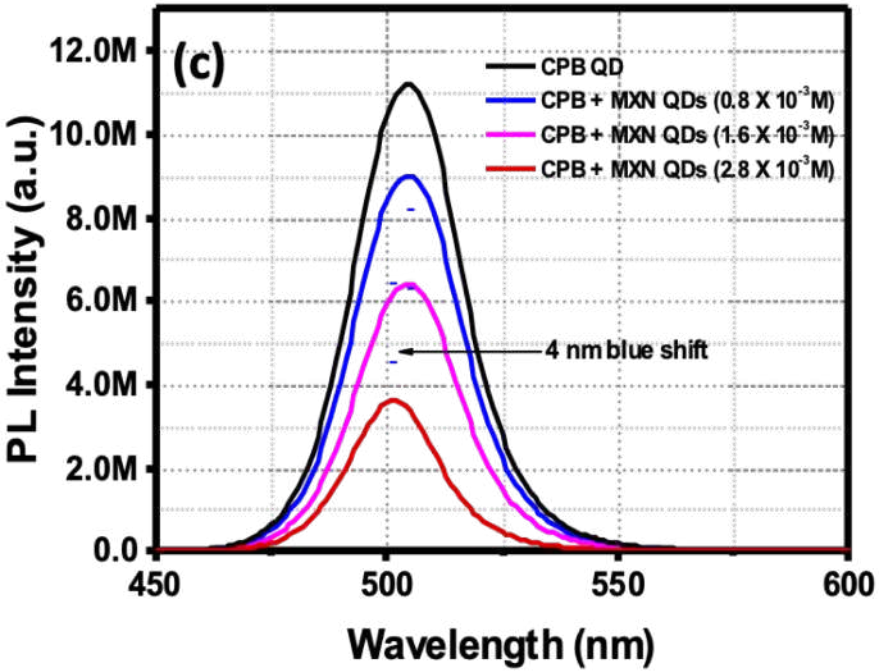
(c)
CPB QD
CPB + MXN QDs (0.8 X 10^{-3}M)
CPB + MXN QDs (1.6 X 10^{-3}M)
CPB + MXN QDs (2.8 X 10^{-3}M)
4 nm blue shift
PL Intensity (a.u.)
Wavelength (nm)

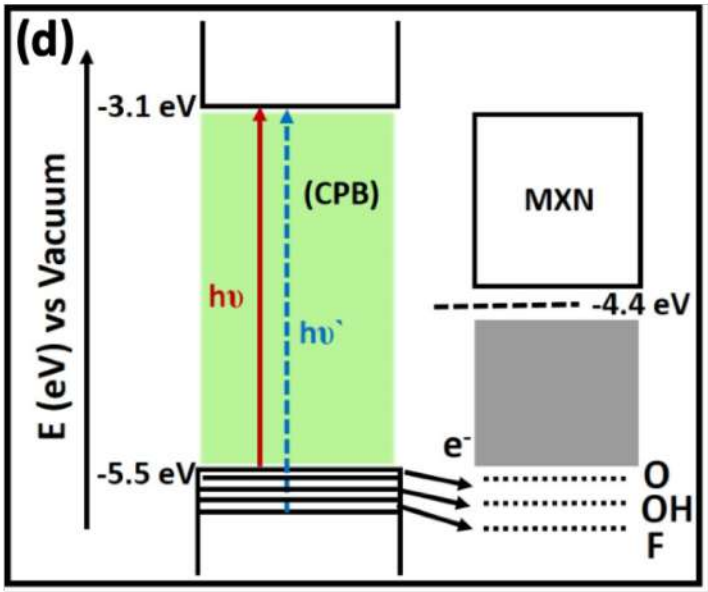
(d)
-3.1 eV
(CPB)
MXN
hυ
hυ`
-4.4 eV
e$^-$
-5.5 eV
O
OH
F
E (eV) vs Vacuum

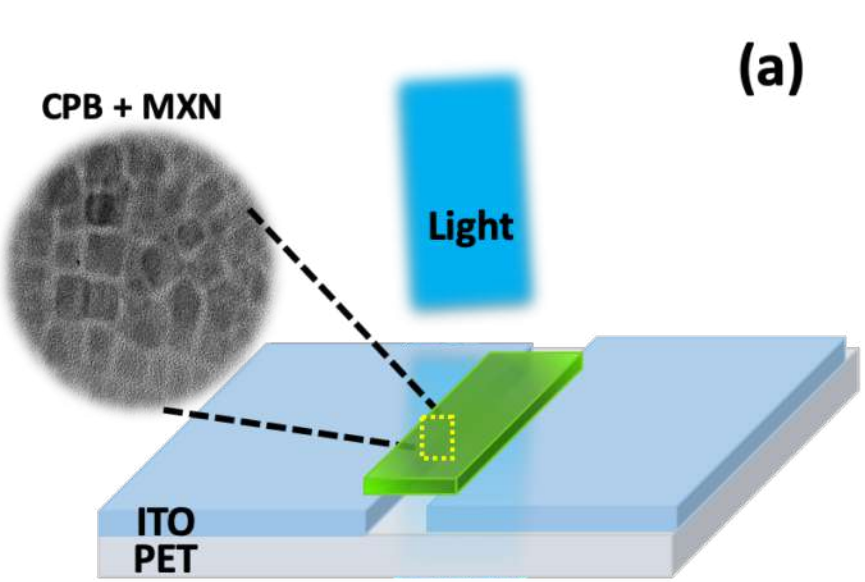
(a)
CPB + MXN
Light
ITO
PET

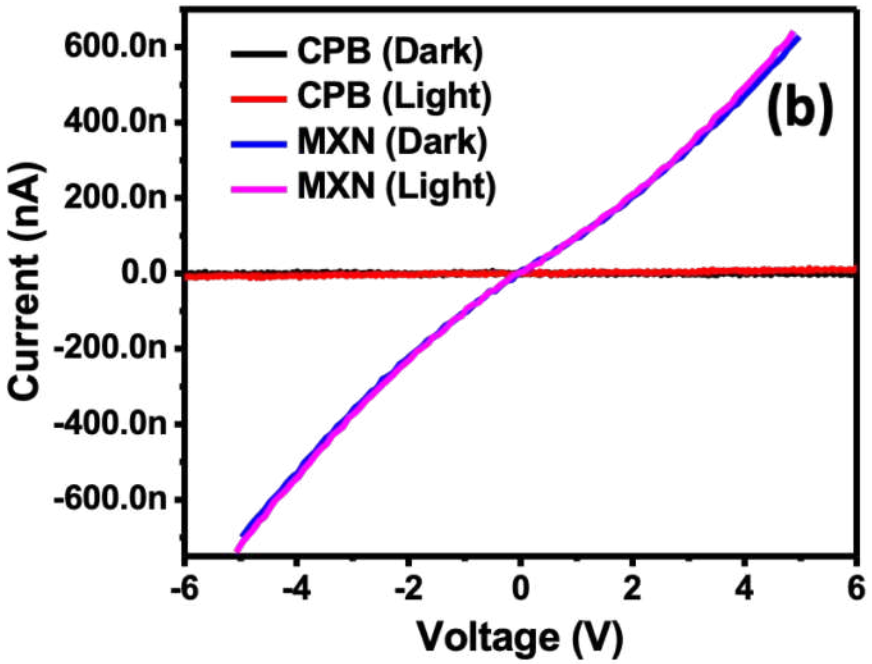
(b)
CPB (Dark)
CPB (Light)
MXN (Dark)
MXN (Light)
Current (nA)
600.0n
400.0n
200.0n
0.0
-200.0n
-400.0n
-600.0n
-6
-4
-2
0
2
4
6
Voltage (V)

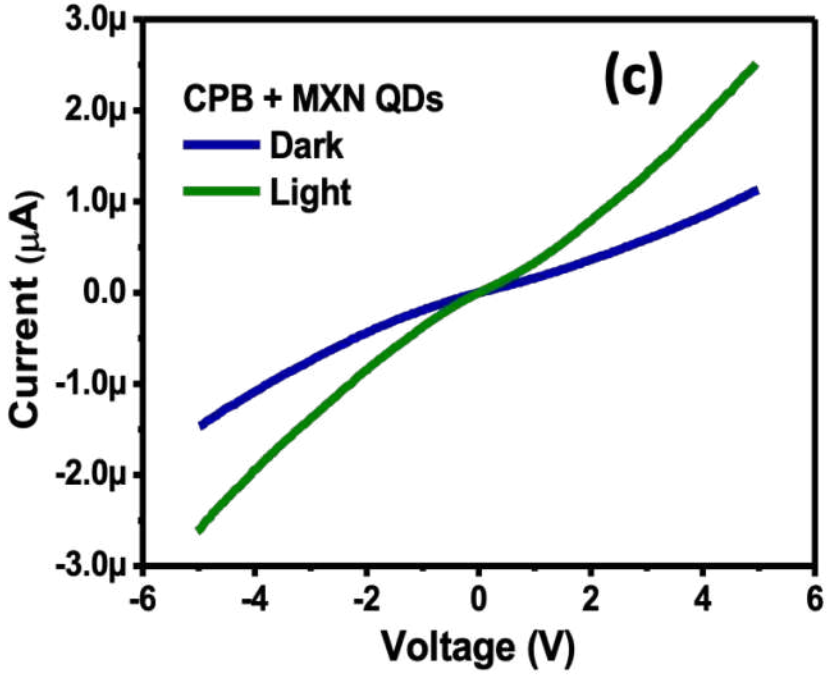
(c)
CPB + MXN QDs
Dark
Light
Current (μA)
3.0μ
2.0μ
1.0μ
0.0
-1.0μ
-2.0μ
-3.0μ
-6
-4
-2
0
2
4
6
Voltage (V)

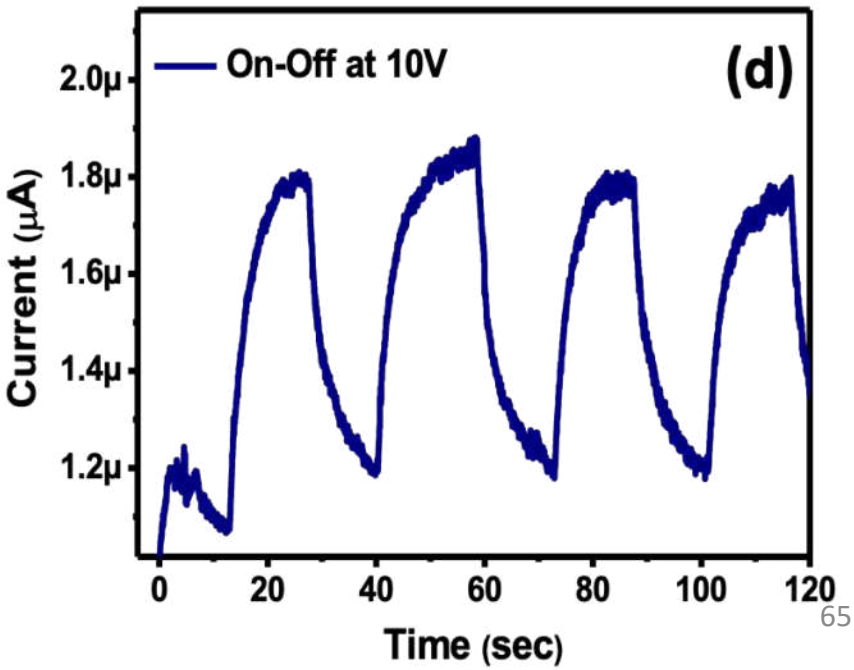
(d)
On-Off at 10V
Current (μA)
2.0μ
1.8μ
1.6μ
1.4μ
1.2μ
0
20
40
60
80
100
120
Time (sec)

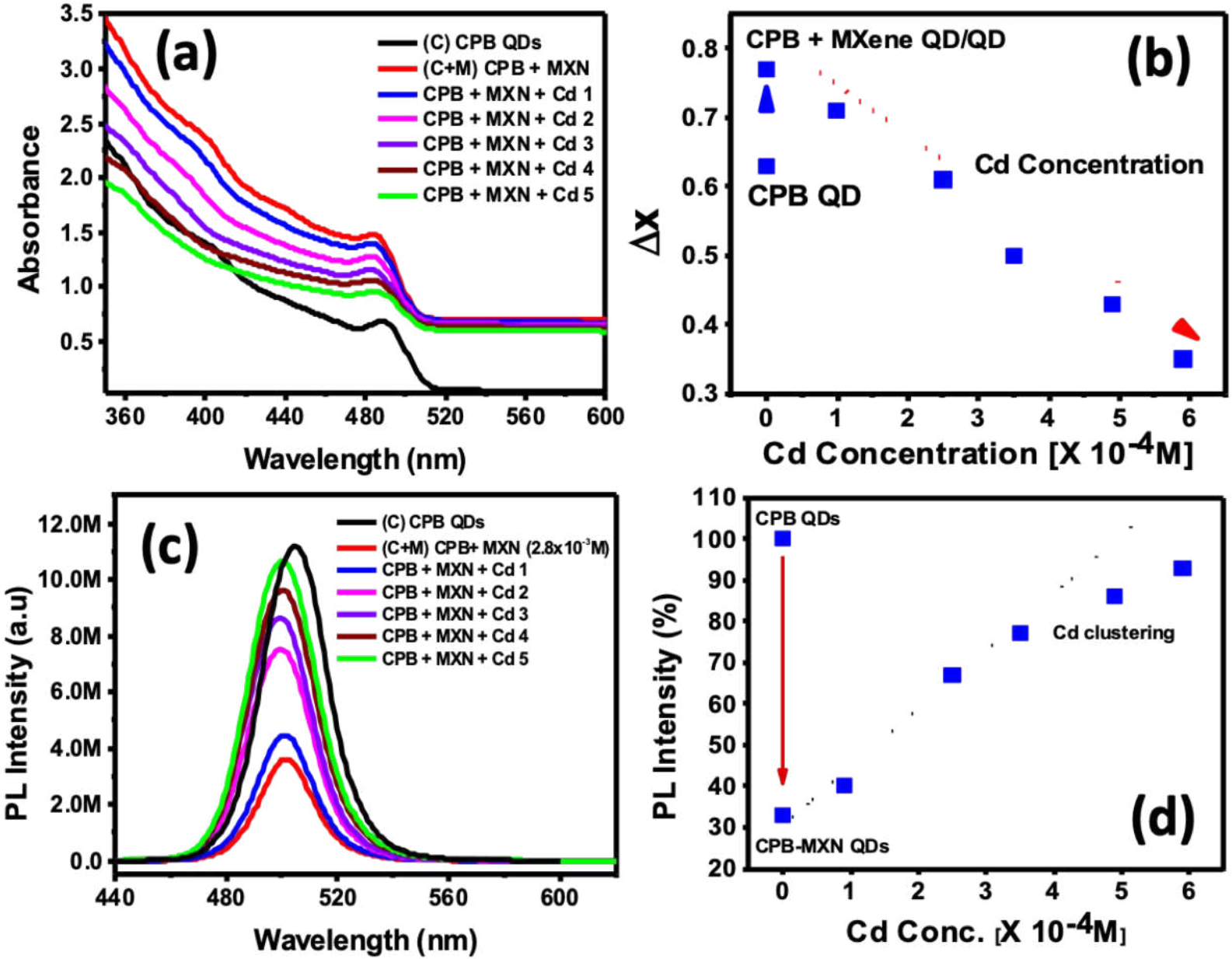
(a)
Absorbance
Wavelength (nm)
(C) CPB QDs
(C+M) CPB + MXN
CPB + MXN + Cd 1
CPB + MXN + Cd 2
CPB + MXN + Cd 3
CPB + MXN + Cd 4
CPB + MXN + Cd 5
(b)
CPB + MXene QD/QD
CPB QD
Cd Concentration
Δx
Cd Concentration [X 10-4M]
(c)
PL Intensity (a.u)
Wavelength (nm)
(C) CPB QDs
(C+M) CPB+ MXN (2.8x10-3M)
CPB + MXN + Cd 1
CPB + MXN + Cd 2
CPB + MXN + Cd 3
CPB + MXN + Cd 4
CPB + MXN + Cd 5
(d)
CPB QDs
CPB-MXN QDs
Cd clustering
PL Intensity (%)
Cd Conc. [X 10-4M]

GDCh Research Articles Angewandte International Edition Chemie

Check for updates

How to cite: *Angew. Chem. Int. Ed.* **2021**, *60*, 18750–18760
International Edition: doi.org/10.1002/anie.202105918
German Edition: doi.org/10.1002/ange.202105918

Perovskite Phases

An Organic–Inorganic Perovskitoid with Zwitterion Cysteamine Linker and its Crystal–Crystal Transformation to Ruddlesden-Popper Phase

Prachi Kour, Mallu Chenna Reddy, Shiv Pal, Siraj Sidhik, Tisita Das, Padmini Pandey, Shatabdi Porel Mukherjee,* Sudip Chakraborty,* Aditya D. Mohite,* and Satishchandra Ogale**

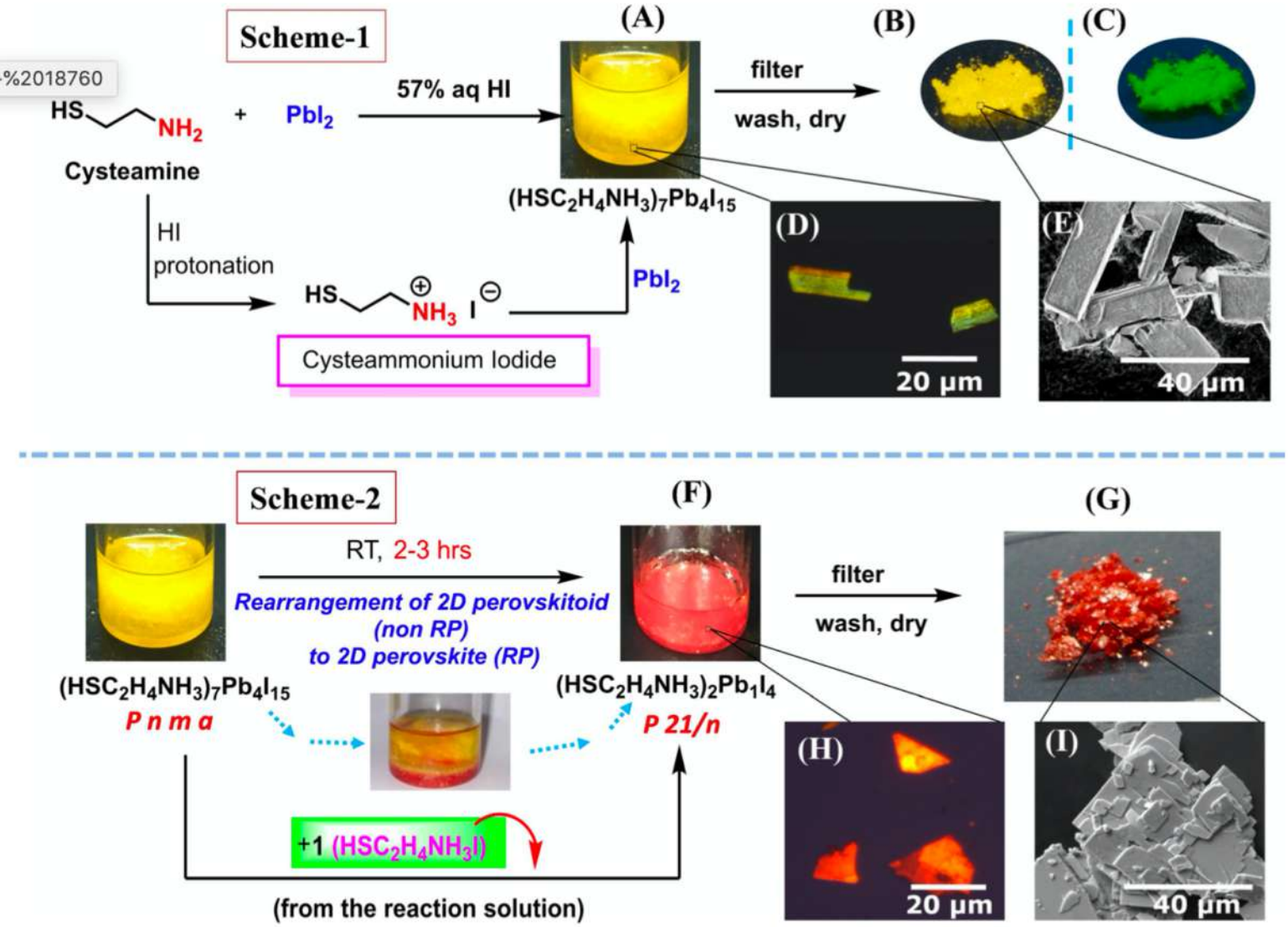

Figure 1. Scheme 1: the reaction and formation of $(HSC_2H_4NH_3)_7Pb_4I_{15}$ (**1**); Crystals of **1** formed in the reaction solution (A); compound **1** in the ambient (B), under the 265 nm UV lamp showing green emission C); polarised microscopy images (D); FESEM image for **1** (E); Scheme 2: the conversion of yellow crystals **1** ($(HSC_2H_4NH_3)_7Pb_4I_{15}$ (2D perovskitoid)) into red crystals **2** ($(HSC_2H_4NH_3)_2Pb_1I_4$ (2D perovskite)) in the mother solution; RP phase crystals **2** in solution (F); Compound **2** crystals under ambient light after filtration (G); polarized microscopy images (H), FESEM image for **2** (I).

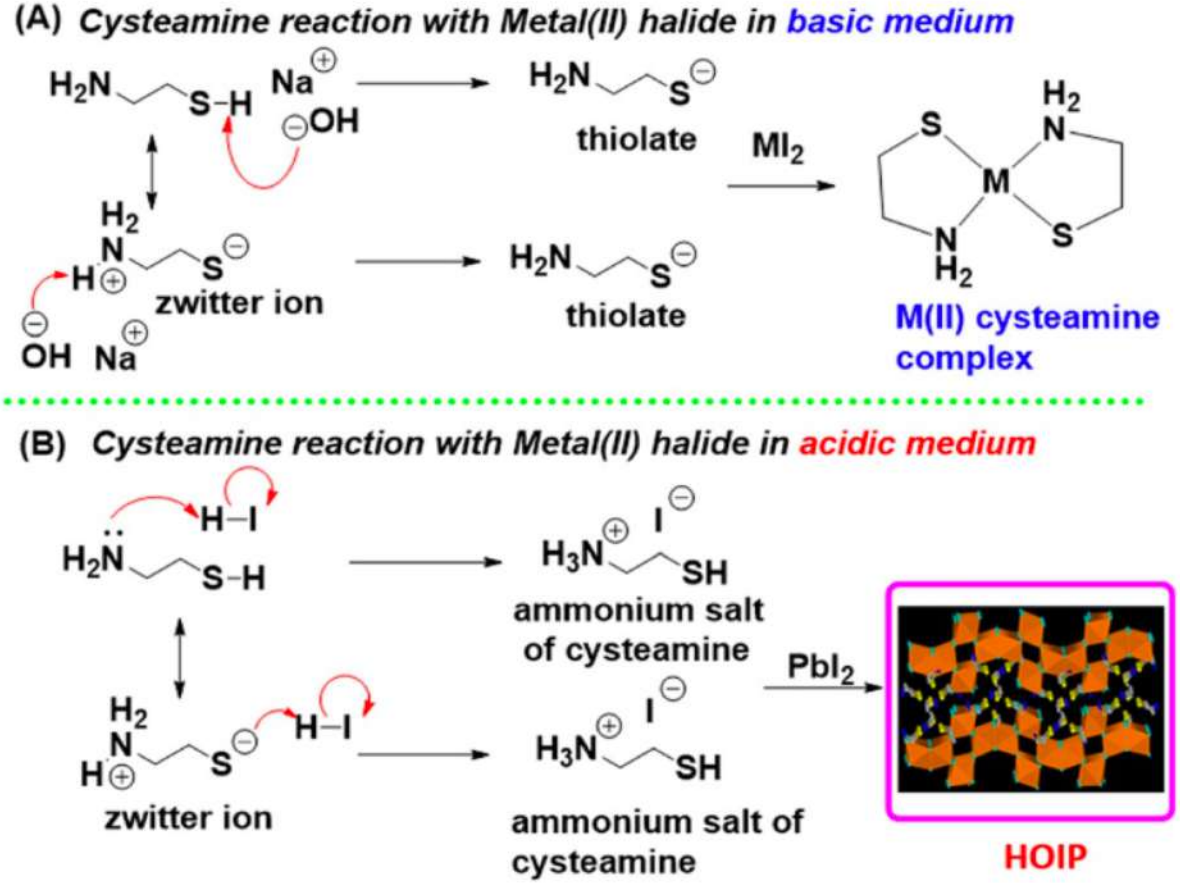

Figure 2. The variation between cysteamine reaction with metal(II) halide in basic medium (A) and acidic medium (B) with the possible mechanism; cysteamine with base (NaOH) generates thiolate intermediate which forms M^{II} cysteamine complex with MI_2 (A); cysteamine with acid (HI) generates cysteammonium iodide salt, which forms HOIP with PbI_2 (B).

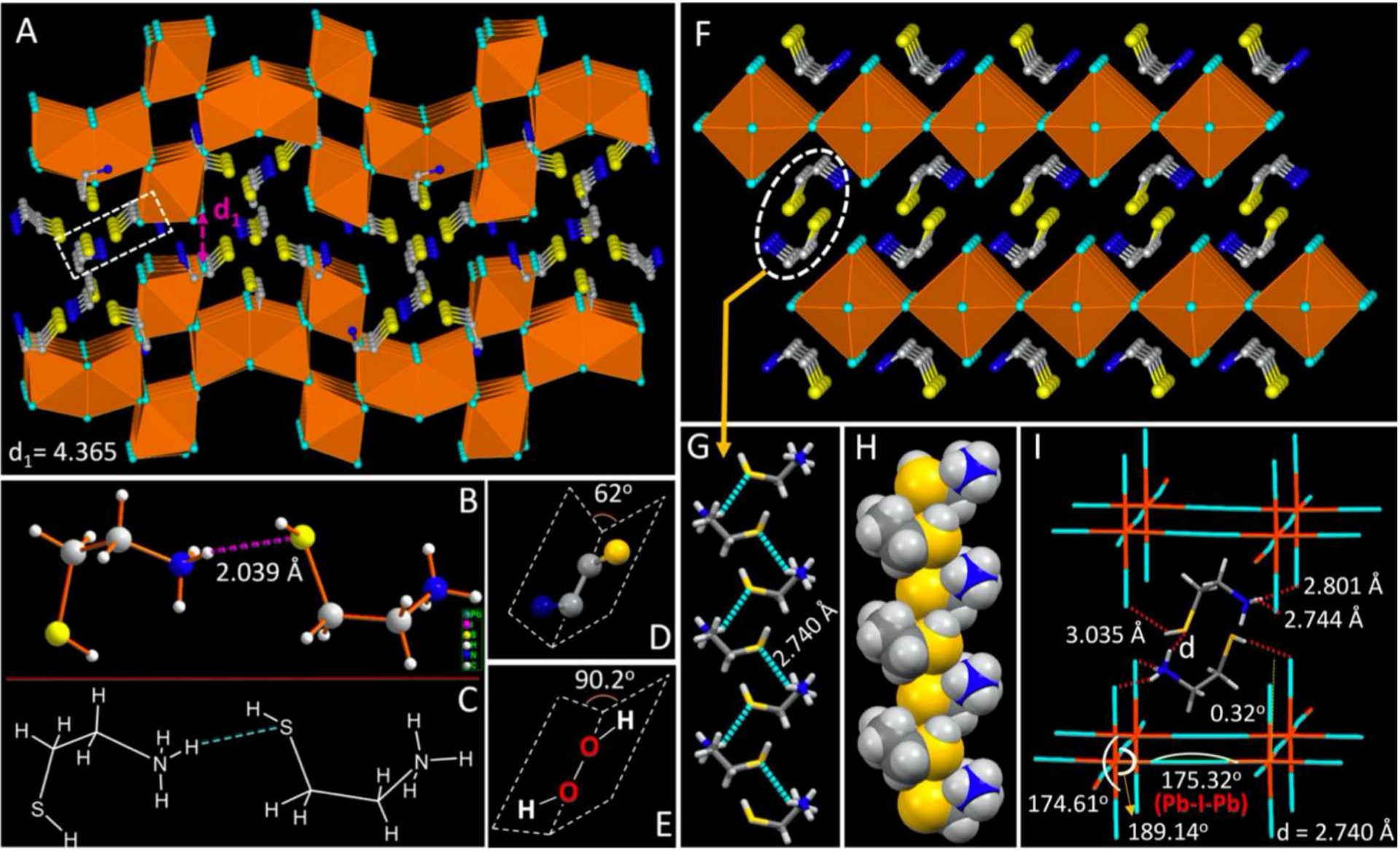
A
d1
d1= 4.365
B
2.039 Å
C
62°
D
90.2°
H
O
O
H
E
F
G
2.740 Å
H
I
2.801 Å
2.744 Å
3.035 Å
d
0.32°
175.32°
(Pb-I-Pb)
174.61°
189.14°
d = 2.740 Å

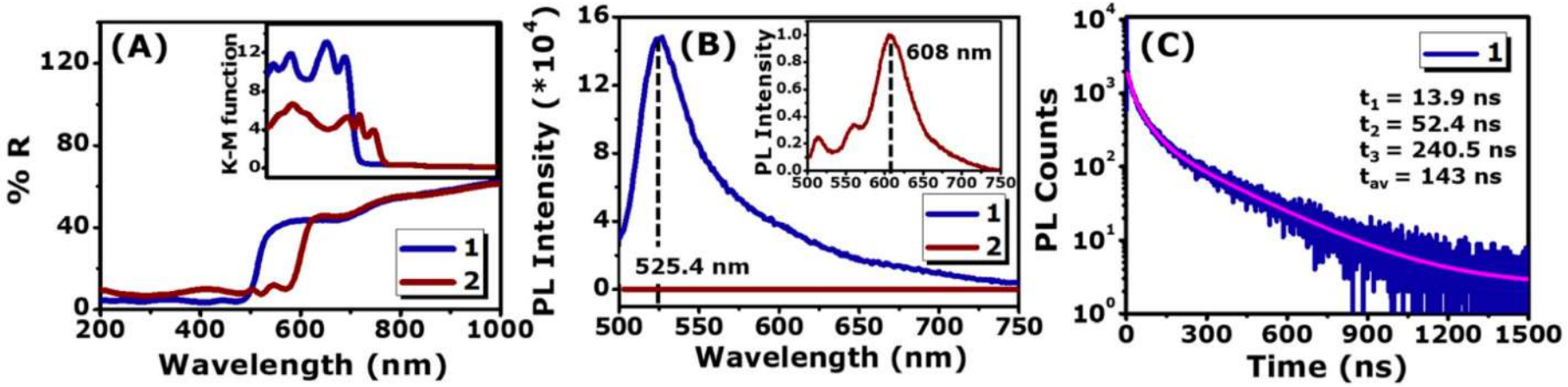

Figure 5. DRS (%R) data with K-M function shown as an inset for the compounds **1** and **2** (A); Comparative PL spectra for compounds **1** and **2**, inset shows the PL for compound **2** (B) at 470 nm excitation; TRPL data for compounds **1** (C). Note: All optical measurements are performed on compound **1** and compound **2** powders.

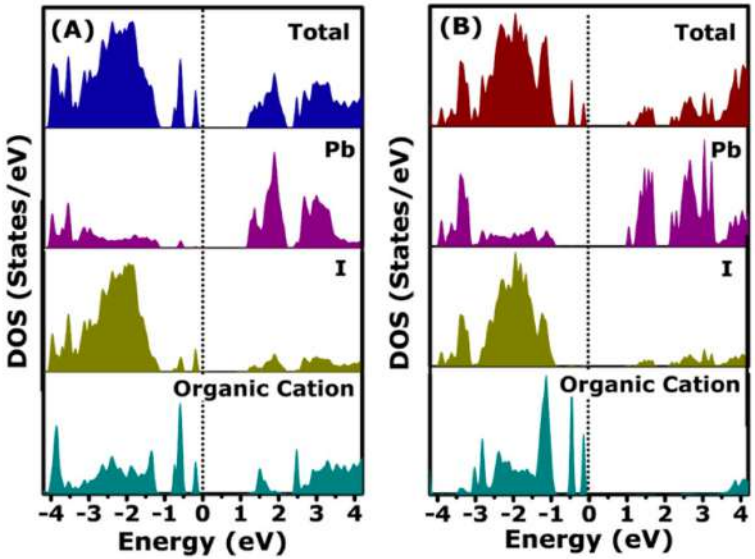

Figure 6. Density of states calculation for **1** (A) and **2** (B) by DFT (For clarity an enlarged image is shown in the Supporting Information, Figure S13).

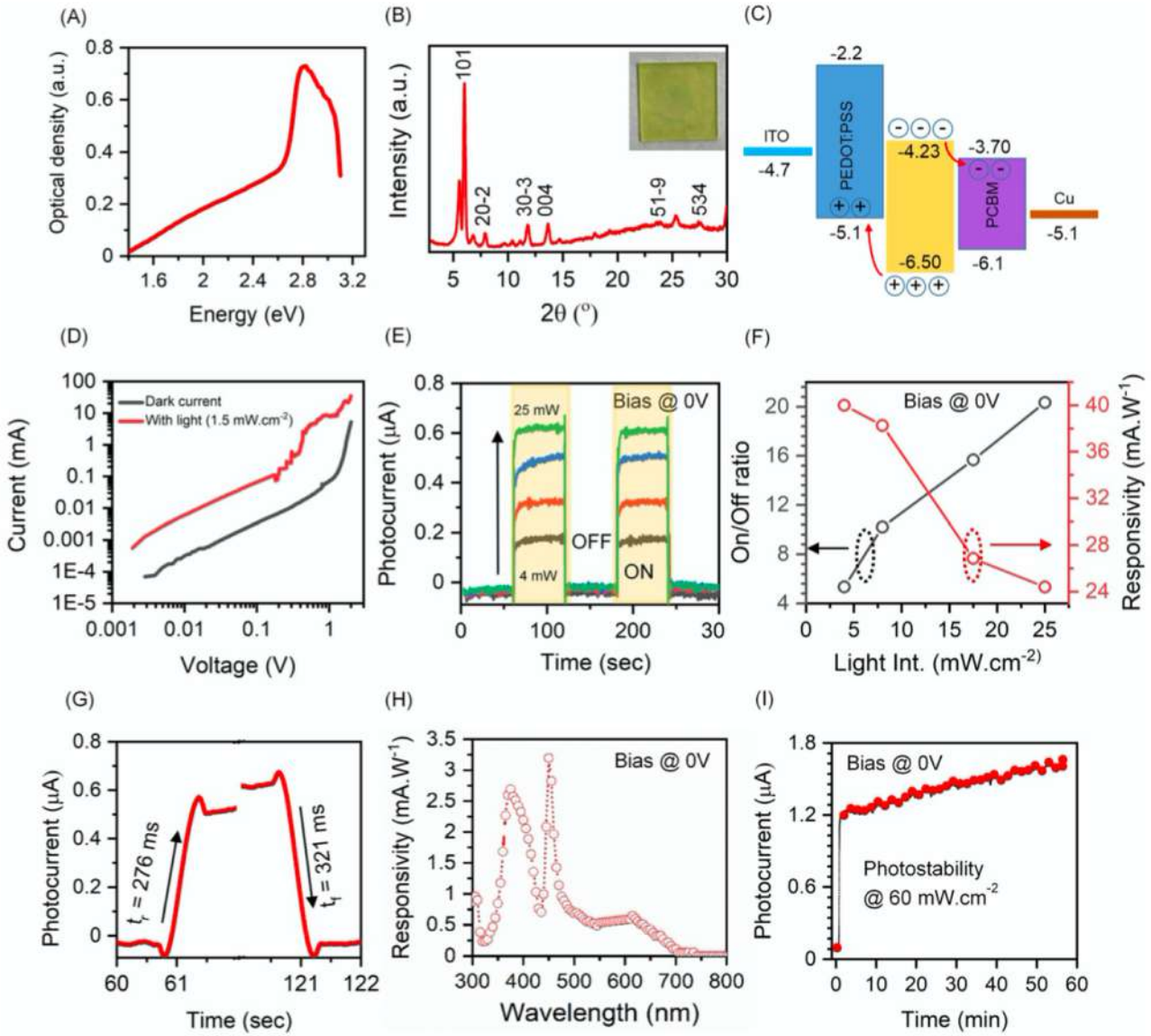

Figure 7. Absorbance of the thin films of compound **1** fabricated by hot-casting technique (A); X-ray diffraction of the thin films of compound **1** fabricated by hot-casting technique (B); Band diagram showing the self-powered photodetector with the synthesized crystals (C); *I–V* curves of the device in the dark and under illumination with light intensity of 1.5 mWcm^{-2} using a broadband source at 0 V (D); current versus time curves of the PD under bias voltage of 0 V using a broad band light source (E); Variation in the ON/OFF ratio and responsivity with the intensity of light at 0 V bias (F); Plot showing the response time of the self-powered photodetector at 25 mWcm^{-2} light intensity under 0 bias (G); Responsivity spectra of the fabricated photodetector at 0 V bias (H); Photostability of the self-powered photodetector at high light intensity of 60 mWcm^{-2} (I). (For clarity an enlarged image is shown in the Supporting Information, Figure S14.)

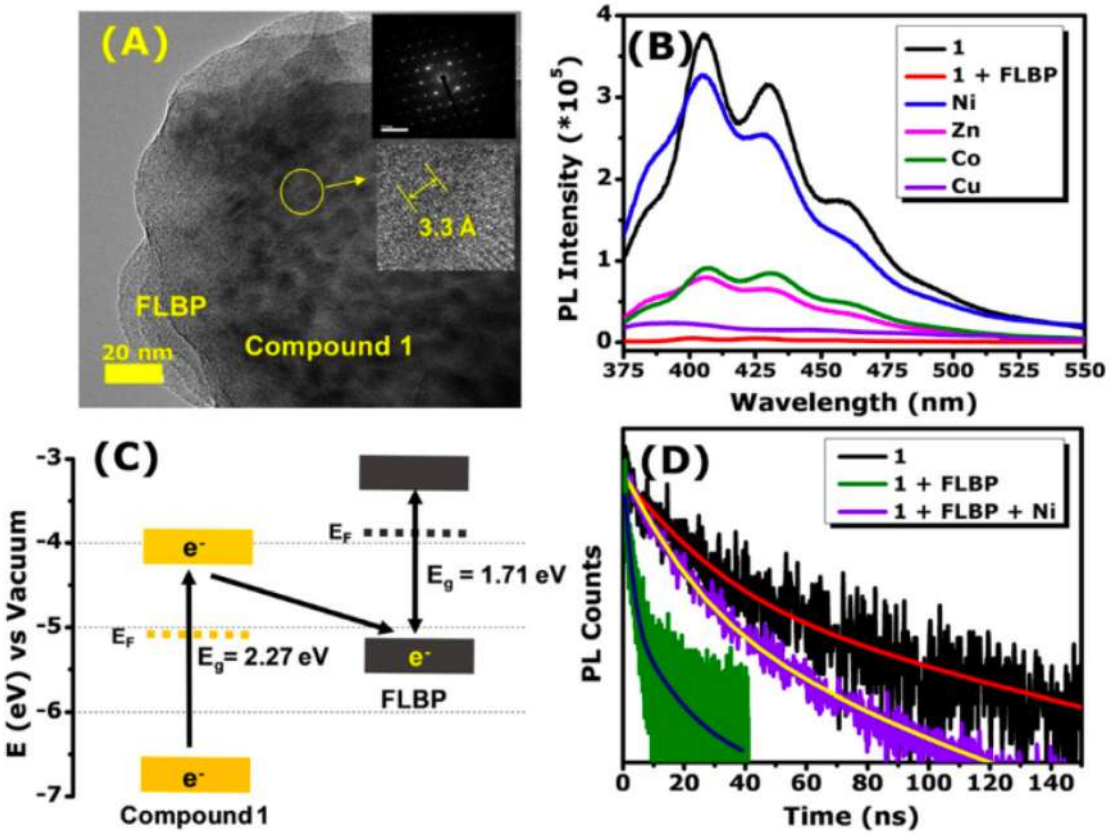

Figure 8. HRTEM image depicting the formation of nanocomposite of compound **1** and FLBP, inset depicts SAED pattern (top) and d-spacing (bottom) (A); PL spectra at 350 nm excitation for perovskitoid/FLBP composite with 1.79×10^{-2} M concentration of various metal ions in toluene (B); Energy-band diagram showing excitionic charge transfer between compound **1** and FLBP (C); TRPL data depicting subsequent recovery of lifetime after addition of 1.79×10^{-3} M Ni^{2+} ions in solution (D). (For clarity an enlarged image is shown in the Supporting Information, Figure S17.)

Journal of Materials Chemistry A

PAPER

View Article Online
View Journal | View Issue

Check for updates

Cite this: *J. Mater. Chem. A*, 2017, **5**, 18634

Low-dimensional hybrid perovskites as high performance anodes for alkali-ion batteries†

Mukta Tathavadekar,[ab] Shrreya Krishnamurthy,[a] Aparna Banerjee,[c] Satyawan Nagane,[ab] Yogesh Gawli,[ab] Anil Suryawanshi,[d] Suresh Bhat,[a] Dhanya Puthusseri,*[cd] Aditya D. Mohite*[e] and Satishchandra Ogale*[d]

Synthesis of the 1D benzidine lead iodide (Bz-Pb-I) hybrid perovskite ($C_6H_9I_3NOPb$)

Synthesis of the 2D butyl ammonium lead iodide hybrid perovskite [$(C_4H_9NH_3)_2PbI_4$/BA_2PbI_4] and 3D methyl ammonium lead iodide hybrid perovskite ($CH_3NH_3PbI_3$/$MAPbI_3$)

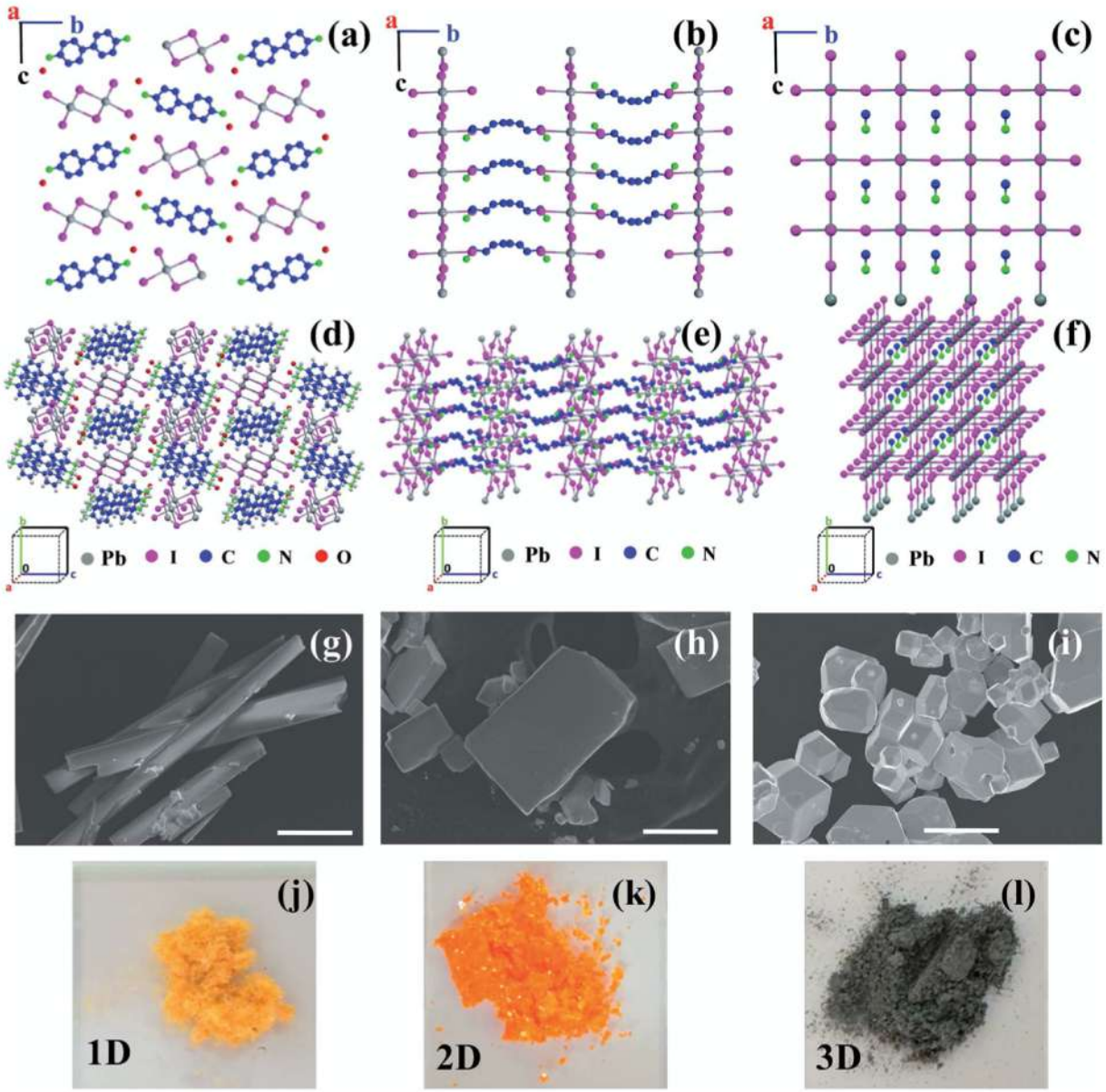

Fig. 1 The Packing diagrams along the *a*-axis of (a) $C_6H_9I_3NOPb$ (1D), (b) $(C_4H_9NH_3)_2PbI_4$ (2D), and (c) $CH_3NH_3PbI_3$ (3D) hybrid perovskite crystals, respectively; (d), (e), and (f) present the corresponding 3D perspectives; (g), (h) and (i) present the FE-SEM micrographs, while (j), (k) and (l) show the optical micrographs of the corresponding 1D, 2D and 3D systems. The scale bar for FE-SEM images is 50 μm.

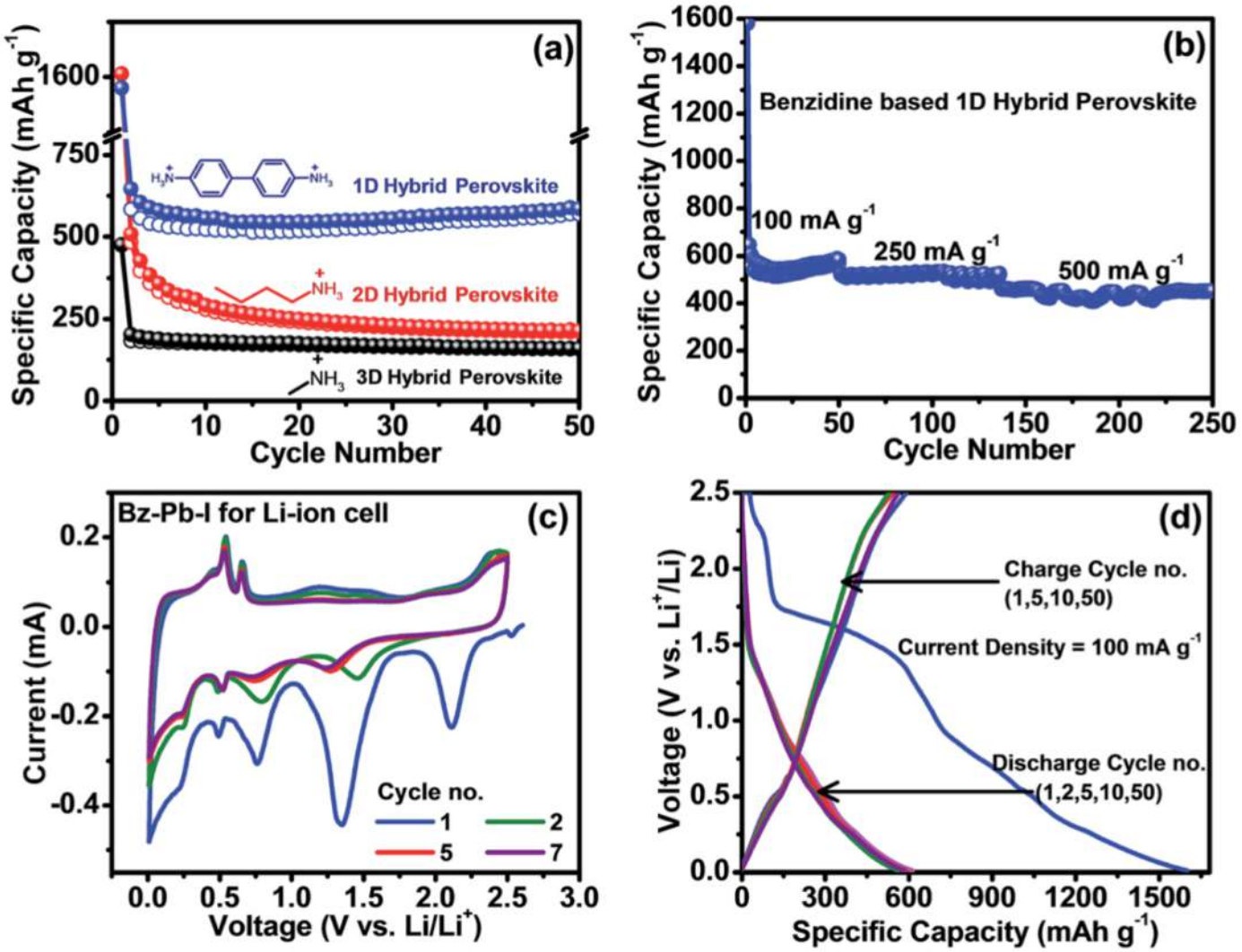

Fig. 2 Results of galvanostatic charge discharge cycling stability measurements for 1-2-3D hybrid perovskite cases and other electrochemical measurements for the 1D Bz-Pb-I case of Li ion batteries in a half cell configuration: (a) cycling stability of 1–2–3D hybrid perovskites at a current density of 100 mA g^{-1} in the potential window of 2.5 to 0.01 V; (b) cycling stability at different charge discharge rates varying from 100 mA g^{-1} to 500 mA g^{-1} in the potential window of 2.5 to 0.01 V for the 1D hybrid perovskite case up to 250 cycles; (c) cyclic voltammogram of 1D Bz-Pb-I at a scan rate of 0.1 mV s^{-1} in a potential window of 0.01 to 2.5 V; (d) charge discharge profiles at a constant current density of 100 mA g^{-1} for 1D Bz-Pb-I.

CENTRE FOR ENERGY SCIENCE

Thank You